Received: 20 April 2019 | Accepted: 27 August 2019

DOI: 10.1111/gcb.14833

PRIMARY RESEARCH ARTICLE

Global Change Biology WILEY

Testing for changes in biomass dynamics in large-scale forest datasets

Ervan Rutishauser[1] | Stuart J. Wright[1] | Richard Condit[2] | Stephen P. Hubbell[3] | Stuart J. Davies[4,5] | Helene C. Muller-Landau[1]

[1]Smithsonian Tropical Research Institute, Ancon, Panama

[2]Morton Arboretum, Lisle, IL, USA

[3]Department of Ecology and Evolutionary Biology, University of California, Los Angeles, CA, USA

[4]Center for Tropical Forest Science-Forest Global Earth Observatory, Smithsonian Tropical Research Institute, Panama City, Panama

[5]Department of Botany, National Museum of Natural History, Washington, DC, USA

Correspondence
Ervan Rutishauser, Smithsonian Tropical Research Institute, Box 0843-03092 Balboa, Ancon, Panama.
Email: er.rutishauser@gmail.com

Funding information
US Department of Energy; National Science Foundation; Smithsonian Tropical Research Institute; MacArthur Foundation

Abstract

Tropical forest responses to climate and atmospheric change are critical to the future of the global carbon budget. Recent studies have reported increases in estimated above-ground biomass (EAGB) stocks, productivity, and mortality in old-growth tropical forests. These increases could reflect a shift in forest functioning due to global change and/or long-lasting recovery from past disturbance. We introduce a novel approach to disentangle the relative contributions of these mechanisms by decomposing changes in whole-plot biomass fluxes into contributions from changes in the distribution of gap-successional stages and changes in fluxes for a given stage. Using 30 years of forest dynamic data at Barro Colorado Island, Panama, we investigated temporal variation in EAGB fluxes as a function of initial EAGB ($EAGB_i$) in 10 × 10 m quadrats. Productivity and mortality fluxes both increased strongly with initial quadrat EAGB. The distribution of EAGB (and thus $EAGB_i$) across quadrats hardly varied over 30 years (and seven censuses). EAGB fluxes as a function of $EAGB_i$ varied largely and significantly among census intervals, with notably higher productivity in 1985–1990 associated with recovery from the 1982–1983 El Niño event. Variation in whole-plot fluxes among census intervals was explained overwhelmingly by variation in fluxes as a function of $EAGB_i$, with essentially no contribution from changes in $EAGB_i$ distributions. The high observed temporal variation in productivity and mortality suggests that this forest is very sensitive to climate variability. There was no consistent long-term trend in productivity, mortality, or biomass in this forest over 30 years, although the temporal variability in productivity and mortality was so strong that it could well mask a substantial trend. Accurate prediction of future tropical forest carbon budgets will require accounting for disturbance-recovery dynamics and understanding temporal variability in productivity and mortality.

KEYWORDS

biomass dynamic, carbon fluxes, long-term change, tropical forests

1 | INTRODUCTION

Understanding tropical forest responses to atmospheric and climate change is critical to modeling the future global carbon cycle. Repeated censuses of forest inventory plots have found increasing stocks of tree carbon in apparently undisturbed tropical forests in Amazonia (Baker et al., 2004; Phillips et al., 1998), Africa (Lewis et al., 2013), and Borneo (Qie et al., 2017). Globally, analysis of long-term forest inventories suggests that old-growth tropical forests are currently carbon sinks, sequestering an average

of 0.34 Mg C ha^{-1} $year^{-1}$ (confidence intervals [CIs] = 0.17–0.47; Muller-Landau, Detto, Chisholm, Hubbell, & Condit, 2014), albeit with a reduction in sink strength over time (Brienen et al., 2015; Qie et al., 2017). The causes of this increase and its consistency in space and time remain uncertain (Lewis, Lloyd, Sitch, Mitchard, & Laurance, 2009; Wright, 2010, 2013). Current knowledge of changes in old-growth tropical forest carbon stocks is hampered by limited spatial and temporal coverage of monitoring plots, sensitivity to measurement errors and data correction procedures, and the confounding influences of disturbance-recovery dynamics (Clark, Clark, et al., 2017; Muller-Landau et al., 2014).

There are multiple pathways through which anthropogenic global change could increase or decrease carbon stocks and fluxes in old-growth tropical forests. Increasing atmospheric carbon dioxide could enhance tropical tree growth and forest productivity through increased photosynthesis and water use efficiency (Lloyd & Farquhar, 2008), and thereby increase forest carbon stocks (Figure 1a–c). Alternatively, rising temperatures and increasing drought frequency and/or intensity could increase tree mortality and thereby decrease forest carbon stocks (McDowell et al., 2018). The "Bigger and Faster" hypothesis proposes that growth, recruitment, and mortality are all increasing (Clark, Clark, et al., 2017); in this case, the net effect on biomass depends on the relative magnitude of the increases in productivity and mortality (Figure 1d–f). Some but not all studies have found evidence of increasing productivity (Brienen et al., 2015; Feeley, Wright, Supardi, Kassim, & Davies, 2007; Körner, 2015) and increasing mortality (Brando et al., 2014; Brienen et al., 2015; Liu et al., 2017; McDowell et al., 2018; Phillips et al., 2010).

It is also possible that the observed increase in tropical forest biomass is due not to global change influences but to long-lasting recovery from past disturbances in some (but not all) tropical forests (Figure 1g–i; Wright, 2010). There is growing evidence that past human-induced or climatic disturbances continue to profoundly shape current forest composition (Brncic, Willis, Harris, & Washington, 2006; Levis et al., 2017; Magnabosco Marra et al., 2018), functioning (Doughty et al., 2015; McMichael, Matthews-Bird, Farfan-Rios, & Feeley, 2017; Oslisly et al., 2013), and extent (Mayle, Burbridge, & Killeen, 2000) in tropical regions. Forest succession after disturbance would generate a pattern of increasing total biomass mortality and biomass productivity over time, similar to that expected under the "Bigger and Faster" hypothesis (Clark, Clark, et al., 2017), and constitutes a null hypothesis or non-global change hypothesis. Forest recovery post-disturbance poses a particular challenge, as it may act at various spatial and temporal scales, and in only a subset of tropical forests.

We propose to separate out the contributions of disturbance-recovery dynamics to temporal variation in forest carbon stocks by decomposing changes in whole-plot biomass fluxes into contributions from changes in the distribution of gap-successional stages and changes in fluxes for a given stage (Figure 2). An old-growth tropical forest is a shifting mosaic of patches at different stages of recovery (Watt, 1947; Whitmore, 1989), of which most are increasing in biomass at any given time (Körner, 2003a). Dividing a plot into small quadrats provides a simple operational way to characterize this mosaic of

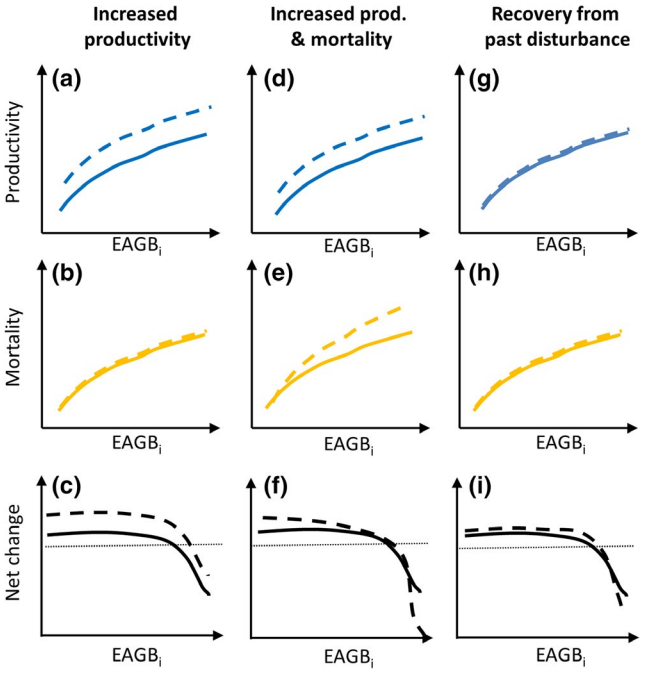

FIGURE 1 Expected patterns of quadrat biomass fluxes in relation to initial estimated above-ground biomass ($EAGB_i$) for three possible scenarios (columns) consistent with increasing biomass stocks in tropical forests. In every panel, the solid line shows the pattern expected for an earlier census interval, and the dashed line for a later census interval. Increasing productivity due to "fertilization" (first column), means higher productivity for a given $EAGB_i$ in the second census interval (a, dashed line) than in the first one (a, solid line), no systematic difference in mortality after controlling for $EAGB_i$ (b), and thus higher net change in EAGB per $EAGB_i$ in the second census interval (c). Increasing productivity and mortality, as expected under "speeding up" (second column), means higher productivity and higher mortality in the second census interval (d, e) and diverse possible patterns for net change (f). Finally, recovery from disturbance (final column) is expected to show no systematic change in fluxes when controlling for $EAGB_i$ (g–i). Note that local quadrat productivity increases with initial quadrat EAGB in all scenarios and census intervals (first row, blue), as does the local mortality flux (second row, yellow). Quadrat-level biomass net change (third row, black) is the difference between productivity and mortality fluxes, and is positive for low $EAGB_i$, and becomes negative for high $EAGB_i$

stages, and quadrat initial EAGB ($EAGB_i$) provides a useful proxy for age/time since disturbance (Bormann & Likens, 1979; Denslow, Ellison, & Sanford, 1998). Plot-level EAGB fluxes (Figure 2c) then reflect the integration of functions for fluxes as a function of $EAGB_i$ (Figure 2a) with the distribution of $EAGB_i$ (Figure 2b). Both quadrat productivity and mortality fluxes (Mg/ha) are expected to increase with $EAGB_i$ (Figure 2a), and consistent global change influences should be evident in directional changes in these functions over time—that is, in increases or decreases in fluxes when controlling for $EAGB_i$. Climate variation could also contribute to temporal variation in productivity and mortality drivers, and thus in fluxes for a given $EAGB_i$ (Dong et al., 2012). In contrast, the distribution of quadrat $EAGB_i$ depends largely on the disturbance history at a site (Espírito-Santo et al., 2014; Fisher, Hurtt,

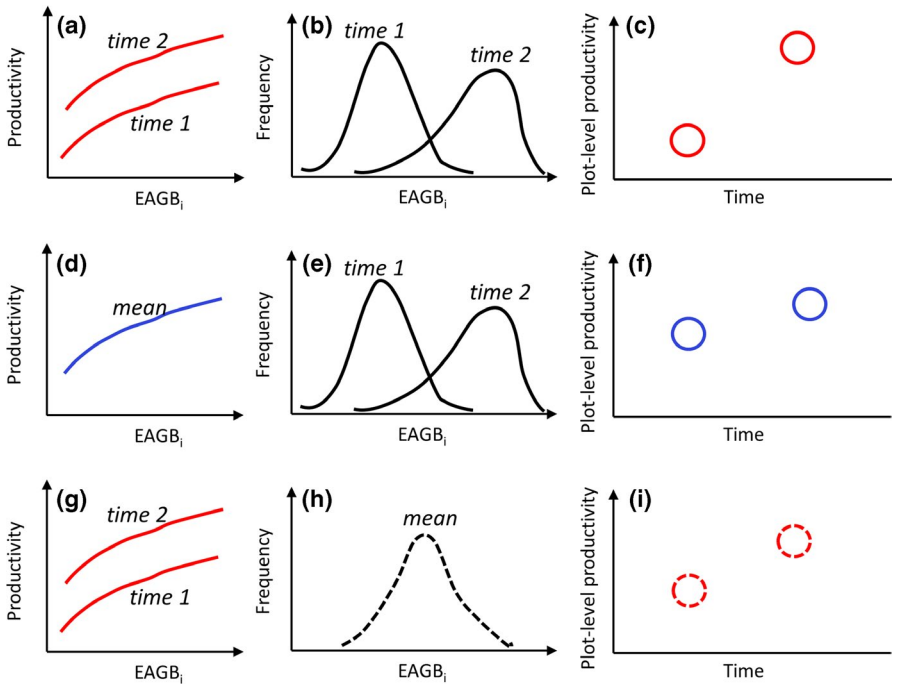

FIGURE 2 Whole plot estimated above-ground biomass (EAGB) fluxes (right column) in a given time period depends on the combination of how small-scale fluxes vary with initial EAGB ($EAGB_i$) (left column) and how $EAGB_i$ varies spatially across the plot and over time (middle column). Here, we illustrate this for productivity; the same integration holds for whole-plot mortality. To distinguish the contribution of flux–$EAGB_i$ relationships from the contribution of $EAGB_i$ distributions to plot-level biomass dynamics, we estimated what whole-plot fluxes would be in each census interval if either the flux–$EAGB_i$ relationship or the $EAGB_i$ distribution were constant across census intervals. To calculate a single constant flux–$EAGB_i$ relationship (d) and a single constant $EAGB_i$ distribution (h), we averaged across all census intervals weighted equally. We then integrated the empirical flux–$EAGB_i$ relationship over the $EAGB_i$ distribution for each census interval under three scenarios: (i) interval-specific flux–$EAGB_i$ relationships and interval-specific $EAGB_i$ distributions (a–c); (ii) the average flux–$EAGB_i$ relationship and interval-specific $EAGB_i$ distributions (d–f); (iii) interval-specific flux–$EAGB_i$ relationships and the average $EAGB_i$ distribution (g–i)

Thomas, & Chambers, 2008), and can fluctuate from a dominance of early successional (i.e., low $EAGB_i$) stages soon after disturbance (Figure 2b, time 1) to higher frequency of late successional quadrats longer after disturbance (Figure 2b, time 2).

Using a large-scale, long-term forest plot dataset for Barro Colorado Island (BCI), Panama, we seek to disentangle the influences of disturbance recovery from potential global change by quantifying how local biomass dynamics vary with initial biomass, and evaluating whether these relationships change over time. Specifically, we tested for temporal variation in quadrat productivity, loss, and net change in biomass when controlling for initial biomass. To assess the degree to which similar biomass patches were consistently associated with similar forest structure across census intervals, we also examined how quadrat initial biomass was related to tree density (per area) and mean tree size at each census and compared these relationships over time.

2 | METHODS

2.1 | Study site

Barro Colorado Island is located in central Panama (9°08' N, 79°510' W). Temperature averages 27°C and annual rainfall averages 2,657 mm (for 1926–2017; Paton, 2018), with a dry season between January and April. The vegetation is moist tropical forest. The 50 ha forest dynamics plot was established in 1982 (Condit, 1998; Hubbell et al., 1999), and recensused in 1985 and every 5 years subsequently (Figure S1). All free-standing woody stems with a diameter at breast height (DBH) ≥1 cm were mapped, tagged, and identified to species, and were measured in diameter at every census in which they remained alive. Diameter measurements were taken at 1.3 m height or above any buttress or major stem deformity. We omitted the initial census of 1982–1983 from analyses of biomass and biomass dynamics due to major differences in the field measurement methods for large trees (Condit, 1998), leaving seven censuses and six 5 year intervals between 1985 and 2015. We omitted 1.2 ha of swamp and 1.9 ha of young forest from the analysis due to differences in species composition, structure, and dynamics (Condit, Hubbell, & Foster, 1996; Harms, Condit, Hubbell, & Foster, 2001), leaving 46.9 ha for analysis. (We note, however, that our results are robust to the inclusion of the young forest, as we would expect; see Supporting information C1). Supplemental materials provide additional details on the census methods (Supporting information A).

2.2 | Individual tree biomass calculation

For all stems of dicot (non-palm) species, we estimated above-ground biomass (EAGB) from individual DBH and species-specific

wood density (WD) using a generic tropical forest biomass equation (Chave et al., 2014). For stems measured at heights other than 1.3 m, we first calculated taper-corrected equivalent diameters at 1.3 m height using a generic taper correction equation for BCI:

$$\mathrm{DBH} = D \times \exp\left(0.0247 \times (\mathrm{HOM} - 1.3)\right),$$

where D is diameter measured at height of measurement (HOM; in m; equation 2, Cushman, Muller-Landau, Condit, & Hubbell, 2014). We applied this taper correction to avoid time-dependent biases in plot-level biomass stocks and fluxes associated with changes over time in the proportion of trees measured above 1.3 m and average measurement heights (Cushman et al., 2014). We also estimated missing diameter measurements (1,192 of the 2,607,014 records) by simple linear interpolation between consecutive measurements. We then EAGB (in Mg dry biomass) of each stem in each census from its DBH, using the updated version of equation 7 of Chave et al. (2014), incorporating species-level WD (in g/cm^3) collected near the study site (Wright et al., 2010 and unpublished) and a climatic index that represents environmental influences on tree height allometries (E = 0.05645985 for BCI):

$$\mathrm{EAGB} = \exp\left(-2.024 - 0.896 \times E + 0.920 \times \log(\mathrm{WD}) + 2.795 \times \log(\mathrm{DBH}) - 0.0461 \times \log(\mathrm{DBH})^2\right)$$

(see Supporting information S2 for details of wood density assignment).

For palms, we estimated biomass using a palm-specific allometric equation based on DBH. For palm species that do not grow in DBH (all local palm species except *Socratea exorrhiza*), we first assigned species-specific median DBH to each palm stem in each census (Table S1). We EAGB (in Mg dry biomass) of each palm stem as

$$\mathrm{AGB} = 0.0417565 \times \mathrm{DBH}^{2.7483},$$

based on the family-wise specific allometric equation of Goodman et al. (2013), modified to include the log-transformation correction factor (Baskerville, 1972). We recognize that this procedure results in systematic errors in biomass fluxes for palms that do not grow in diameter, because it fails to consider their height growth, and that better estimates would be possible if height data were available. Overall, palms other than *Socratea* account for 0.9% of the woody biomass and 1.8% of the estimated woody productivity on BCI.

For multi-stemmed trees, individual tree biomass was calculated as the sum of biomass of all live stems. Large (DBH > 50 cm) individuals of strangler fig species (*Ficus costaricana*, *Ficus obtusifolia*, *Ficus popenoei*, and *Ficus trigonata*), for which diameter measurements are unreliable measures of size, were excluded from the analysis by excluding associated quadrats (Table S2).

2.3 | Quadrat-level biomass stocks and fluxes

Biomass stocks and fluxes were analyzed at the scale of 10 m quadrats and for the plot as a whole. Analysis at the quadrat level aimed to quantify how local biomass fluxes vary with local initial biomass for each census interval, and to compare these relationships across census intervals. Initial biomass was calculated as the sum of biomass of all trees alive at the initial census. We calculated biomass fluxes per time in productivity, mortality, and net change using simple arithmetic estimators. That is, we calculated fluxes for each quadrat by summing over relevant trees (i) and dividing by the time interval measured separately for each tree:

$$\text{EAGB change} = \sum \frac{(\mathrm{EAGB}_{\text{final}\,i} - \mathrm{EAGB}_{\text{initial}\,i})}{\text{time}_i}.$$

Productivity was calculated as the sum of the EAGB changes of surviving trees and the EAGB of recruits (including resprouts). Because the census dataset includes all stems >1 cm in diameter, biomass increment accounts for the vast majority of the woody productivity (97.5%; Figure S2). Biomass loss was calculated as the sum of EAGB_i of all trees that died by the next census, as well as of large individual stems that died on multi-stemmed individuals (see Supporting information A for details on the treatment of multi-stemmed trees). For recruits and dead stems, the time interval used was the mean time between measurements for that quadrat and census interval. These arithmetic estimators systematically underestimate fluxes because they miss contributions from trees that recruited and died during the census interval, with larger biases for longer census intervals (Kohyama, Kohyama, & Sheil, 2019). However, all our census intervals were very similar in length (Figure S1), and thus, these biases do not confound our analysis. Estimated biomass stocks and fluxes are expressed on a quadrat basis (100 m^{-2}), and can be converted to units of Mg/ha by multiplying by 100.

We quantified the relationship of quadrat-level biomass fluxes to initial biomass for each census interval using local regression and power function fits. We first illustrate the relationships for productivity, mortality, and net change using local polynomial regression, specifically the *locfit()* function in R (Loader, 1999) with smoothing parameter (alpha) set to 0.7. To formally test for variation in EAGB productivity and loss among census intervals, each of these fluxes was modeled as power functions of EAGB_i, with a power variance function structure (using package lme4; Bates, Mächler, Bolker, & Walker, 2015). We tested for differences among census intervals in power function "slopes" (exponents) and normalized intercepts, with these intercepts calculated as the predictions for the median EAGB value of 125.0 Mg/ha. CIs were computed by bootstrapping over quadrats (1,000 times). We evaluated the sensitivity of the results to different local regression models, and the consistency between the power function and local regression results.

For each census interval, our analyses of quadrat-level fluxes excluded quadrats affected by any one or more of three problems. First, analyses excluded quadrats if any stem had a change in HOM >10 cm during that census interval. Second, analyses excluded quadrats that ever had a strangler fig larger than 50 cm DBH. Finally, analyses excluded quadrats where an individual stem had an unreasonably large change in DBH in that census interval, such that its absolute biomass change was >0.98 Mg/ha (this threshold was

chosen because it is 20% of the mean productivity per hectare computed over all quadrats and census intervals that met the first two criteria). We excluded between 389 and 1,288 of the 4,669 possible quadrats (i.e., not in swamps or in young forest), depending on the census interval, mostly because of the first rule removing quadrats with a change in measurement height (Table S2). We did not remove or correct unlikely but less influential diameter changes, because in a dataset of this size, these random errors will tend to cancel out, whereas attempts to filter or correct such changes have strong potential to introduce systematic biases (because it is easier to detect some types of errors than others, Muller-Landau et al., 2014). The results were robust to varying filtering methods (Figure S7).

We evaluated consistency in or differences among censuses in the probability distribution of quadrat-level EAGB using empirical cumulative density functions. We specifically tested for differences among censuses in selected percentiles (5th, 10th, 25th, 50th, 75th, 90th, and 95th), by evaluating whether CIs overlapped. We estimated CIs on the percentiles by bootstrapping over quadrats.

We evaluated the sensitivity of our results to the spatial grain of quadrats, applying the same methods for smaller (8.33 m) and larger (12.5, 15.15 m) quadrats (Figures S8–S10).

2.4 | Disentangling sources of temporal variation in whole-plot fluxes

To distinguish the contribution of flux–$EAGB_i$ relationships from the contribution of $EAGB_i$ distributions to plot-level biomass dynamics, we estimated what whole-plot fluxes would be in each census interval if either the flux–$EAGB_i$ relationship or the $EAGB_i$ distribution was constant across census intervals. To calculate a single constant flux–$EAGB_i$ relationship and a single constant $EAGB_i$ distribution, we averaged across all census intervals weighted equally. We then integrated the empirical flux–$EAGB_i$ relationship over the $EAGB_i$ distribution (Figure 2) for each census interval under three scenarios: (a) interval-specific flux–$EAGB_i$ relationships and the average $EAGB_i$ distribution; (b) the average flux–$EAGB_i$ relationship and interval-specific $EAGB_i$ distributions; and (c) interval-specific flux–$EAGB_i$ relationships and interval-specific $EAGB_i$ distributions. For each flux–$EAGB_i$ relationship, fluxes for the central 90% of the EAGBI distribution (from the 5th to 95th percentile) were estimated from $EAGB_i$ using fits of the *locfit* function to the full distribution, as above (α = 0.7). In the tails of the distribution, fluxes were estimated as equal to the means for the corresponding interval (i.e., the 0–5th percentile interval or the 95th–100th percentile interval), to avoid undue influence of a few points.

2.5 | Forest structure

For each census interval, forest structure was quantified by analyzing the distributions over 10 × 10 m quadrats of the numbers of trees ≥ 1, 10, and 60 cm, and of quadratic mean diameter ($D_g = \sqrt{\sum \mathrm{DBH}^2/n}$, in cm). We quantified how these structure measures varied with quadrat EAGB in each census interval by fitting local regressions (R function *locfit* with α = 0.7), and calculating values expected for select quadrat EAGB (corresponding to the 10th, 25th, 50th, 75th, and 90th percentiles computed for all censuses combined). We tested whether there were changes over time in the values expected for selected quadrat EAGB or in the plot-level means, by comparing CIs obtained by bootstrapping over quadrats.

3 | RESULTS

3.1 | Quadrat-level biomass fluxes

Mean quadrat EAGB productivity and EAGB mortality loss both increased with initial quadrat EAGB in each census interval, with uncertainty rising in parallel (Figures 3 and 4a,b; Figure S2). Both fluxes were well-fit by power functions of $EAGB_i$ (Figure 4a,b; Figures S5 and S6). Mean EAGB net change was positive for low $EAGB_i$ and became negative in quadrats with EAGB> ~3 Mg/100 m^2 (equivalently 300 Mg/ha; Figure 4c).

There was substantial variation among census intervals in EAGB fluxes as a function of $EAGB_i$. This is visually evident from examination of the differences in EAGB-specific fluxes from the mean flux over census intervals (Figure 4d–f), and is quantified by differences in parameter values of the power function fits (Figure 5; power functions were good fits to the data, as is evident from their concordance with local regressions in Figures S5 and S6). Productivity fluxes in the 1985–1990 census interval averaged 10%–30% higher than the mean over census intervals for all but the highest values of $EAGB_i$ (Figure 4d, blue line). The next highest productivity fluxes were in the most recent census interval, and the lowest productivity fluxes were in 2000–2005 (Table S6). EAGB loss also varied among census intervals, with above-average EAGB loss for lower $EAGB_i$ in some census intervals (2005–2010 and 2010–2015) and for higher $EAGB_i$ in other intervals (1995–2000). The power function fits reflected these patterns, with significant variation among census intervals in the normalized intercepts, the estimated fluxes at the midpoint of the $EAGB_i$ distribution (here 125 Mg/ha; Figure 5a,b; Table S6). For productivity, the first census interval had by far the largest intercept, with subsequent declines to 2000–2005, and then increases since 2005 (Figure 5a). For mortality, the intercept tended to increase after the 1990–1995 census interval. The slopes (exponents) of the power functions showed little variation among census intervals (mostly overlapping CIs, Figure 5c,d). CIs for EAGB loss and net flux were wide (Figures S3 and S4), limiting the power to test for significant differences among census intervals (Figure 4d–f; Figure S3 and S4). Results were qualitatively consistent for other quadrat sizes (Figures S8–S10).

3.2 | Whole plot biomass stocks and fluxes

The probability distribution of EAGB density over 10 × 10 m quadrats varied only slightly among censuses, and showed no clear directional change (Figure 6a). The 5th–50th percentiles of quadrat EAGB increased slightly from 1985 to 2000, and then decreased again to values similar to initial ones (Figure 6c). In contrast, the 90th percentile increased slightly over the study period (Figure 6c).

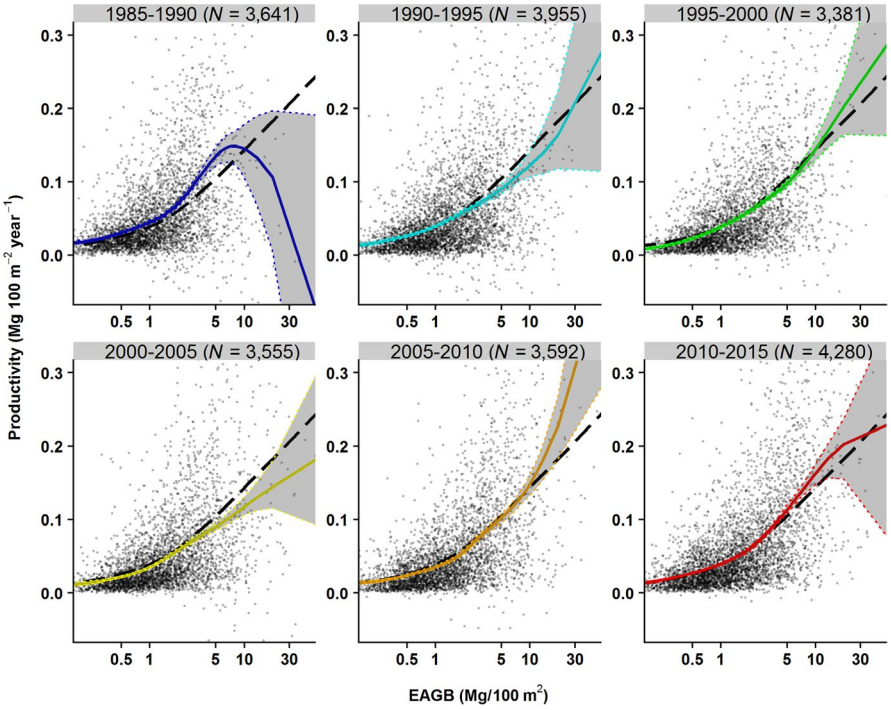

FIGURE 3 Quadrat-level mean annual estimated above-ground biomass (EAGB) productivity (Mg 100 m^{-2} year^{-1}) as a function of initial quadrat biomass (EAGB in Mg/100 m^2) for each 5 year census interval, for individual 10 × 10 m quadrats (points), together with local polynomial regression lines for individual census intervals (colored solid lines) and for all census intervals combined (black dashed lines). Confidence envelopes were computed from bootstrapping over quadrats. For each census interval, analyses excluded quadrats with problematic EAGB change measurements (see Section 2 for details); *N* is the number of quadrats included for each census interval. The range of data shown here is truncated, but all points were included in the analyses. Note that EAGB stocks and fluxes can be converted to units of Mg/ha by multiplying by 100

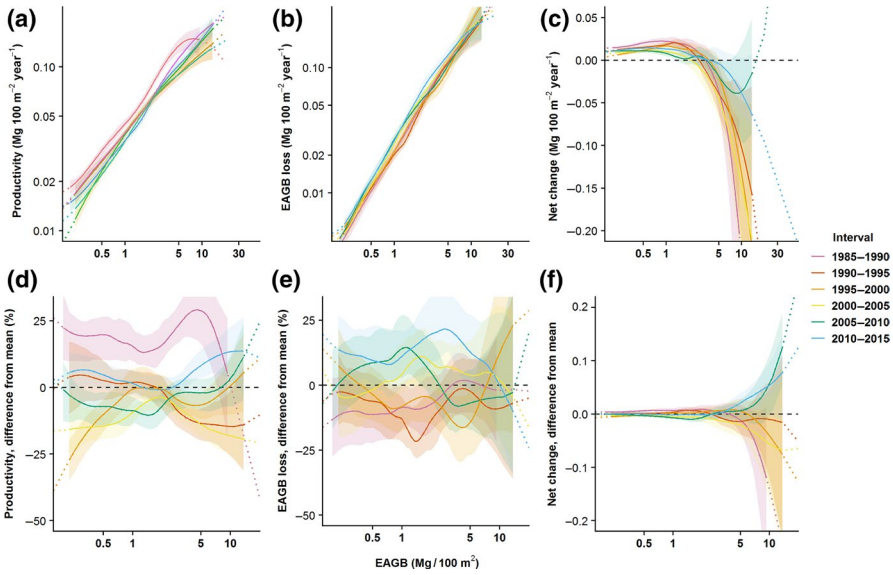

FIGURE 4 Variation among census intervals in quadrat estimated above-ground biomass (EAGB) productivity (a), loss (b), and net change (c) as a function of above-ground biomass (EAGB) at the initial census for 10 × 10 m quadrats, together with the corresponding differences from the mean (per initial EAGB) across all census intervals (d–f). Patterns were quantified using local polynomial regression; regression lines are displayed as solid lines for initial EAGB values spanning the 2nd–98th percentiles of the respective census interval, and as dotted lines outside this range. Confidence envelopes were computed by bootstrapping over quadrats, and are shown for the 2nd–98th percentiles of initial EAGB using shading. Analyses excluded quadrats with problematic EAGB change measurements (see methods for details). Note that productivity (a) and loss (b) are shown on log scales, and their differences from the mean are expressed in percentages (d,e) whereas the net change (c) and its difference from the mean (f) are shown on linear scales. Note that EAGB stocks and fluxes can be converted to units of Mg/ha by multiplying by 100

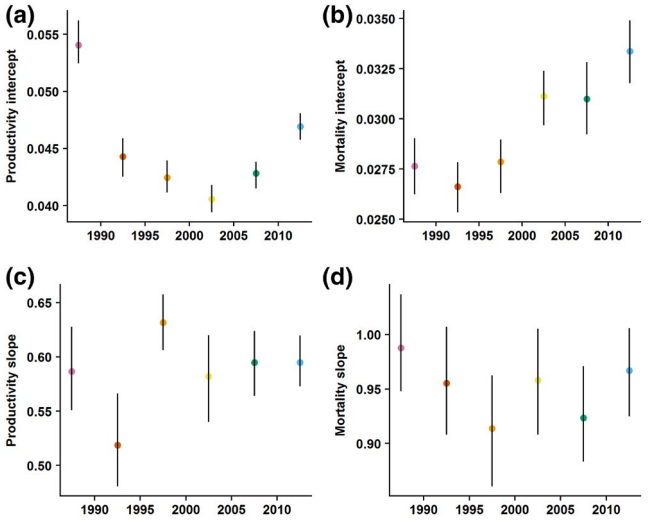

FIGURE 5 Variation among census intervals in the intercepts (a, b) and slopes (c, d) of power function relationships of quadrat-level productivity (a, c) and losses to mortality (b, d) to initial above-ground biomass. Intercepts are normalized, and represent the values at the overall midpoint estimated above-ground biomass (EAGB) value (1.25 Mg/100 m^2, i.e., an EAGB density of 125 Mg/ha). Confidence intervals were computed from bootstrapping over quadrats (see Table S2 for parameter values). Analyses excluded quadrats with problematic EAGB change measurements (see Section 2 for details)

Temporal variation in whole-plot EAGB fluxes as estimated by integrating temporal variation in flux–$EAGB_i$ relationships and $EAGB_i$ distributions was due almost entirely to temporal variation in flux–$EAGB_i$ relationships for a given $EAGB_i$, with almost no contribution of temporal variation in the $EAGB_i$ distribution (Figure 7; Table S4 scenario b). Temporal patterns in whole-plot fluxes thus roughly mirrored those in fluxes as a function of $EAGB_i$. Productivity flux was highest in 1985–1990, then dropped steeply, and has increased over the last three census intervals. Mortality loss flux dropped between the first and second census interval, and tended to increase since then, albeit CIs are wide. These patterns in estimated whole-plot fluxes mirrored calculated fluxes from summing over quadrats, although the exact pattern in productivity is highly sensitive to data cleaning and correction procedures (Figures S7–S17).

3.3 | Changes in forest structure

The mean density of stems >1 cm dbh increased modestly after the 1982–1983 drought, then thinned rapidly from 1990 to 2005, and was stable from 2005 to 2015 (Figure 8a, black points and lines). The same pattern was evident when controlling for focal quadrat biomass density (Figure 8a, colored lines). The density of stems ≥10 cm dbh in the plot as a whole increased slowly to 1995 and then decreased to 2010, with parallel patterns in all but the lowest biomass quadrats (Figure 8b). The density of large stems (≥60 cm dbh) remained essentially constant over time (Figure 8c; Table S5). Quadratic mean

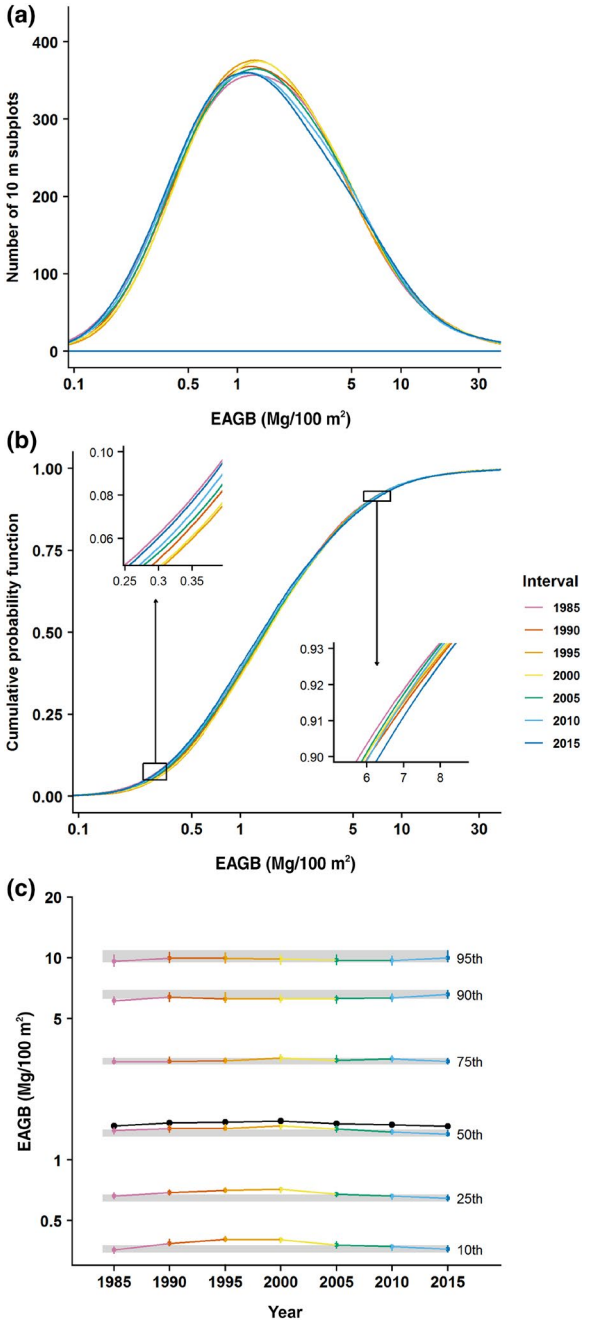

FIGURE 6 Probability density distribution (a) and cumulative probability distribution (b) of estimated above-ground biomass (EAGB) density across all 10 × 10 m quadrats, with insets in (b) magnified to show inter-census variation for cumulative probabilities of 0.05–0.1 and 0.9–0.95. (c) Variation over time in seven specific percentiles of the EAGB distribution over quadrats (colored points and lines) and in the overall mean EAGB density at the 50 ha scale (black solid points and lines). In panel (c), vertical lines show the 95% confidence intervals (CIs) from bootstrapping over quadrats, and horizontal gray shading shows the CIs for values in 2015 to enable easy visual assessment of how other years compare. The illustrated curves in panels (a) and (b) are truncated at the 0.2th and 99.8th percentiles of the distribution, but all values were included in analyses. Note that the EAGB densities can be converted to units of Mg/ha by multiplying by 100

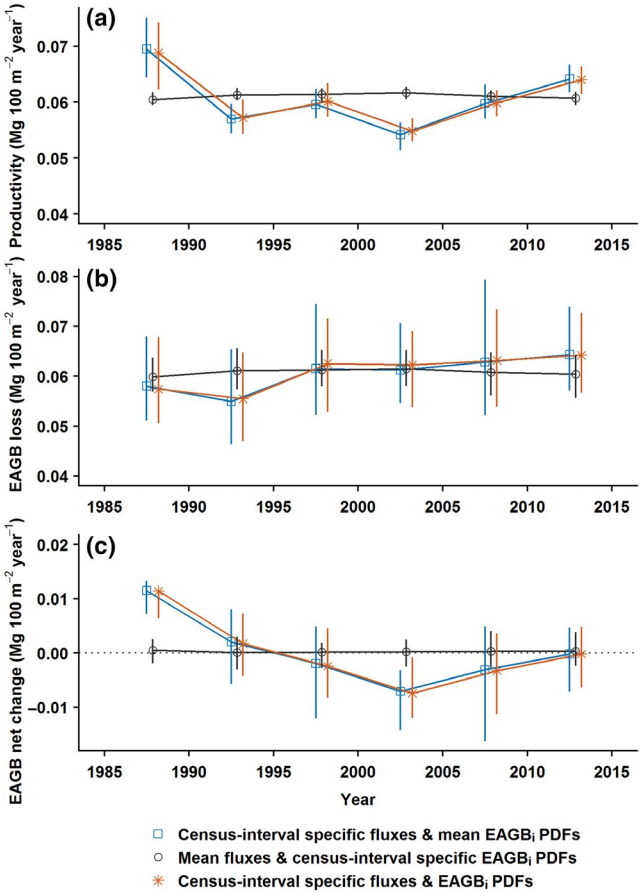

FIGURE 7 Time series of hypothetical whole-plot productivity (a), loss (b), and net change (c) expected with and without variation among census intervals in functions specifying how estimated above-ground biomass (EAGB) fluxes vary with initial biomass, and with and without variation among census intervals in initial EAGB distributions (EAGB$_i$). See Section 2 for details. Vertical lines show 95% confidence intervals obtained by bootstrapping over quadrats. The points are placed at the mid-points of the census intervals, and jiggered horizontally to increase readability. Values are given in Table S3. Note that EAGB stocks and fluxes can be converted to units of Mg/ha by multiplying by 100. PDF, probability density function

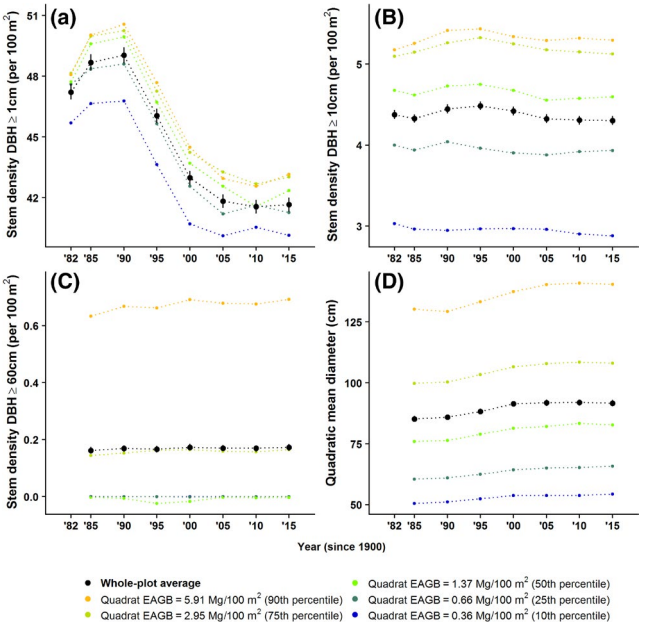

FIGURE 8 Variation among censuses in forest size structure at the whole plot level (black) and for different initial EAGB in 10 × 10 m quadrats (colors). 95% Confidence intervals (vertical lines) were obtained from bootstrapping over quadrats, but are generally smaller than the dot size. The density of large stems and mean diameter are not reported for 1982 due to inconsistencies in measurement methods (Condit, 1998). DBH, diameter at breast height

stem DBH increased from 1985 to 2000, and then leveled off, with parallel patterns for all quadrat biomass densities (Figure 8d).

4 | DISCUSSION

Here, we proposed and applied a straightforward way to control for successional stage in analyses of forest biomass change, by comparing forest patches at similar stages of gap recovery, as inferred by similar EAGB$_i$ density. Our analyses revealed strong temporal variation in forest woody productivity and loss fluxes both at the whole plot level and when controlling for local (10 × 10 m) gap phase. There was no consistent long-term trend in productivity, mortality, or biomass in this forest over 30 years, although the interannual variability in productivity and mortality is so strong that it could well mask a substantial trend. Woody productivity varied ~25% among 5 year census intervals, and woody losses ~15%, between 1985 and 2015. Because this variability is consistent even after controlling for gap phase, we conclude it arises from interannual variation in driving factors, most obviously climate.

4.1 | Temporal climate variation in the tropics and its impacts

Tropical forests experience biologically important interannual climate variation in temperature, solar radiation, water availability, and the frequency and intensity of major storms. Interannual climate variation in tropical forests is related in part to irregularly periodic climate oscillations, including the El Niño Southern Oscillation (ENSO) and the Atlantic Multidecadal Oscillation (AMO). In much of the tropics, the El Niño phase of ENSO is associated with drier, sunnier, and hotter conditions, whereas the La Niña phase is associated with wetter, cloudier, and cooler conditions (Holmgren, Scheffer, Ezcurra, Gutiérrez, & Mohren, 2001; Marengo, Tomasella, Alves, Soares, & Rodriguez, 2011). The AMO also influences climate variation at our site and other areas in the region (Elder, Balling, Cerveny, & Krahenbuhl, 2014). Tropical tree recruitment, growth, and mortality all vary among years in relation to such local climate variation, and thus, stand-level productivity and mortality fluxes vary as well.

Extended periods of drier than normal conditions—that is, droughts—are associated with increased mortality and decreased

productivity in many tropical forests (Feldpausch et al., 2016; Phillips et al., 2009). The severe 1982–1983 El Niño made the dry season on BCI longer and harsher than normal, and was associated with higher tree mortality rates. Similarly, many sites in the Amazon and southeast Asia experienced elevated mortality during and after El Niño droughts (e.g., Brando et al., 2014; McDowell et al., 2018; Phillips et al., 2010; Qie et al., 2017; Rowland et al., 2015). El Niño droughts in the Amazon were also associated with decreased leaf area index, decreased photosynthesis (attributed to both stomatal closure and lower leaf area), and decreased woody productivity during the drought periods (Aguilos, Hérault, Burban, Wagner, & Bonal, 2018; Asner, Townsend, & Braswell, 2000; Rowland et al., 2014; Santos et al., 2018). Tree-ring studies generally find that woody productivity is positively correlated with annual precipitation (Alfaro-Sánchez, Muller-Landau, Wright, & Camarero, 2017; Schippers, Sterck, Vlam, & Zuidema, 2015), consistent with the idea that dry years are bad for productivity. Temporal variation in woody growth in relation to water availability could be explained in part by shifts in allocation (rather than simply differences in total GPP and NPP), with trees allocating to increased xylem growth in wet periods after droughts in order to replace drought-damaged xylem (Trugman et al., 2018).

Although most studies have emphasized the negative effects of drier periods, drier years also bring higher solar radiation, and this can lead to more favorable conditions for forest productivity and tree survival if the dryness is not too extreme. On BCI, the drier periods of the 1987–1988 and 1997–1998 El Niños (Figure S18) were associated with elevated fruit production (Detto, Wright, Calderón, & Muller-Landau, 2018), and the 5 year census periods encompassing these events featured above-average woody productivity (this study, Meakem et al., 2017). El Niño events are associated with reduced rainfall during the wet season across northern South American and southern Central America (Ropelewski & Halpert, 1987). Moisture availability remains ample and reduced cloud cover and great solar radiation relieves light limitation (Graham, Mulkey, Kitajima, Phillips, & Wright, 2003), providing a straightforward explanation for observed increases in productivity (Detto et al., 2018; Wright & Calderón, 2006). Consistent with these findings, a previous analysis of multiple moist and wet tropical forests, including BCI, found higher tree growth in census intervals with higher solar radiation (Dong et al., 2012). There are also reasons why dry years might exhibit lower rather than higher mortality. Reduced light limitation in sunnier years might reduce mortality rates for shaded understory tree, and fewer and smaller storms may reduce mortality due to windthrows, lightning, and landslides (Aubry-Kientz, Rossi, Wagner, & Hérault, 2015; Espírito-Santo et al., 2010; Guzzetti, Peruccacci, Rossi, & Stark, 2008; Yanoviak, Gora, Burchfield, Bitzer, & Detto, 2017).

Interannual variation in temperature may also contribute to interannual variation in tropical forest carbon dynamics. Warmer years have been associated with lower tropical tree growth in several studies (Clark, Piper, Keeling, & Clark, 2003; Dong et al., 2012; Schippers et al., 2015). Temperature directly affects photosynthesis and respiration rates, with photosynthesis responding unimodally to temperature, and respiration increasing continuously with temperature (Lloyd & Farquhar, 2008; Slot & Winter, 2017). Furthermore, high leaf temperatures increase vapor pressure deficits and water demand, leading to stomatal closure, and it is this effect on water relations that appears to be the main contributor to temperature limitation on productivity (Aguilos et al., 2018; Slot & Winter, 2017). Higher atmospheric carbon dioxide concentrations increase plant water use efficiency, and may thereby partly mitigate the negative effects of higher temperatures and drier conditions on productivity (Holtum & Winter, 2010).

In addition to the direct effects of climate on plant physiological function and mortality risk, climate may also influence forest carbon cycles indirectly by causing shifts in allocation, stand structure, functional composition, and influences of interacting species. Plants may increase or decrease allocation to woody growth, including adding to or drawing down carbon stores, depending on past and current climate conditions (Clark, Clark, & Oberbauer, 2013; Doughty et al., 2014; Trugman et al., 2018). Past mortality events from climate alter tree age and size distributions, gap phase distributions, and thereby stand-level carbon budgets (Anderegg, Schwalm, et al., 2015; Chazdon, 2003; Clark, 2007). Differential recruitment, survival, and growth of plant functional types under particular climate conditions also alters functional composition, and thereby the response of forests to future climate. For example, mortality of drought-intolerant species under drought can shift composition toward more drought-tolerant species, with implications for forest carbon budgets and resilience to future droughts (Esquivel-Muelbert et al., 2019; McDowell et al., 2008; Ouédraogo, Mortier, Gourlet-Fleury, Freycon, & Picard, 2013). The proliferation of pathogens and insect herbivores, and thus their effects on trees, is also highly sensitive to climate conditions (Anderegg, Hicke, et al., 2015; Van Bael et al., 2004).

4.2 | Detecting and attributing long-term change

Tropical forests are experiencing global atmospheric and climate change. Mean atmospheric CO_2 concentration is increasing continuously, with an increase of 15% over the duration of our study (from 346 ppm in 1985 to 400 ppm in 2015, Figure S18g). Temperatures are increasing in most tropical regions, and precipitation patterns are changing in region-specific ways (Buckley & Huey, 2016; Malhi & Wright, 2004). At our site, the focal 30 year period exhibited trends of +0.15°C per decade in daily maximum temperature, +0.04°C per decade in daily minimum temperature, +5 mm/year in annual precipitation, +0.05% soil moisture per year, and −1.3 W m^{-2} $year^{-1}$ in annual solar radiation. Trends in annual means of these BCI climate metrics over the 30 year period alone were not statistically significant after Bonferroni correction (individual p-values of .075, .44, .66, .033, and .48, respectively), reflecting the relative strength of interannual variation. This interannual variation limits the ability to detect long-term trends—but failure to reject the null hypothesis of

no increase should not be misinterpreted as support for constant climate conditions.

These atmospheric and climate changes are hypothesized to be changing tropical forest carbon dynamics (Lewis, Malhi, & Phillips, 2004). CO_2 is needed for photosynthesis, and physiological models suggest that the observed increase in CO_2 should increase growth (Phillips & Lewis, 2014), although there is uncertainty about the degree to which growth responses are limited by availability of other nutrients, and within-plant carbon demands (Körner, 2009, 2003b; Wright et al., 2011). Spatial variation in climate among tropical forests is associated with variation in tropical forest carbon stocks and fluxes (Álvarez-Dávila et al., 2017; Becknell, Kissing Kucek, & Powers, 2012; Poorter et al., 2016; Taylor et al., 2017), suggesting that directional climate changes should also change forest carbon budgets in the long term. As discussed above, tropical forests are also sensitive to temporal variation in climate conditions, further suggesting that climate change will matter. However, the relationship of short-term to long-term climate responses is not straightforward, because the importance of particular mechanisms shifts with the timescale. Allocational shifts to/from woody productivity, reproductive output, and carbohydrate stores play a large role in variation over seasonal to annual time scales (Dickman et al., 2018; Doughty et al., 2014), but are likely to play little role at decadal and longer time scales. In contrast, shifts in functional composition of the tree community are likely to play a large role in responses to long-term climate variation (van der Sande et al., 2016), but very little role in short-term responses. Such compositional shifts are in general expected to decrease the sensitivity of forest carbon fluxes to climate variation, as the forest becomes increasingly dominated by species that do relatively well in the new climate conditions (Esquivel-Muelbert et al., 2019; Fauset et al.., 2015; Feldpausch et al., 2016).

However, evidence of long-term changes in tropical forest carbon cycling is mixed, with divergent patterns across studies. Increasing woody productivity and mortality were found in analyses of the RAINFOR network of Amazonian plots (Brienen et al., 2015), but not in site-specific studies of BCI (this study) or La Selva (Clark, Asao, et al., 2017; Clark et al., 2013; Clark, Clark, et al., 2017). On average, studies report increased biomass densities in old-growth tropical forests (Brienen et al., 2015; Chave et al., 2008, Lewis et al., 2009; Muller-Landau et al., 2014; Qie et al., 2017; Rutishauser, Wagner, Herault, Nicolini, & Blanc, 2010), but this pattern too is not universal (this study, Chave et al., 2008; Clark, Clark, et al., 2017; Feeley et al., 2007) and the causes of observed increases continue to be debated (Clark, 2004; Lewis et al., 2009; Muller-Landau, 2009; Wright, 2013). It is notable that two of the most intensive long-term studies of focal sites, this 30 year study of BCI and Clark, Clark, et al. (2017)'s 40 year study of La Selva, find multidecadal stability in forest structure and dynamics, in striking contrast to the "Bigger and Faster" hypothesis.

The large uncertainty surrounding estimated fluxes and their long-term trends observed here, even with such a large-scale long-term study, highlights the difficulty of accurately capturing changes in forest dynamics from field data (Clark, Asao, et al., 2017). Wagner, Rutishauser, Blanc, and Herault (2010) calculated that estimating even the mean EAGB loss within 20% error with 95% confidence in a particular forest would require ~200 ha-years of monitoring, far more than the usual size and duration of most forest monitoring experiments. The effort required to accurately estimate a long-term trend is much higher still—even a trend as large as 1% a year amounts to only 10% a decade, within the error limits of the Wagner et al. (2010) calculation. Detection of long-term trends is further complicated by sensitivity of estimated trends to the precise methods of data quality assessment and quality control (QAQC; Figure S18). Many common QAQC procedures result in systematic biases in whole-plot statistics (Cushman et al., 2014; Muller-Landau et al., 2014). Our analysis followed current best practices for calculating EAGB fluxes, including standardizing effective POM (Cushman et al., 2014) and avoiding data "cleaning" procedures that can systematically bias whole-plot statistics (Muller-Landau et al., 2014).

4.3 | Conclusion and future directions

The tropical forest on BCI exhibited large temporal variability in stand-level productivity and mortality fluxes over 30 years, even after controlling for disturbance-recovery dynamics, but no long-term trend. Observed temporal variability was aligned to some degree with ENSO-related climate variation, but with a markedly different pattern than is usually reported, highlighting the complexity of tropical forest climate responses. While the drier conditions of El Niño events have been associated with increased tree mortality and reduced productivity in the Amazon (Feldpausch et al., 2016; Lewis, Brando, Phillips, Heijden, & Nepstad, 2011), the drier and sunnier conditions during El Niño events were associated with enhanced productivity and no change in mortality on BCI (Detto et al., 2018; Meakem et al., 2017). No long-term directional trend in productivity, mortality, or biomass was evident in our data, but such a trend could well be obscured by the strong interannual variation.

A better understanding of tropical forest responses to climate variation and long-term trends requires both more data and integration with mechanistic models. Although climate and atmospheric change is global, climate effects are locally variable, and forest responses are dependent on a myriad of other local factors, including species composition and disturbance history, resulting in highly variable EAGB dynamics (Clark et al., 2013). Future multisite analyses of large plot datasets using the methods developed here could provide insights into temporal and spatial variation in tropical forest carbon fluxes (Chave et al., 2008; van der Sande et al., 2016; Wagner et al., 2016). However, any studies based on extant plot datasets are likely to fall short of what is needed to quantify overall trends given high temporal and spatial variability, and the nonsystematic placement of sampling plots (Marvin et al., 2014; McMichael et al., 2017; Saatchi et al., 2015; Wright, 2006). Improvements in remote sensing ultimately promise more comprehensive and consistent measurements of tropical forest structure

and function, and their change over time (Bastin et al., 2018; Rödig et al., 2018; Saatchi et al., 2011), although the contribution of recovery from past disturbances remains to be resolved (McMichael et al., 2017; Palace et al., 2017). Studies integrating mechanistic models with data on climate drivers and forest dynamics are uniquely well suited to gleaning insights into the ultimate mechanisms behind observed patterns and to disentangling the roles of temperature, rainfall, atmospheric carbon dioxide, soils, species composition, and site history (Levine et al., 2016; Schippers et al., 2015).

ACKNOWLEDGEMENTS

E.R. and S.J.D. were supported by the Next Generation Ecosystem Experiments-Tropics, funded by the US Department of Energy, Office of Science, Office of Biological and Environmental Research. We gratefully acknowledge the contributions to the Barro Colorado Island 50 ha plot of Robin Foster, co-founder of the plot; Rolando Pérez and Salomón Aguilar for species identification; Suzanne Lao for data management; Steven Dolins for database design; and hundreds of field-workers over the years. The BCI forest dynamics plot dataset was made possible by the financial support of the National Science Foundation, the Smithsonian Tropical Research Institute, and the MacArthur Foundation. We thank Deborah A. Clark and an anonymous reviewer for constructive comments on this manuscript.

CONFLICT OF INTEREST

All authors declare no conflict of interest.

ORCID

Ervan Rutishauser https://orcid.org/0000-0003-1182-4032

REFERENCES

Aguilos, M., Hérault, B., Burban, B., Wagner, F., & Bonal, D. (2018). What drives long-term variations in carbon flux and balance in a tropical rainforest in French Guiana? *Agricultural & Forest Meteorology*, *253–254*, 114–123. https://doi.org/10.1016/j.agrformet.2018.02.009

Alfaro-Sánchez, R., Muller-Landau, H. C., Wright, S. J., & Camarero, J. J. (2017). Growth and reproduction respond differently to climate in three Neotropical tree species. *Oecologia*, *184*, 531–541. https://doi.org/10.1007/s00442-017-3879-3

Álvarez-Dávila, E., Cayuela, L., González-Caro, S., Aldana, A. M., Stevenson, P. R., Phillips, O., … Rey-Benayas, J. M. (2017). Forest biomass density across large climate gradients in northern South America is related to water availability but not with temperature. *PLoS ONE*, *12*(3), e0171072. https://doi.org/10.1371/journal.pone.0171072

Anderegg, W. R. L., Hicke, J. A., Fisher, R. A., Allen, C. D., Aukema, J., Bentz, B., … Zeppel, M. (2015). Tree mortality from drought, insects, and their interactions in a changing climate. *New Phytologist*, *208*, 674–683. https://doi.org/10.1111/nph.13477

Anderegg, W. R. L., Schwalm, C., Biondi, F., Camarero, J. J., Koch, G., Litvak, M., … Pacala, S. (2015). Pervasive drought legacies in forest ecosystems and their implications for carbon cycle models. *Science*, *349*, 528–532. https://doi.org/10.1126/science.aab1833

Asner, G. P., Townsend, A. R., & Braswell, B. H. (2000). Satellite observation of El Niño effects on Amazon Forest phenology and productivity. *Geophysical Research Letters*, *27*, 981–984. https://doi.org/10.1029/1999GL011113

Aubry-Kientz, M., Rossi, V., Wagner, F., & Hérault, B. (2015). Identifying climatic drivers of tropical forest dynamics. *Biogeosciences*, *12*, 5583–5596. https://doi.org/10.5194/bg-12-5583-2015

Baker, T. R., Phillips, O. L., Malhi, Y., Almeida, S., Arroyo, L., Di Fiore, A., … Vasquez Martinez, R. (2004). Increasing biomass in Amazonian forest plots. *Philosophical Transactions of the Royal Society of London. Series B: Biological Sciences*, *359*, 353–365. https://doi.org/10.1098/rstb.2003.1422

Baskerville, G. (1972). Use of logarithmic regression in the estimation of plant biomass. *Canadian Journal of Forest Research*, *2*, 49–53. https://doi.org/10.1139/x72-009

Bastin, J.-F., Rutishauser, E., Kellner, J. R., Saatchi, S., Pélissier, R., Hérault, B., … Zebaze, D. (2018). Pan-tropical prediction of forest structure from the largest trees. *Global Ecology and Biogeography*, *27*, 1366–1383. https://doi.org/10.1111/geb.12803

Bates, D., Mächler, M., Bolker, B., & Walker, S. (2015). Fitting linear mixed-effects models using lme4. *Journal of Statistical Software*, *67*(1), 1–48. https://doi.org/10.18637/jss.v067.i01

Becknell, J. M., Kissing Kucek, L., & Powers, J. S. (2012). Aboveground biomass in mature and secondary seasonally dry tropical forests: A literature review and global synthesis. *Forest Ecology and Management*, *276*, 88–95.

Bormann, F. H., & Likens, G. E. (1979). *Pattern and process in a forested ecosystem: Disturbance, development and the steady state based on the Hubbard Brook Ecosystem Study* (1st ed.). New York, NY: Springer-Verlag.

Brando, P. M., Balch, J. K., Nepstad, D. C., Morton, D. C., Putz, F. E., Coe, M. T., … Soares-Filho, B. S. (2014). Abrupt increases in Amazonian tree mortality due to drought-fire interactions. *Proceedings of the National Academy of Sciences of the United States of America*, *111*, 6347–6352. https://doi.org/10.1073/pnas.1305499111

Brienen, R. J. W., Phillips, O. L., Feldpausch, T. R., Gloor, E., Baker, T. R., Lloyd, J., … Zagt, R. J. (2015). Long-term decline of the Amazon carbon sink. *Nature*, *519*, 344–348. https://doi.org/10.1038/nature14283

Brncic, T. M., Willis, K. J., Harris, D. J., & Washington, R. (2006). Culture or climate? The relative influences of past processes on the composition of the lowland Congo rainforest. *Philosophical Transactions of the Royal Society B: Biological Sciences*, *362*, 229–242. https://doi.org/10.1098/rstb.2006.1982

Buckley, L. B., & Huey, R. B. (2016). Temperature extremes: Geographic patterns, recent changes, and implications for organismal vulnerabilities. *Global Change Biology*, *22*, 3829–3842. https://doi.org/10.1111/gcb.13313

Chave, J., Condit, R., Muller-Landau, H. C., Thomas, S. C., Ashton, P. S., Bunyavejchewin, S., … Losos, E. C. (2008). Assessing evidence for a pervasive alteration in tropical tree communities. *PLoS Biology*, *6*, 455–462. https://doi.org/10.1371/journal.pbio.0060045

Chave, J., Réjou-Méchain, M., Búrquez, A., Chidumayo, E., Colgan, M. S., Delitti, W. B., … Vieilledent, G. (2014). Improved allometric models to estimate the aboveground biomass of tropical trees. *Global Change Biology*, *20*, 3177–3190. https://doi.org/10.1111/gcb.12629

Chazdon, R. L. (2003). Tropical forest recovery: Legacies of human impact and natural disturbances. *Perspectives in Plant Ecology, Evolution and Systematics*, *6*, 51–71. https://doi.org/10.1078/1433-8319-00042

Clark, D. (2004). Sources or sinks? The responses of tropical forests to current and future climate and atmospheric composition. *Philosophical*

Transactions of the Royal Society of London. Series B: Biological Sciences, *359*, 477–491. https://doi.org/10.1098/rstb.2003.1426

Clark, D. A. (2007). Detecting tropical forests' responses to global climatic and atmospheric change: Current challenges and a way forward. *Biotropica*, *39*, 4–19. https://doi.org/10.1111/j.1744-7429.2006.00227.x

Clark, D. A., Asao, S., Fisher, R., Reed, S., Reich, P. B., Ryan, M. G., … Yang, X. (2017). Field data to benchmark the carbon cycle models for tropical forests. *Biogeosciences*, *14*(20), 4663–4690. https://doi.org/10.5194/bg-14-4663-2017

Clark, D. A., Clark, D. B., & Oberbauer, S. F. (2013). Field-quantified responses of tropical rainforest aboveground productivity to increasing CO_2 and climatic stress, 1997–2009: Tropical rainforest productivity responses. *Journal of Geophysical Research: Biogeosciences*, *118*, 783–794. https://doi.org/10.1002/jgrg.20067

Clark, D. B., Clark, D. A., Oberbauer, S. F., & Kellner, J. R. (2017). Multidecadal stability in tropical rain forest structure and dynamics across an old-growth landscape. *PLoS ONE*, *12*, e0183819. https://doi.org/10.1371/journal.pone.0183819

Clark, D. A., Piper, S. C., Keeling, C. D., & Clark, D. B. (2003). Tropical rain forest tree growth and atmospheric carbon dynamics linked to interannual temperature variation during 1984–2000. *Proceedings of the National Academy of Sciences of the United States of America*, *100*, 5852–5857. https://doi.org/10.1073/pnas.0935903100

Condit, R. (1998). *Tropical forest census plots: Methods and results from Barro Colorado Island, Panama and a comparison with other plots*. Berlin, Germany: Springer Science & Business Media.

Condit, R., Hubbell, S. P., & Foster, R. B. (1996). Changes in tree species abundance in a Neotropical forest: Impact of climate change. *Journal of Tropical Ecology*, *12*, 231–256. https://doi.org/10.1017/S0266467400009433

Cushman, K. C., Muller-Landau, H. C., Condit, R. S., & Hubbell, S. P. (2014). Improving estimates of biomass change in buttressed trees using tree taper models. *Methods in Ecology and Evolution*, *5*, 573–582. https://doi.org/10.1111/2041-210X.12187

Denslow, J. S., Ellison, A. M., & Sanford, R. E. (1998). Treefall gap size effects on above- and below-ground processes in a tropical wet forest. *Journal of Ecology*, *86*, 597–609. https://doi.org/10.1046/j.1365-2745.1998.00295.x

Detto, M., Wright, S. J., Calderón, O., & Muller-Landau, H. C. (2018). Resource acquisition and reproductive strategies of tropical forest in response to the El Niño-Southern Oscillation. *Nature Communications*, *9*, 913. https://doi.org/10.1038/s41467-018-03306-9

Dickman, L. T., McDowell, N. G., Grossiord, C., Collins, A. D., Wolfe, B. T., Detto, M., … Chambers, J. Q. (2018). Homoeostatic maintenance of nonstructural carbohydrates during the 2015–2016 El Niño drought across a tropical forest precipitation gradient. *Plant, Cell and Environment*, *42*(5), 1705–1714. https://doi.org/10.1111/pce.13501

Dong, S. X., Davies, S. J., Ashton, P. S., Bunyavejchewin, S., Supardi, M. N., Kassim, A. R., … Moorcroft, P. R. (2012). Variability in solar radiation and temperature explains observed patterns and trends in tree growth rates across four tropical forests. *Proceedings of the Royal Society B: Biological Sciences*, *279*, 3923–3931. https://doi.org/10.1098/rspb.2012.1124

dos Santos, V. A. H. F., Ferreira, M. J., Rodrigues, J. V. F. C., Garcia, M. N., Ceron, J. V. B., Nelson, B. W., & Saleska, S. R. (2018). Causes of reduced leaf-level photosynthesis during strong El Niño drought in a Central Amazon forest. *Global Change Biology*, *24*, 4266–4279. https://doi.org/10.1111/gcb.14293

Doughty, C. E., Malhi, Y., Araujo-Murakami, A., Metcalfe, D. B., Silva-Espejo, J. E., Arroyo, L., … Ledezma, R. (2014). Allocation trade-offs dominate the response of tropical forest growth to seasonal and interannual drought. *Ecology*, *95*, 2192–2201. https://doi.org/10.1890/13-1507.1

Doughty, C. E., Metcalfe, D. B., Girardin, C. A. J., Amézquita, F. F., Cabrera, D. G., Huasco, W. H., … Malhi, Y. (2015). Drought impact on forest carbon dynamics and fluxes in Amazonia. *Nature*, *519*, 78–82. https://doi.org/10.1038/nature14213

Elder, R. C., Balling, R. C., Cerveny, R. S., & Krahenbuhl, D. (2014). Regional variability in drought as a function of the Atlantic Multidecadal Oscillation. *Caribbean Journal of Science*, *48*, 31–44. https://doi.org/10.18475/cjos.v48i1.a5

Espírito-Santo, F. D. B., Gloor, M., Keller, M., Malhi, Y., Saatchi, S., Nelson, B., … Phillips, O. L. (2014). Size and frequency of natural forest disturbances and the Amazon forest carbon balance. *Nature Communications*, *5*, 3434. https://doi.org/10.1038/ncomms4434

Espírito-Santo, F. D. B., Keller, M., Braswell, B., Nelson, B. W., Frolking, S., & Vicente, G. (2010). Storm intensity and old-growth forest disturbances in the Amazon region. *Geophysical Research Letters*, *37*, L11403. https://doi.org/10.1029/2010gl043146

Esquivel-Muelbert, A., Baker, T. R., Dexter, K. G., Lewis, S. L., Brienen, R. J. W., Feldpausch, T. R., … Phillips, O. L. (2019). Compositional response of Amazon forests to climate change. *Global Change Biology*, *25*, 39–56. https://doi.org/10.1111/gcb.14413

Fauset, S., Johnson, M. O., Gloor, M., Baker, T. R., Monteagudo, A. M., Brienen, R. J. W., … Phillips, O. L. (2015). Hyperdominance in Amazonian forest carbon cycling. *Nature Communications*, *6*, 6857. https://doi.org/10.1038/ncomms7857

Feeley, K. J., Wright, J., Supardi, N., Kassim, A. R., & Davies, S. J. (2007). Decelerating growth in tropical forest trees. *Ecology Letters*, *10*, 461–469. https://doi.org/10.1111/j.1461-0248.2007.01033.x

Feldpausch, T. R., Phillips, O. L., Brienen, R. J. W., Gloor, E., Lloyd, J., Lopez-Gonzalez, G., … Dávila, E. Á. (2016). Amazon forest response to repeated droughts. *Global Biogeochemical Cycles*, *30*, 964–982. https://doi.org/10.1002/2015GB005133

Fisher, J. I., Hurtt, G. C., Thomas, R. Q., & Chambers, J. Q. (2008). Clustered disturbances lead to bias in large-scale estimates based on forest sample plots. *Ecology Letters*, *11*, 554–563. https://doi.org/10.1111/j.1461-0248.2008.01169.x

Goodman, R. C., Phillips, O. L., del Castillo Torres, D., Freitas, L., Cortese, S. T., Monteagudo, A., & Baker, T. R. (2013). Amazon palm biomass and allometry. *Forest Ecology and Management*, *310*, 994–1004. https://doi.org/10.1016/j.foreco.2013.09.045

Graham, E. A., Mulkey, S. S., Kitajima, K., Phillips, N. G., & Wright, S. J. (2003). Cloud cover limits net CO_2 uptake and growth of a rainforest tree during tropical rainy seasons. *Proceedings of the National Academy of Sciences of the United States of America*, *100*, 572–576. https://doi.org/10.1073/pnas.0133045100

Guzzetti, F., Peruccacci, S., Rossi, M., & Stark, C. P. (2008). The rainfall intensity–duration control of shallow landslides and debris flows: An update. *Landslides*, *5*, 3–17. https://doi.org/10.1007/s10346-007-0112-1

Harms, K. E., Condit, R., Hubbell, S. P., & Foster, R. B. (2001). Habitat associations of trees and shrubs in a 50-ha Neotropical forest plot. *Journal of Ecology*, *89*, 947–959. https://doi.org/10.1046/j.0022-0477.2001.00615.x

Holmgren, M., Scheffer, M., Ezcurra, E., Gutiérrez, J. R., & Mohren, G. M. J. (2001). El Niño effects on the dynamics of terrestrial ecosystems. *Trends in Ecology & Evolution*, *16*, 89–94. https://doi.org/10.1016/S0169-5347(00)02052-8

Holtum, J. A., & Winter, K. (2010). Elevated [CO_2] and forest vegetation: More a water issue than a carbon issue? *Functional Plant Biology*, *37*, 694–702. https://doi.org/10.1071/FP10001

Hubbell, S. P., Foster, R. B., O'Brien, S. T., Harms, K. E., Condit, R., Wechsler, B., … De Lao, S. L. (1999). Light-gap disturbances, recruitment limitation, and tree diversity in a neotropical forest. *Science*, *283*, 554–557. https://doi.org/10.1126/science.283.5401.554

Kohyama, T. S., Kohyama, T. I., & Sheil, D. (2019). Estimating net biomass production and loss from repeated measurements of trees in forests

and woodlands: Formulae, biases and recommendations. *Forest Ecology and Management*, *433*, 729–740. https://doi.org/10.1016/j.foreco.2018.11.010

Körner, C. (2003a). Slow in, rapid out – Carbon flux studies and Kyoto targets. *Science*, *300*, 1242–1243. https://doi.org/10.1126/science.1084460

Körner, C. (2003b). Carbon limitation in trees. *Journal of Ecology*, *91*, 4–17. https://doi.org/10.1046/j.1365-2745.2003.00742.x

Körner, C. (2009). Responses of humid tropical trees to rising CO_2. *Annual Review of Ecology Evolution and Systematics*, *40*, 61–79. https://doi.org/10.1146/annurev.ecolsys.110308.120217

Körner, C. (2015). Paradigm shift in plant growth control. *Current Opinion in Plant Biology*, *25*, 107–114. https://doi.org/10.1016/j.pbi.2015.05.003

Levine, N. M., Zhang, K., Longo, M., Baccini, A., Phillips, O. L., Lewis, S. L., … Moorcroft, P. R. (2016). Ecosystem heterogeneity determines the ecological resilience of the Amazon to climate change. *Proceedings of the National Academy of Sciences of the United States of America*, *113*, 793–797. https://doi.org/10.1073/pnas.1511344112

Levis, C., Costa, F. R. C., Bongers, F., Peña-Claros, M., Clement, C. R., Junqueira, A. B., … Ter Steege, H. (2017). Persistent effects of pre-Columbian plant domestication on Amazonian forest composition. *Science*, *355*, 925–931. https://doi.org/10.1126/science.aal0157

Lewis, S. L., Brando, P. M., Phillips, O. L., van der Heijden, G. M. F., & Nepstad, D. (2011). The 2010 Amazon drought. *Science*, *331*, 554. https://doi.org/10.1126/science.1200807

Lewis, S. L., Lloyd, J., Sitch, S., Mitchard, E. T. A., & Laurance, W. F. (2009). Changing ecology of tropical forests: Evidence and drivers. *Annual Review of Ecology, Evolution, and Systematics*, *40*, 529–549. https://doi.org/10.1146/annurev.ecolsys.39.110707.173345

Lewis, S. L., Malhi, Y., & Phillips, O. L. (2004). Fingerprinting the impacts of global change on tropical forests. *Philosophical Transactions of the Royal Society B: Biological Sciences*, *359*, 437–462. https://doi.org/10.1098/rstb.2003.1432

Lewis, S. L., Sonke, B., Sunderland, T., Begne, S. K., Lopez-Gonzalez, G., van der Heijden, G. M. F., … Zemagho, L. (2013). Above-ground biomass and structure of 260 African tropical forests. *Philosophical Transactions of the Royal Society B: Biological Sciences*, *368*, 20120295–20120295. https://doi.org/10.1098/rstb.2012.0295

Liu, J., Bowman, K. W., Schimel, D. S., Parazoo, N. C., Jiang, Z., Lee, M., … Eldering, A. (2017). Contrasting carbon cycle responses of the tropical continents to the 2015–2016 El Niño. *Science*, *358*, eaam5690. https://doi.org/10.1126/science.aam5690

Lloyd, J., & Farquhar, G. D. (2008). Effects of rising temperatures and $[CO_2]$ on the physiology of tropical forest trees. *Philosophical Transactions of the Royal Society B: Biological Sciences*, *363*, 1811–1817. https://doi.org/10.1098/rstb.2007.0032

Loader, C. (1999). *Local regression and likelihood*. New York, NY: Springer Science & Business Media.

Magnabosco Marra, D., Trumbore, S. E., Higuchi, N., Ribeiro, G. H. P. M., Negrón-Juárez, R. I., Holzwarth, F., … Wirth, C. (2018). Windthrows control biomass patterns and functional composition of Amazon forests. *Global Change Biology*, *24*, 5867–5881. https://doi.org/10.1111/gcb.14457

Malhi, Y., & Wright, J. (2004). Spatial patterns and recent trends in the climate of tropical rainforest regions. *Philosophical Transactions of the Royal Society of London. Series B: Biological Sciences*, *359*, 311–329. https://doi.org/10.1098/rstb.2003.1433

Marengo, J. A., Tomasella, J., Alves, L. M., Soares, W. R., & Rodriguez, D. A. (2011). The drought of 2010 in the context of historical droughts in the Amazon region. *Geophysical Research Letters*, *38*. https://doi.org/10.1029/2011GL047436

Marvin, D. C., Asner, G. P., Knapp, D. E., Anderson, C. B., Martin, R. E., Sinca, F., & Tupayachi, R. (2014). Amazonian landscapes and the bias in field studies of forest structure and biomass. *Proceedings of the National Academy of Sciences of the United States of America*, *111*, E5224–E5232. https://doi.org/10.1073/pnas.1412999111

Mayle, F. E., Burbridge, R., & Killeen, T. J. (2000). Millennial-scale dynamics of southern Amazonian Rain Forests. *Science*, *290*, 2291–2294. https://doi.org/10.1126/science.290.5500.2291

McDowell, N., Allen, C. D., Anderson-Teixeira, K., Brando, P., Brienen, R., Chambers, J., … Xu, X. (2018). Drivers and mechanisms of tree mortality in moist tropical forests. *New Phytologist*, *219*, 851–869. https://doi.org/10.1111/nph.15027

McDowell, N., Pockman, W. T., Allen, C. D., Breshears, D. D., Cobb, N., Kolb, T., … Yepez, E. A. (2008). Mechanisms of plant survival and mortality during drought: Why do some plants survive while others succumb to drought? *New Phytologist*, *178*, 719–739. https://doi.org/10.1111/j.1469-8137.2008.02436.x

McMichael, C. N. H., Matthews-Bird, F., Farfan-Rios, W., & Feeley, K. J. (2017). Ancient human disturbances may be skewing our understanding of Amazonian forests. *Proceedings of the National Academy of Sciences of the United States of America*, *114*, 522–527. https://doi.org/10.1073/pnas.1614577114

Meakem, V., Tepley, A. J., Gonzalez-Akre, E. B., Herrmann, V., Muller-Landau, H. C., Wright, S. J., … Anderson-Teixeira, K. J. (2017). Role of tree size in moist tropical forest carbon cycling and water deficit responses. *New Phytologist*, *219*, 947–958. https://doi.org/10.1111/nph.14633

Muller-Landau, H. C. (2009). Carbon cycle: Sink in the African jungle. *Nature*, *457*, 969–970. https://doi.org/10.1038/457969a

Muller-Landau, H. C., Detto, M., Chisholm, R. A., Hubbell, S. P., & Condit, R. (2014). Detecting and projecting changes in forest biomass from plot data. In D. A. Coomes, D. F. R. P. Burslem, & W. D. Simonson (Eds.), *Forests and global change*, *ecological review* (pp. 381–416). Cambridge, UK: Cambridge University Press.

Oslisly, R., White, L., Bentaleb, I., Favier, C., Fontugne, M., Gillet, J.-F., & Sebag, D. (2013). Climatic and cultural changes in the west Congo Basin forests over the past 5000 years. *Philosophical Transactions of the Royal Society B: Biological Sciences*, *368*, 20120304. https://doi.org/10.1098/rstb.2012.0304

Ouédraogo, D.-Y., Mortier, F., Gourlet-Fleury, S., Freycon, V., & Picard, N. (2013). Slow-growing species cope best with drought: Evidence from long-term measurements in a tropical semi-deciduous moist forest of Central Africa. *Journal of Ecology*, *101*, 1459–1470. https://doi.org/10.1111/1365-2745.12165

Palace, M. W., McMichael, C. N. H., Braswell, B. H., Hagen, S. C., Bush, M. B., Neves, E., … Frolking, S. (2017). Ancient Amazonian populations left lasting impacts on forest structure. *Ecosphere*, *8*, e02035. https://doi.org/10.1002/ecs2.2035

Paton, S. (2018). *2017 Meteorological and hydrological summary for Barro Colorado Island*. Balboa, Panama: Smithsonian Tropical Research Institute.

Phillips, O. L., Aragao, L. E. O. C., Lewis, S. L., Fisher, J. B., Lloyd, J., Lopez-Gonzalez, G., … Torres-Lezama, A. (2009). Drought sensitivity of the Amazon Rainforest. *Science*, *323*, 1344–1347. https://doi.org/10.1126/science.1164033

Phillips, O. L., & Lewis, S. L. (2014). Recent changes in tropical forest biomass and dynamics. In D. A. Coomes, D. F. R. P. Burslem, & W. D. Simonson (Eds.), *Forests and global change*, *ecological review* (pp. 77–108). Cambridge, UK: Cambridge University Press.

Phillips, O. L., Malhi, Y., Higuchi, N., Laurance, W., Nunez, P. V., Vasquez, R. M., … Grace, J. (1998). Changes in the carbon balance of tropical forest: Evidence from long-term plots. *Science*, *282*, 439–442. https://doi.org/10.1126/science.282.5388.439

Phillips, O. L., van der Heijden, G., Lewis, S. L., López-González, G., Aragão, L. E. O. C., Lloyd, J., … Vilanova, E. (2010). Drought–mortality relationships for tropical forests. *New Phytologist*, *187*, 631–646. https://doi.org/10.1111/j.1469-8137.2010.03359.x

Poorter, L., Bongers, F., Aide, T. M., Almeyda Zambrano, A. M., Balvanera, P., Becknell, J. M., … Rozendaal, D. M. A. (2016). Biomass resilience of

Neotropical secondary forests. *Nature*, *530*(7589), 211–214. https://doi.org/10.1038/nature16512

Qie, L., Lewis, S. L., Sullivan, M. J. P., Lopez-Gonzalez, G., Pickavance, G. C., Sunderland, T., … Phillips, O. L. (2017). Long-term carbon sink in Borneo's forests halted by drought and vulnerable to edge effects. *Nature Communications*, *8*(1), 1966. https://doi.org/10.1038/s41467-017-01997-0

Rödig, E., Cuntz, M., Rammig, A., Fischer, R., Taubert, F., & Huth, A. (2018). The importance of forest structure for carbon flux estimates in the Amazon rainforest. *Environmental Research Letters*, *13*, 054013. https://doi.org/10.1088/1748-9326/aabc61

Ropelewski, C. F., & Halpert, M. S. (1987). Global and regional scale precipitation patterns associated with the El Niño/Southern Oscillation. *Monthly Weather Review*, *115*, 1606–1626. https://doi.org/10.1175/1520-0493(1987)115<1606:GARSPP>2.0.CO;2

Rowland, L., Lobo-do-Vale, R. L., Christoffersen, B. O., Melém, E. A., Kruijt, B., Vasconcelos, S. S., … Meir, P. (2015). After more than a decade of soil moisture deficit, tropical rainforest trees maintain photosynthetic capacity, despite increased leaf respiration. *Global Change Biology*, *21*, 4662–4672. https://doi.org/10.1111/gcb.13035

Rowland, L., Malhi, Y., Silva-Espejo, J. E., Farfán-Amézquita, F., Halladay, K., Doughty, C. E., … Phillips, O. L. (2014). The sensitivity of wood production to seasonal and interannual variations in climate in a lowland Amazonian rainforest. *Oecologia*, *174*, 295–306. https://doi.org/10.1007/s00442-013-2766-9

Rutishauser, E., Wagner, F., Herault, B., Nicolini, E. A., & Blanc, L. (2010). Contrasting above-ground biomass balance in a Neotropical rain forest. *Journal of Vegetation Science*, *21*, 672–682. https://doi.org/10.1111/j.1654-1103.2010.01175.x

Saatchi, S. S., Harris, N. L., Brown, S., Lefsky, M., Mitchard, E. T. A., Salas, W., … Morel, A. (2011). Benchmark map of forest carbon stocks in tropical regions across three continents. *Proceedings of the National Academy of Sciences of the United States of America*, *108*, 9899–9904. https://doi.org/10.1073/pnas.1019576108

Saatchi, S., Mascaro, J., Xu, L., Keller, M., Yang, Y., Duffy, P., … Schimel, D. (2015). Seeing the forest beyond the trees. *Global Ecology and Biogeography*, *24*, 606–610. https://doi.org/10.1111/geb.12256

Schippers, P., Sterck, F., Vlam, M., & Zuidema, P. A. (2015). Tree growth variation in the tropical forest: Understanding effects of temperature, rainfall and CO_2. *Global Change Biology*, *21*, 2749–2761. https://doi.org/10.1111/gcb.12877

Slot, M., & Winter, K. (2017). In situ temperature relationships of biochemical and stomatal controls of photosynthesis in four lowland tropical tree species. *Plant, Cell and Environment*, *40*, 3055–3068. https://doi.org/10.1111/pce.13071

Taylor, P. G., Cleveland, C. C., Wieder, W. R., Sullivan, B. W., Doughty, C. E., Dobrowski, S. Z., & Townsend, A. R. (2017). Temperature and rainfall interact to control carbon cycling in tropical forests. *Ecology Letters*, *20*(6), 779–788. https://doi.org/10.1111/ele.12765

Trugman, A. T., Detto, M., Bartlett, M. K., Medvigy, D., Anderegg, W. R. L., Schwalm, C., … Pacala, S. W. (2018). Tree carbon allocation explains forest drought-kill and recovery patterns. *Ecology Letters*, *21*, 1552–1560. https://doi.org/10.1111/ele.13136

Van Bael, S. A., Aiello, A., Valderrama, A., Medianero, E., Samaniego, M., & Wright, S. J. (2004). General herbivore outbreak following an El Nino-related drought in a lowland Panamanian forest. *Journal of Tropical Ecology*, *20*, 625–633. https://doi.org/10.1017/s0266467404001725

van der Sande, M. T., Arets, E. J. M. M., Peña-Claros, M., de Avila, A. L., Roopsind, A., Mazzei, L., … Poorter, L. (2016). Old-growth Neotropical forests are shifting in species and trait composition. *Ecological Monographs*, *86*, 228–243. https://doi.org/10.1890/15-1815.1

Wagner, F. H., Hérault, B., Bonal, D., Stahl, C., Anderson, L. O., Baker, T. R., … Aragão, L. E. O. C. (2016). Climate seasonality limits leaf carbon assimilation and wood productivity in tropical forests. *Biogeosciences*, *13*, 2537–2562. https://doi.org/10.5194/bg-13-2537-2016

Wagner, F., Rutishauser, E., Blanc, L., & Herault, B. (2010). Assessing effects of plot size and census interval on estimates of tropical forest structure and dynamics. *Biotropica*, *42*, 664–671. https://doi.org/10.1111/j.1744-7429.2010.00644.x

Watt, A. S. (1947). Pattern and process in plant ecology. *Journal of Ecology*, *35*, 1–22.

Whitmore, T. C. (1989). Canopy gaps and the two major groups of forest trees. *Ecology*, *70*, 536–538. https://doi.org/10.2307/1940195

Wright, S. J. (2006). Response to Lewis et al.: The uncertain response of tropical forests to global change. *Trends in Ecology & Evolution*, *21*(4), 174–175. https://doi.org/10.1016/j.tree.2006.02.003

Wright, S. J. (2010). The future of tropical forests. *Annals of the New York Academy of Sciences*, *1195*, 1–27. https://doi.org/10.1111/j.1749-6632..2010.05455.x

Wright, S. J. (2013). The carbon sink in intact tropical forests. *Global Change Biology*, *19*(2), 337–339. https://doi.org/10.1111/gcb.12052

Wright, S. J., & Calderón, O. (2006). Seasonal, El Nino and longer term changes in flower and seed production in a moist tropical forest. *Ecology Letters*, *9*, 35–44. https://doi.org/10.1111/j.1461-0248.2005.00851.x

Wright, S. J., Kitajima, K., Kraft, N. J. B., Reich, P. B., Wright, I. J., Bunker, D. E., … Zanne, A. E. (2010). Functional traits and the growth–mortality trade-off in tropical trees. *Ecology*, *91*, 3664–3674. https://doi.org/10.1890/09-2335.1

Wright, S. J., Yavitt, J. B., Wurzburger, N., Turner, B. L., Tanner, E. V. J., Sayer, E. J., … Corre, M. D. (2011). Potassium, phosphorus, or nitrogen limit root allocation, tree growth, or litter production in a lowland tropical forest. *Ecology*, *92*, 1616–1625. https://doi.org/10.1890/10-1558.1

Yanoviak, S. P., Gora, E. M., Burchfield, J. M., Bitzer, P. M., & Detto, M. (2017). Quantification and identification of lightning damage in tropical forests. *Ecology and Evolution*, *7*, 5111–5122. https://doi.org/10.1002/ece3.3095

SUPPORTING INFORMATION

Additional supporting information may be found online in the Supporting Information section at the end of the article.

How to cite this article: Rutishauser E, Wright SJ, Condit R, Hubbell SP, Davies SJ, Muller-Landau HC. Testing for changes in biomass dynamics in large-scale forest datasets. *Glob Change Biol*. 2019;00:1–15. https://doi.org/10.1111/gcb.14833

Supplemental information

"Testing for changes in biomass dynamics in large-scale forest datasets"

Ervan Rutishauser, S. Joseph Wright, Richard Condit, Stephen P. Hubbell, Stuart J. Davies, and Helene C. Muller-Landau

Global Change Biology

Contents

A. Details of census methods

In the first two censuses (1982 and 1985), diameters of stems with DBH < 55 mm were rounded down to the nearest 5 mm (10, 15, 20, 25, 30, 35, 40, 45, 50). To remove associated biases in tree growth measurements in the 1985-1990 interval, we substituted DBH values of trees DBH < 55 mm in 1985 and 1990, with median DBH values measured in 1990 for each rounding class. That is, trees recorded as 10 mm in 1985 or 10-14 mm in 1990 were analysed as having a diameter of 12 mm, and so forth. The medians by 5 mm diameter class were 12, 17, 22, 27, 32, 37, 42, 47 and 52 mm. This treatment affected 1990 data only for analysis of 1985-1990 growth, not for analysis of 1990-95 growth.

Before 2010, stems of multi-stemmed individuals were not individually tagged, making it impossible to unambiguously identify cases in which one stem died and another of similar size resprouted. We thus summed biomass over stems at the tree level, and treated most changes in total biomass of an individual tree as positive or negative growth (productivity). However, there were two types of cases in which we could confidently identify biomass losses and classify them as such. The first concerned cases in which main stems > 10 cm DBH died and resprouted, which we treated as a combination of biomass loss (mortality) fluxes of the stem that died and recruitment (productivity) fluxes of the resprouts. We classified cases as main stem deaths followed by resprouting if the DBH of the main stem was > 10 cm in one census, and at least 20% smaller in the next census (N=716). The second concerned cases in which multiple-stemmed individuals experienced a loss in biomass accompanied by a decrease in stem number; in these cases, the loss in biomass was counted entirely as mortality, with zero growth (productivity). We applied the same methods across all censuses, thereby avoiding a bias over time due to changing methods.

Table S1 Species-specific median DBH (cm) for palm species that do not grow in diameter. In these species, all changes in DBH over censuses are treated as measurement errors. To avoid associated errors in biomass fluxes, we assigned the species-specific median DBH to every stem at every census in these species.

Name	Median DBH (cm)	Name	Median DBH (cm)
Astrocaryum standleyanum	133	*Bactris major*	37
Attalea rostrata	376	*Chamaedorea tepejilote*	30
Bactris barronis	40	*Elaeis oleifera*	382
Bactris coloniata	35	*Geonoma interrupta*	35
Bactris coloradonis	40	*Oenocarpus mapora*	85

Table S2 Number of 10x10m quadrats meeting criteria for removal from the analyses by census interval and reason for removal. The reasons for removal are (i) presence of large (DBH>50 cm) strangler figs (*Ficus costaricana, F. obtusifolia, F. popenoei or F. trigonata*), (ii) at least one tree with change in POM > 10 cm, and (iii) at least one tree with an extreme productivity value (defined below). For consistency, quadrats containing at least one large strangler fig in any census were discarded from all analyses (N=13). Note that some quadrats are affected by more than one reason of removal and the total of quadrat excluded does not correspond to the sum of reasons of removal.

Census year	1990	1995	2000	2005	2010	2015
large strangler figs	4	5	7	5	5	4
change of POM > 10 cm	1010	701	1271	1104	1068	372
extreme productivity	20	12	18	10	10	15
Total quadrat excluded	1028	714	1288	1114	1077	389
(Total quadrat included	3641	3955	3381	3555	3592	4280)

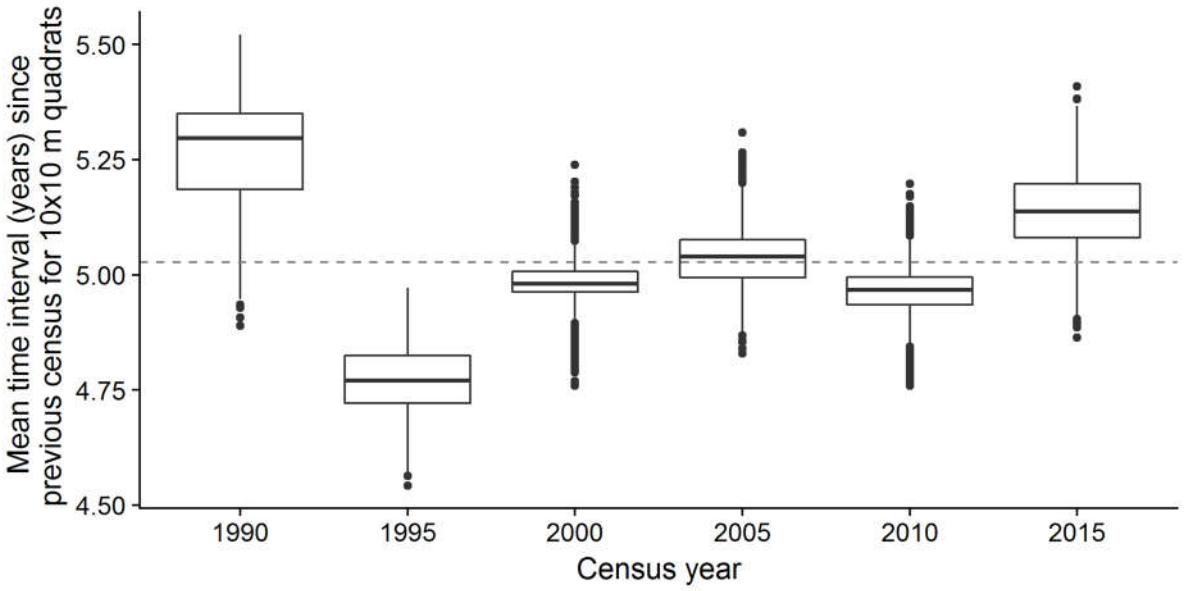

Figure S1 Variation in census interval length among census intervals and among 10x10 m quadrats. Biomass fluxes calculated with the simple formulas used here are increasingly biased downwards at longer census intervals (Kohyama et al. 2019). This would confound comparisons across census intervals if census interval lengths varied, but we show here that there is little variation among census intervals. Quadrat-level census intervals were computed as the means over each individual present in the quadrat in one or both censuses. For recruits, the initial date is the mean date at which other stems in the quadrat were censused. The boxes show medians, 25th, and 75th percentiles, the bars extend to -/+ 1.5 x IQR below the first and third quartiles respectively, and additional outlying quadrats are shown individually. The analysis covers 48.8 ha of the BCI plot, excluding the 1.2 ha of swamp that were discarded from all analyses.

Table S3 Mean biomass increment per tree (in kg.yr-1), sample size of trees used to calculate the mean (N), and the number of trees whose growth rates were substituted with these mean values (NSub) for the analysis of whole-plot fluxes (Figure 7), by initial DBH class and census interval. Growth rates were substituted for trees that had a change in the point of measurement, or that had an unreasonably large change in dbh such that biomass growth > $t * \overline{P}$ (or < $-t * \overline{P}$), where t is a threshold (0.2 in our study) and $\overline{P}$ is the mean productivity per hectare for all census intervals combined. The analysis covers 46.9 ha of the BCI plot, excluding 1.2 ha of swamp and 1.9 ha of young forest. Most substitutions were related to changes in POM (Table S2). Note that the analyses of quadrat-level fluxes (Figures 3, 4, 5) excluded quadrats with trees affected by any of these problems, and thus are not affected by these substitutions.

Census interval	< 5 cm			5-9.9 cm			10-19.9 cm			20-39.9 cm			40-59.9 cm			> 60 cm		
	mean	N	N_{sub}	mean	N	N_{sub}	mean	N	N_{sub}	mean	N	N_{sub}	mean	N	N_{sub}	mean	N	N_{sub}
1985-1990	0.13	144,282	3	1.16	21,402	51	4.57	9,414	23	19.22	3,920	380	70.63	803	408	146.90	350	392
1990-1995	0.09	147,457	1	0.88	24,347	67	4.14	9,953	72	16.98	4,114	321	44.19	1,031	211	87.74	599	199
1995-2000	0.09	137,564	277	0.77	23,867	290	3.98	9,794	365	17.43	4,147	357	44.58	1,031	215	92.81	637	168
2000-2005	0.09	129,288	140	0.83	23,402	206	3.86	9,559	295	16.35	4,094	336	45.31	973	260	77.62	581	235
2005-2010	0.12	124,829	206	0.90	23,061	234	3.94	9,451	266	15.96	3,824	479	46.31	1,056	166	101.28	667	149
2010-2015	0.12	123,822	90	1.00	23,485	129	4.29	9,476	87	17.31	4,085	87	48.63	1,169	22	109.56	748	48

B. Detailed results on analyses of biomass fluxes

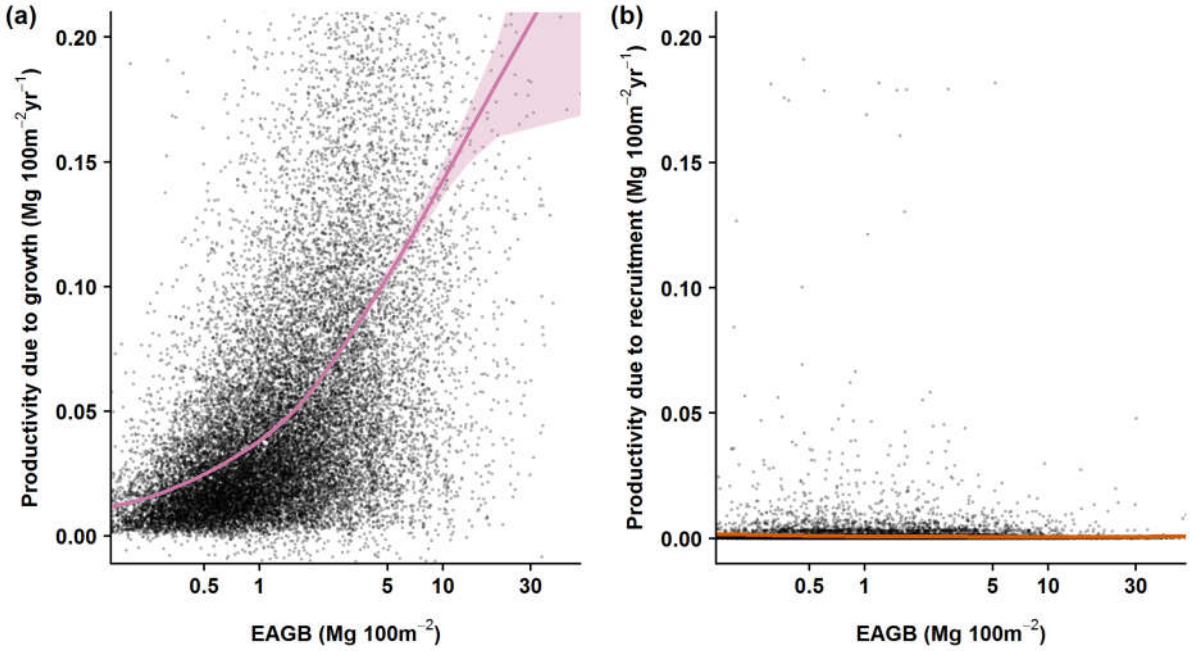

Figure S2 Quadrat-level annual EAGB productivity due to growth of surviving trees (a) and recruitment of new trees (b) (Mg.100m^{-2}.yr^{-1}) as a function of initial quadrat biomass for each 5-year census interval, for 10x10 m quadrats (points) with local polynomial regression lines for individual census intervals (colored solid lines) and for all census intervals combined (black dashed lines). For each census interval, analyses excluded quadrats containing one or more trees that (a) are large strangler figs, (b) have a change in POM, or (c) have an obvious major measurement error during the census interval (see methods for details; N is the number of quadrats included for each census interval). Regression lines are shown only for the ranges of the 2nd to 98th percentile values of the respective datasets (avoiding the distribution extremes where uncertainty increases). The range of data shown here is truncated for illustration purposes, but all points (including those outside the graphed range) were included in analyses.

Table S4 Time series of hypothetical whole-plot productivity, loss, and net change under three scenarios: (a) census-interval specific fluxes & mean EAGBi PDFs, (b) mean fluxes & census-interval specific EAGBi PDFs and (c) census-interval specific fluxes & EAGBi PDFs. Here "fluxes" refers to functions for quadrat biomass flux as a function of initial quadrat biomass, "EAGBi PDF" refers to the probability distribution of initial biomass density over quadrats, and means are based on combining data for all census intervals. Note that the analysis covers 46.9 ha of the BCI plot, excluding 1.2 ha of swamp and 1.9 ha of young forest.

Scenario	Census interval	Productivity	EAGB loss	Net change
a	1985-1990	0.070 (0.064-0.075)	0.058 (0.049-0.070)	0.012 (0.005-0.014)
a	1990-1995	0.057 (0.053-0.060)	0.054 (0.045-0.064)	0.003 (-0.004-0.009)
a	1995-2000	0.059 (0.057-0.061)	0.061 (0.051-0.069)	-0.002 (-0.008-0.006)
a	2000-2005	0.054 (0.051-0.056)	0.062 (0.055-0.071)	-0.008 (-0.015--0.003)
a	2005-2010	0.059 (0.056-0.062)	0.062 (0.052-0.071)	-0.003 (-0.009-0.004)
a	2010-2015	0.064 (0.061-0.066)	0.063 (0.057-0.070)	0.000 (-0.005-0.004)
b	1985-1990	0.060 (0.059-0.061)	0.059 (0.055-0.062)	0.001 (-0.001-0.003)
b	1990-1995	0.061 (0.060-0.062)	0.061 (0.057-0.065)	0.000 (-0.003-0.003)
b	1995-2000	0.061 (0.060-0.062)	0.061 (0.058-0.065)	0.000 (-0.002-0.002)
b	2000-2005	0.061 (0.060-0.062)	0.061 (0.057-0.065)	0.000 (-0.002-0.003)
b	2005-2010	0.061 (0.060-0.062)	0.060 (0.057-0.064)	0.001 (-0.002-0.003)
b	2010-2015	0.060 (0.059-0.062)	0.060 (0.057-0.064)	0.001 (-0.002-0.002)
c	1985-1990	0.069 (0.062-0.075)	0.057 (0.049-0.067)	0.012 (0.008-0.013)
c	1990-1995	0.057 (0.054-0.060)	0.055 (0.045-0.066)	0.002 (-0.006-0.009)
c	1995-2000	0.060 (0.057-0.062)	0.062 (0.054-0.072)	-0.002 (-0.009-0.003)
c	2000-2005	0.054 (0.052-0.057)	0.063 (0.055-0.071)	-0.008 (-0.015--0.003)
c	2005-2010	0.059 (0.057-0.063)	0.062 (0.052-0.072)	-0.003 (-0.010-0.005)
c	2010-2015	0.064 (0.061-0.066)	0.063 (0.056-0.072)	0.000 (-0.006-0.005)

Table S5 Plot-level average (value) and 95% confidence intervals for quadratic mean diameter and density of trees with DBH ≥ 1, 10 and 60 cm by census (Figure 8). The density of large trees and mean diameter are not reported for 1982 due to inconsistencies in measurement methods (see Condit, 1998). Letters indicate significant differences within a given column. Note that the analysis covers 46.9 ha of the BCI plot, excluding 1.2 ha of swamp and 1.9 ha of young forest.

Census year	Quadratic mean diameter (cm)			Tree density DBH ≥ 1 cm (ha^{-1})			Tree density DBH ≥ 10 cm (ha^{-1})			Tree density DBH ≥ 60 cm (ha^{-1})		
	value	5%CI	95%CI	value	5%CI	95%CI	value	5%CI	95%CI	value	5%CI	95%CI
1982	-	-	-	47.21a	46.85	47.63	4.38a	4.32	4.43	-	-	-
1985	85.2a	84.0	86.5	48.68b	48.27	49.09	4.33a	4.28	4.38	0.16a	0.15	0.17
1990	85.9a	84.8	87.0	49.04b	48.64	49.43	4.45b	4.39	4.50	0.17a	0.16	0.18
1995	88.3b	87.2	89.5	46.05c	45.69	46.39	4.49b	4.42	4.54	0.17a	0.15	0.18
2000	91.4c	90.3	92.6	42.98d	42.62	43.31	4.42b	4.39	4.48	0.17a	0.16	0.19
2005	91.9c	90.5	93.1	41.82e	41.50	42.16	4.33a	4.27	4.38	0.17a	0.16	0.18
2010	91.9c	90.7	93.1	41.55e	41.21	41.89	4.31a	4.25	4.36	0.17a	0.16	0.18
2015	91.7c	90.4	93.0	41.66e	41.31	42.00	4.30a	4.25	4.36	0.17a	0.16	0.18

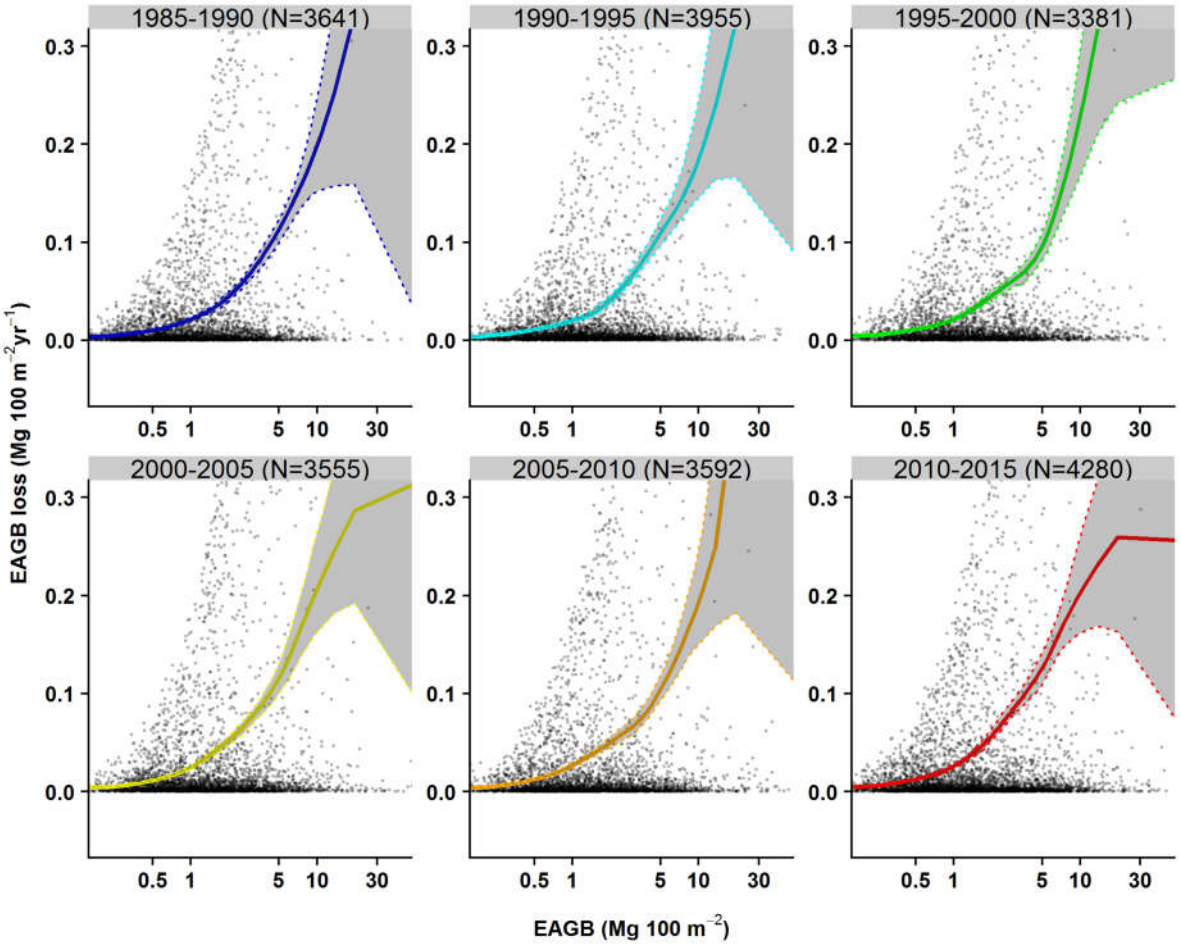

Figure S3 Quadrat-level annual EAGB mortality (Mg.100m^{-2}.yr^{-1}) as a function of initial quadrat biomass for each 5-year census interval, for 10x10 m quadrats (points) with local polynomial regression lines for individual census intervals (colored solid lines) and for all census intervals combined (black dashed lines). For each census interval, analyses excluded quadrats containing one or more trees that (a) are large strangler figs, (b) have a change in POM, or (c) have an obvious major measurement error during the census interval (see methods for details; N is the number of quadrats included for each census interval). Regression lines are shown only for the ranges of the 2nd to 98th percentile values of the respective datasets (avoiding the distribution extremes where uncertainty increases). The range of data shown here is truncated for illustration purposes, but all points (including those outside the graphed range) were included in analyses.

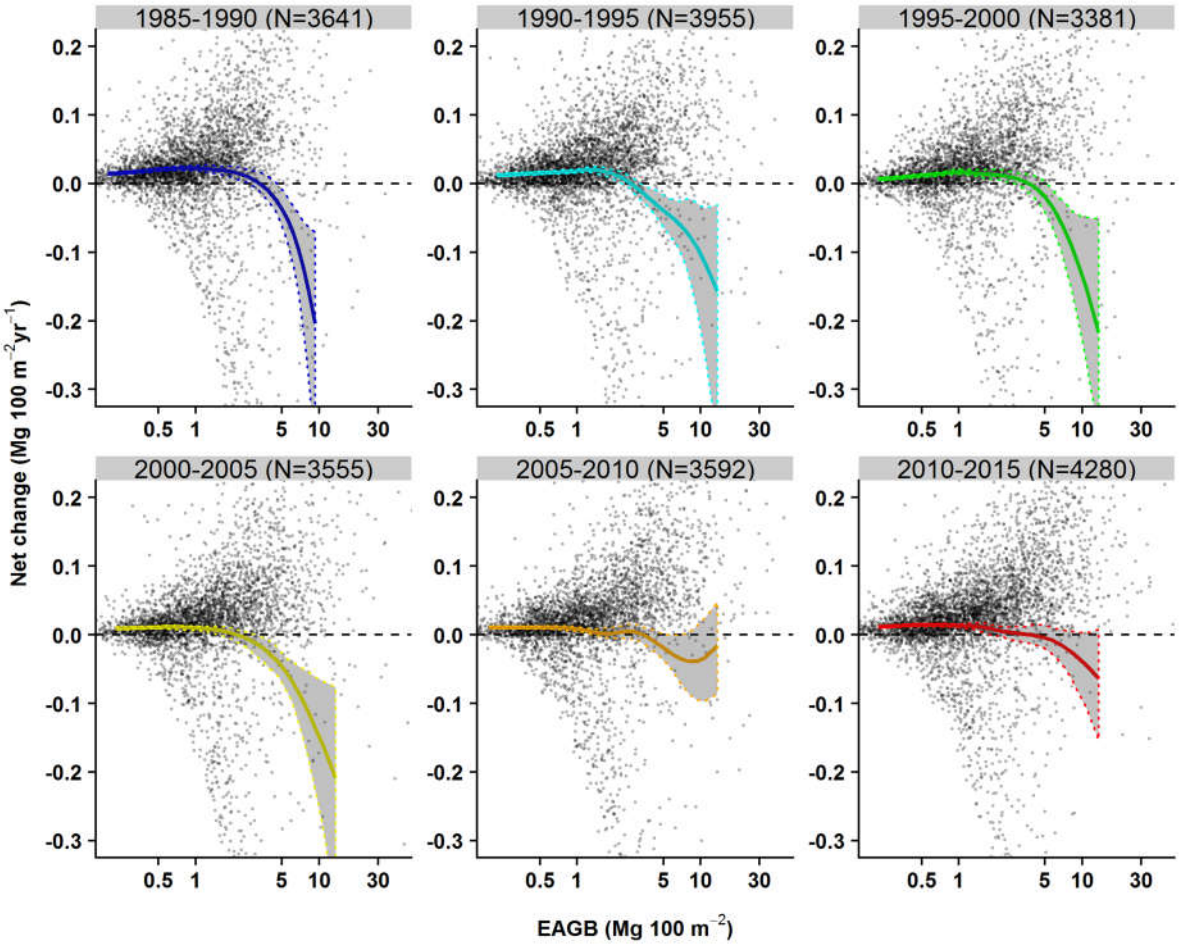

Figure S4 Quadrat-level annual EAGB net change (Mg.ha^{-1}.yr^{-1}) as a function of initial quadrat biomass for each 5-year census interval, for 10x10 m quadrats (points) with local polynomial regression lines for individual census intervals (colored solid lines) and for all census intervals combined (black dashed lines). Confidence envelopes (dotted lines) were computed from bootstrapping over quadrats. For each census interval, analyses excluded quadrats containing one or more trees that (a) are large strangler figs, (b) have a change in POM, or (c) have an obvious major measurement error during the census interval (see methods for details; N is the number of quadrats included for each census interval). Regression lines are shown only for the ranges of the 2nd to 98th percentile values of the respective datasets (avoiding the distribution extremes where uncertainty increases). The range of data shown here is truncated for illustration purposes, but all points (including those outside the graphed range) were included in analyses.

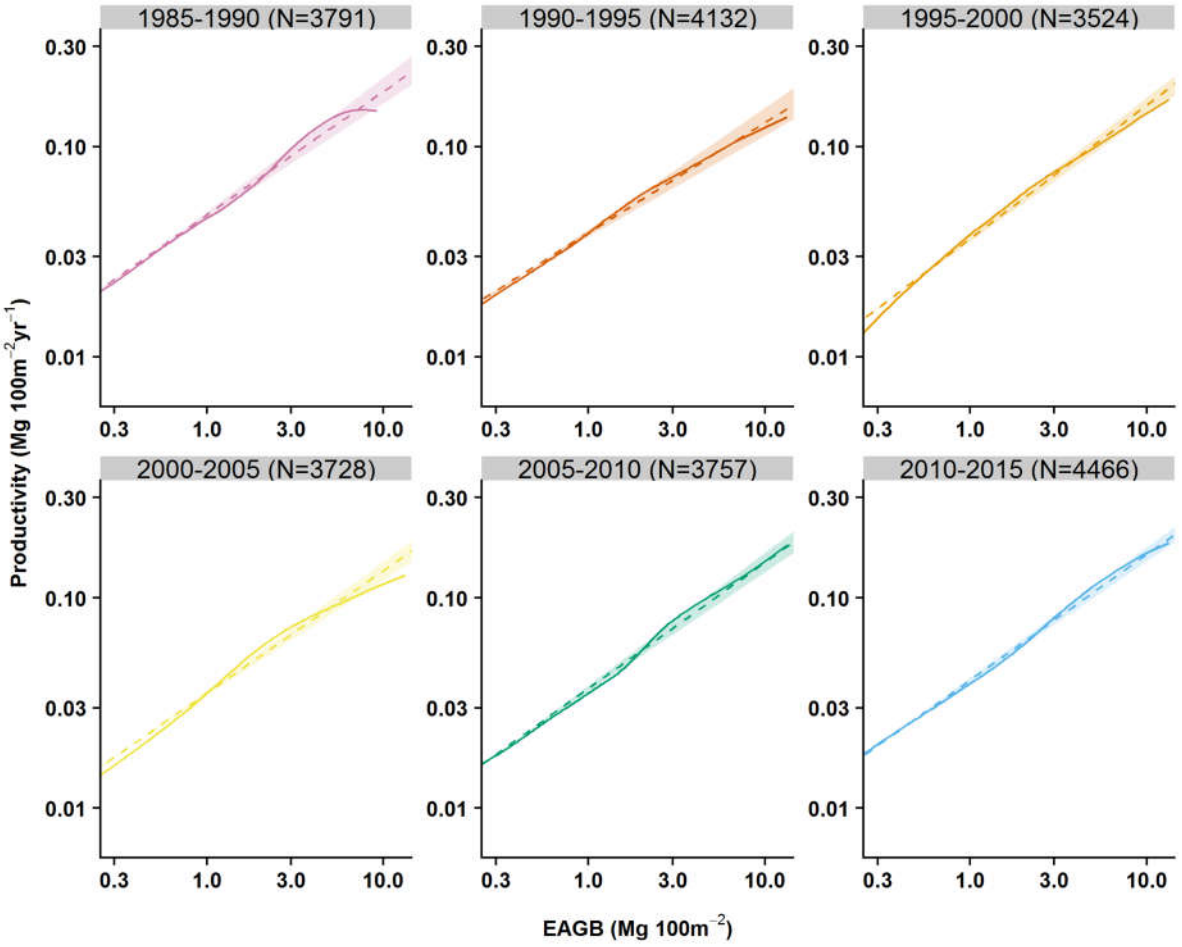

Figure S5 Comparisons of local polynomial regression lines (solid lines) and power function fits (dashed lines) for the relationships of quadrat-level mean annual EAGB productivity (Mg ha^{-1} yr^{-1}) to initial quadrat biomass for each 5-year census interval (panels). Confidence envelopes for the power function fits (shading) were computed from bootstrapping over quadrats. Note that both axes are log-scaled. For each census interval, analyses excluded quadrats with problematic EAGB measurements (see methods for details). N is the number of quadrats included for each census interval. Regression lines are shown only for the ranges of the 2nd to 98th percentile values of the respective datasets, thereby avoiding the distribution extremes where uncertainty increases.

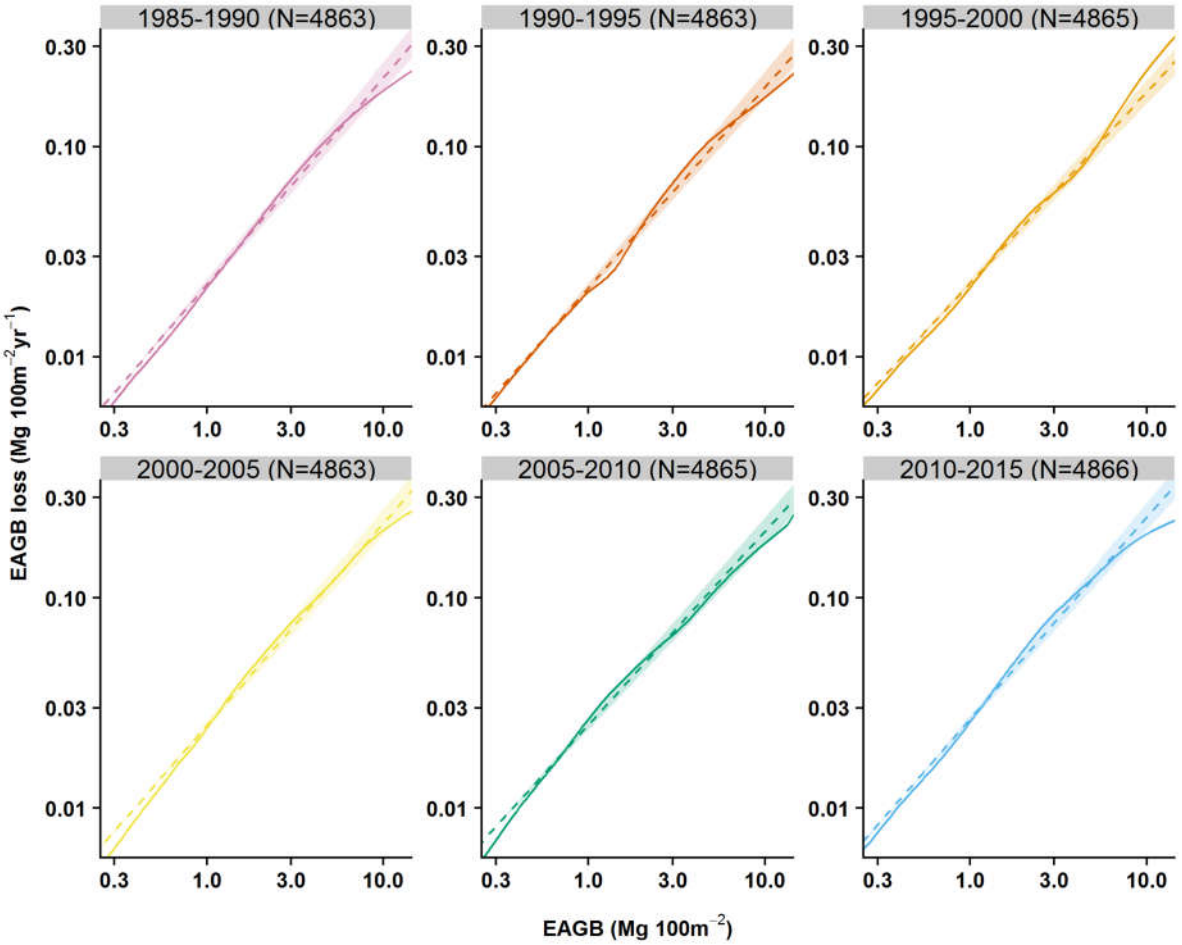

Figure S6 Comparisons of local polynomial regression lines (solid lines) and power function fits (dashed lines) for the relationships of quadrat-level mean annual EAGB loss (Mg ha^{-1} yr^{-1}) to initial quadrat biomass for each 5-year census interval (panels). Confidence envelopes for the power function fits (shading) were computed from bootstrapping over quadrats. Note that both axis are log-scaled. For each census interval, analyses excluded quadrats with problematic EAGB measurements (see methods for details). N is the number of quadrats included for each census interval. Regression lines are shown only for the ranges of the 2nd to 98th percentile values of the respective datasets thereby avoiding the distribution extremes where uncertainty increases.

Table S6 The estimated normalized intercepts (or coefficients, alpha) and slopes (or exponents, beta) of power functions fitted to quadrat-level productivity and mortality as a function of initial quadrat biomass for each census interval, as shown in figure 5.

Flux	Census interval	Normalized intercepts	Slopes
Productivity	1985-1990	0.587 (0.553-0.629)	5.422 (6.333-6.779)
Productivity	1990-1995	0.525 (0.492-0.568)	4.387 (4.964-5.320)
Productivity	1995-2000	0.635 (0.612-0.667)	4.223 (4.983-5.314)
Productivity	2000-2005	0.583 (0.552-0.619)	4.032 (4.692-4.970)
Productivity	2005-2010	0.600 (0.573-0.635)	4.257 (4.996-5.272)
Productivity	2010-2015	0.598 (0.575-0.625)	4.659 (5.483-5.707)
Mortality	1985-1990	0.955 (0.896-1.024)	2.649 (3.349-3.804)
Mortality	1990-1995	0.910 (0.858-0.950)	2.755 (3.497-3.872)
Mortality	1995-2000	0.962 (0.918-1.008)	3.083 (3.987-4.345)
Mortality	2000-2005	0.923 (0.877-0.965)	3.072 (3.904-4.333)
Mortality	2005-2010	0.961 (0.906-0.994)	3.298 (4.196-4.696)
Mortality	2010-2015	0.587 (0.553-0.629)	5.422 (6.333-6.779)

C. Sensitivity analyses

Here we evaluate the robustness of our results to different data filtering methods and quadrat sizes.

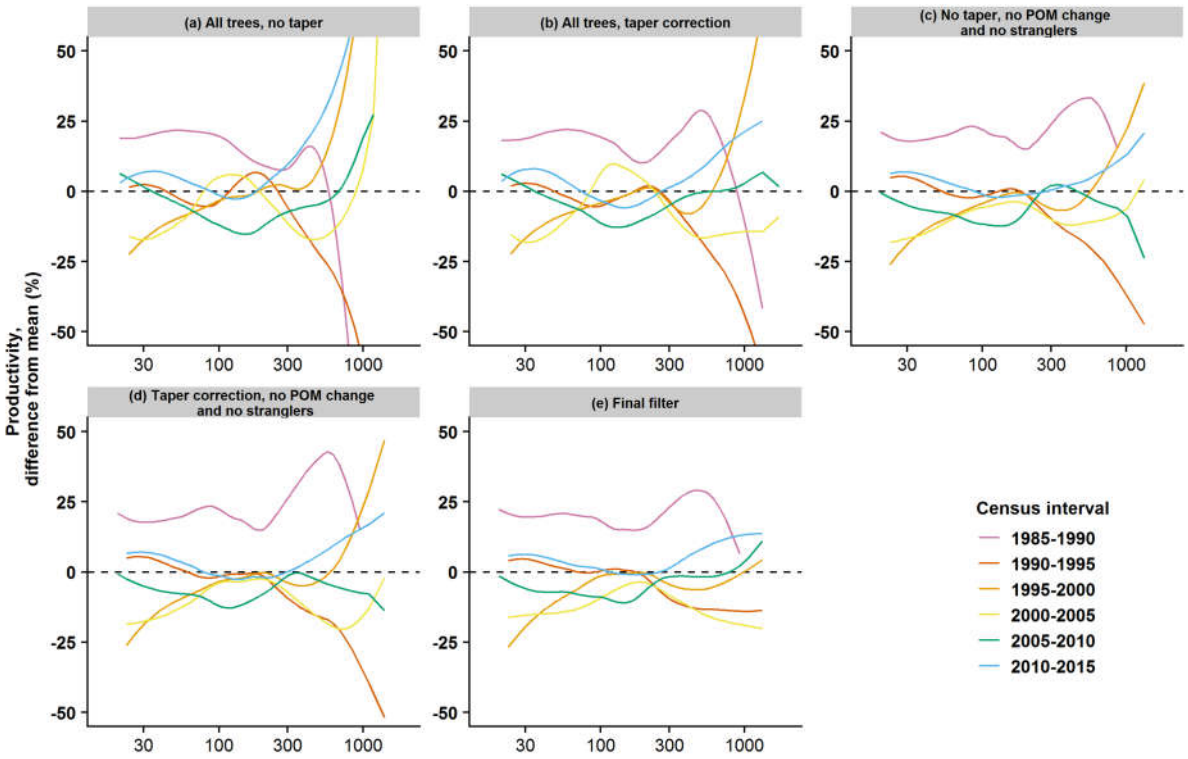

Figure S7 Effects of data filtering rules on variation among census intervals in patterns of productivity as a function of initial biomass for 10m quadrats. Alternative rule sets are: (a) all trees without taper correction, (b) all trees with taper correction, exclusion of quadrats with POM change and large strangler figs without (c) or with (d) taper correction, and (d) exclusion of quadrats with one or more trees with a highly suspicious and highly influential measurement error (i.e. productivity > 20% of mean productivity for 1 ha), large strangler figs and/or POM change. In all case, quadrats in swamps (1.2 ha) were discarded and POM changes were defined as a difference in POM greater than 10 cm.

A. Scale: 8.3 (500/60) m

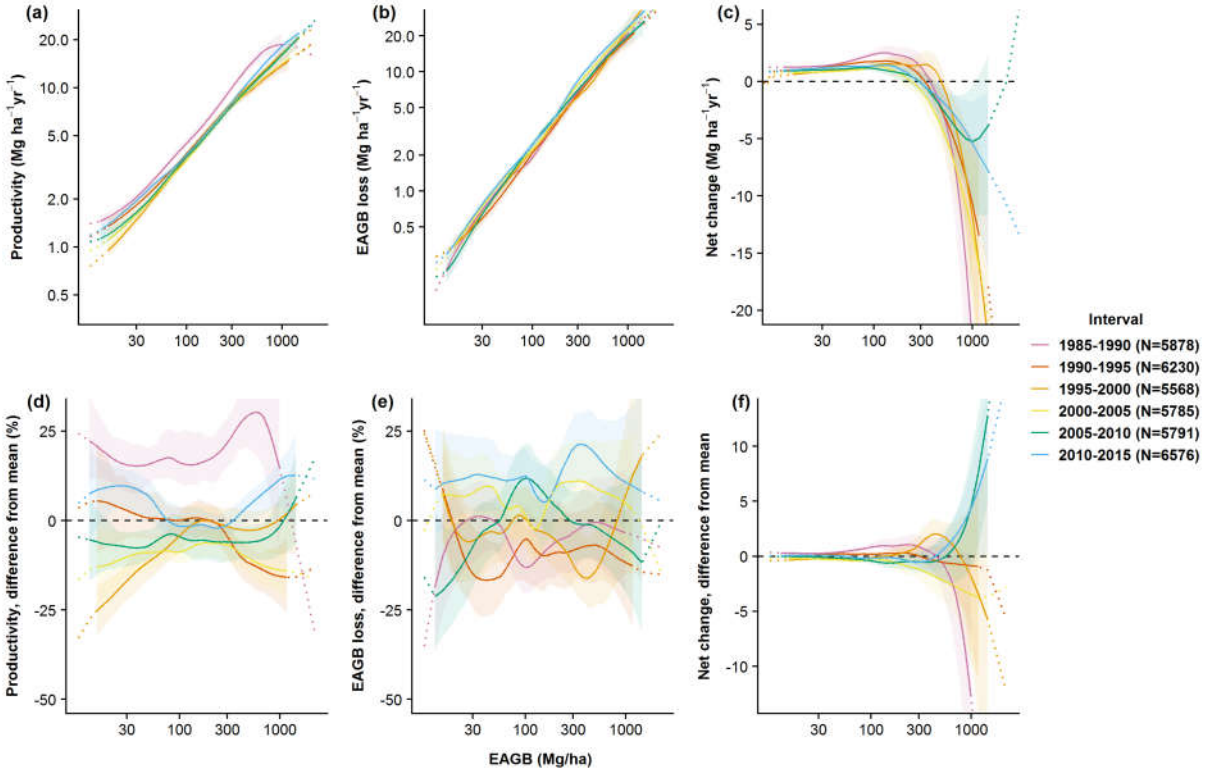

B. Scale: 12.5 m

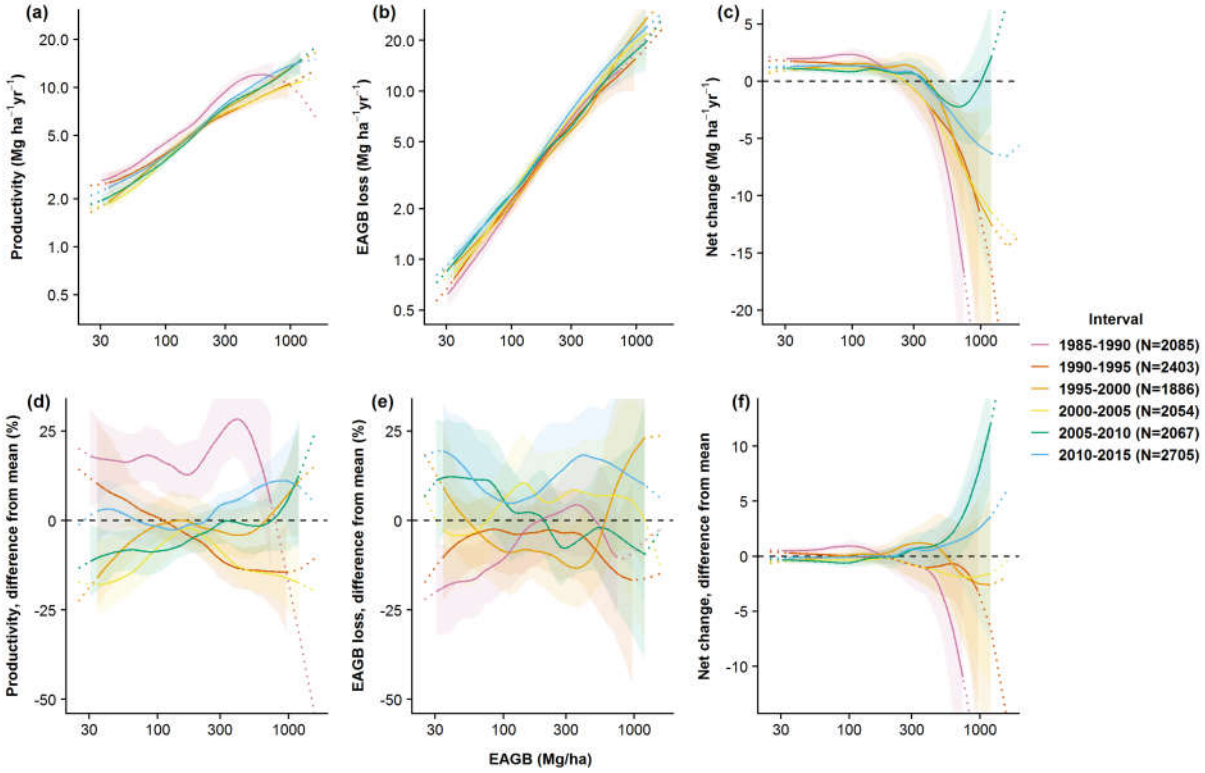

C. Scale: 15.15 m

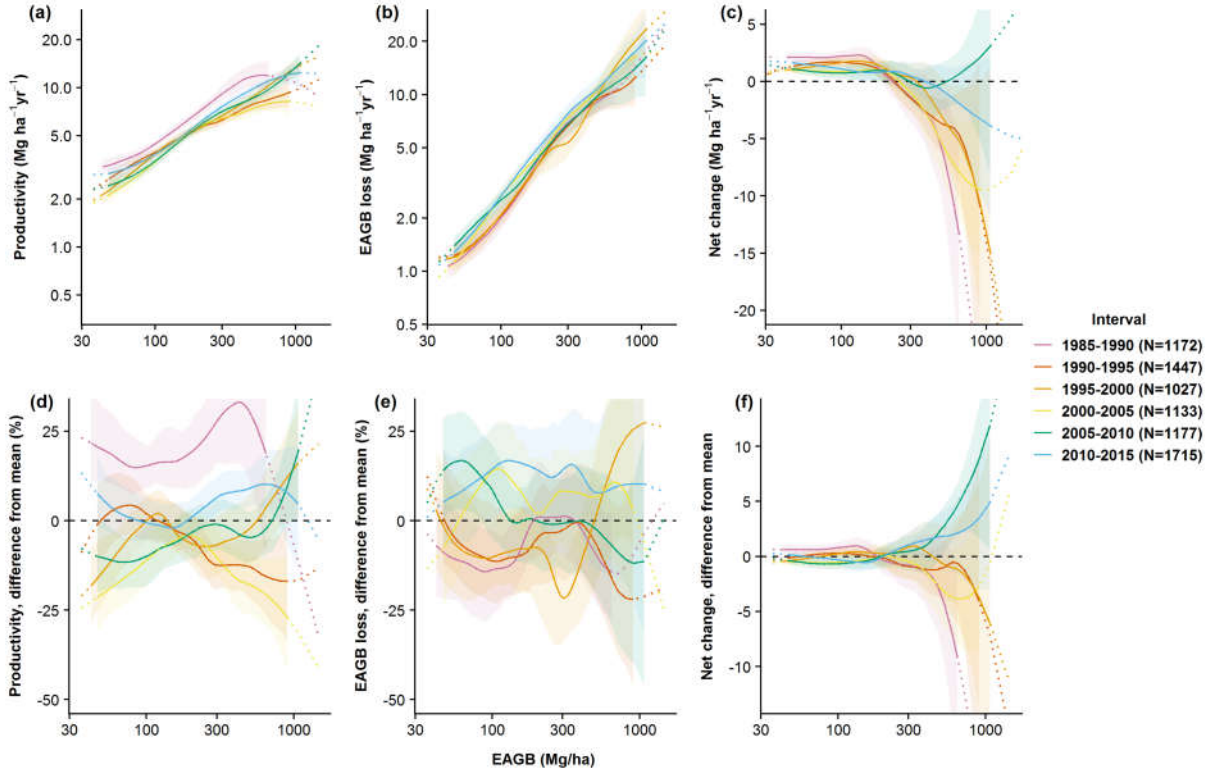

Figure S8 Comparison of qualitative patterns of quadrat biomass fluxes across different quadrat sizes, for 8.93, 12.5 and 15.15-m square quadrats (A, B, and C respectively). Variation among census intervals in EAGB productivity (a), loss (b) and net change (c) as a function of aboveground biomass (EAGB) at the initial census for 10-m quadrats, computed using local polynomial regression, together with the corresponding differences from the mean (per initial EAGB) across all census intervals (d,e,f). Note that productivity (a) and loss (c) are shown on log scales, whereas the net change (e) is on a linear scale. Analyses excluded quadrats containing large strangler figs, one or more trees with a change in POM, or obvious major measurement error during the census interval (see methods). Regression lines are displayed for values spanning the 2nd to 98th percentiles of the respective census interval (solid lines), and outside this range (dotted lines). Note that extreme values (dotted lines) have large uncertainty and for (f), difference are not expressed as percentage. Confidence envelops were computed by bootstrapping over quadrats. Number of quadrats included per census interval is given in the legend. Figures are given in Mg/ha to ease comparison among different quadrat sizes.

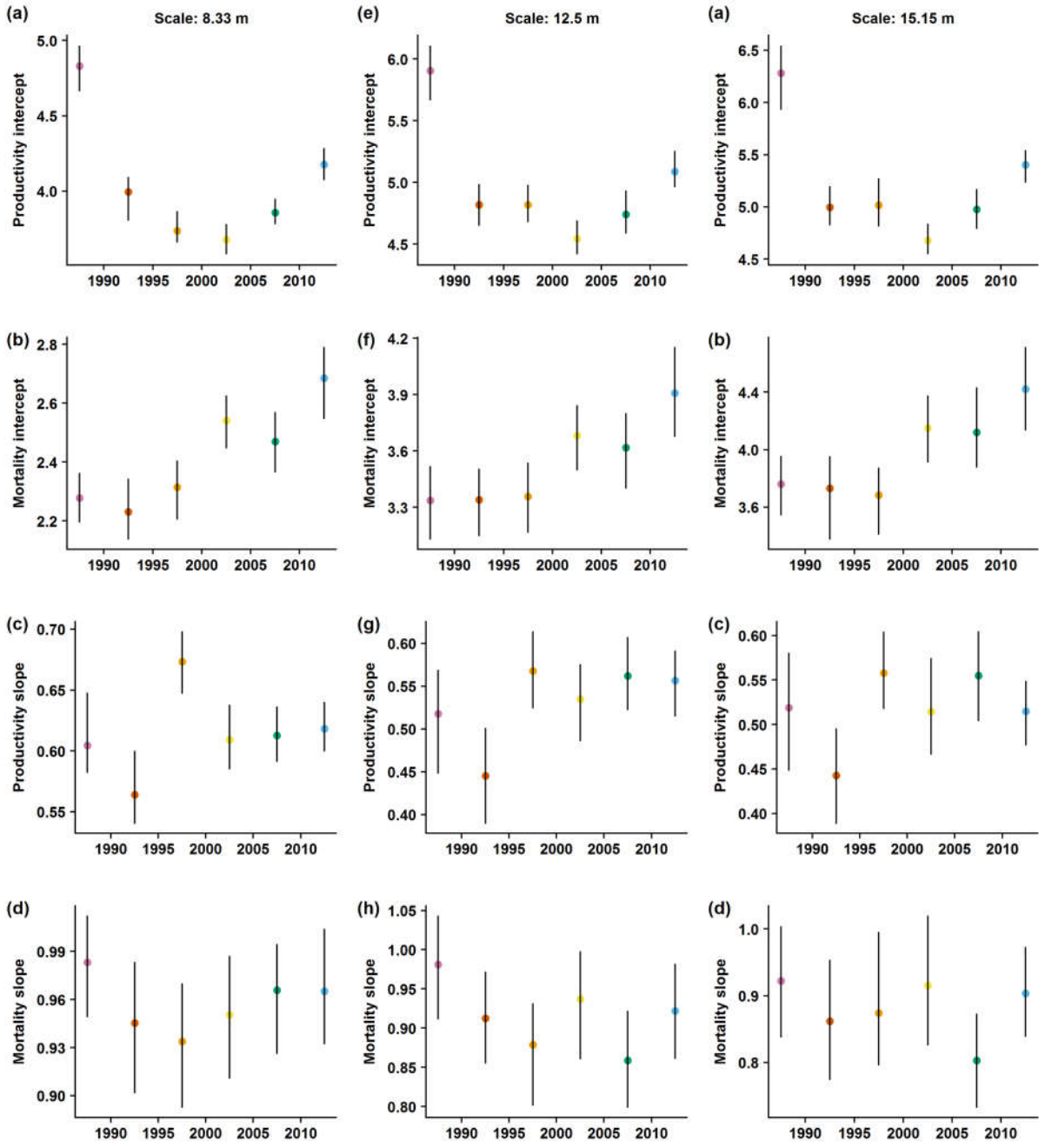

Figure S9 Intercept (a,b,e,f,I,j) and slope (c,d,g,h,k,l) of power function fits of quadrat-level productivity and mortality by census intervals, for quadrat sizes of 8.3, 12.5 and 15.15 m. The intercepts are normalized; they are the values at the midpoint EAGB value over all census intervals (125 Mg ha-1). Points are placed at the mid-points of the census intervals Confidence intervals were computed from bootstrapping over quadrats.

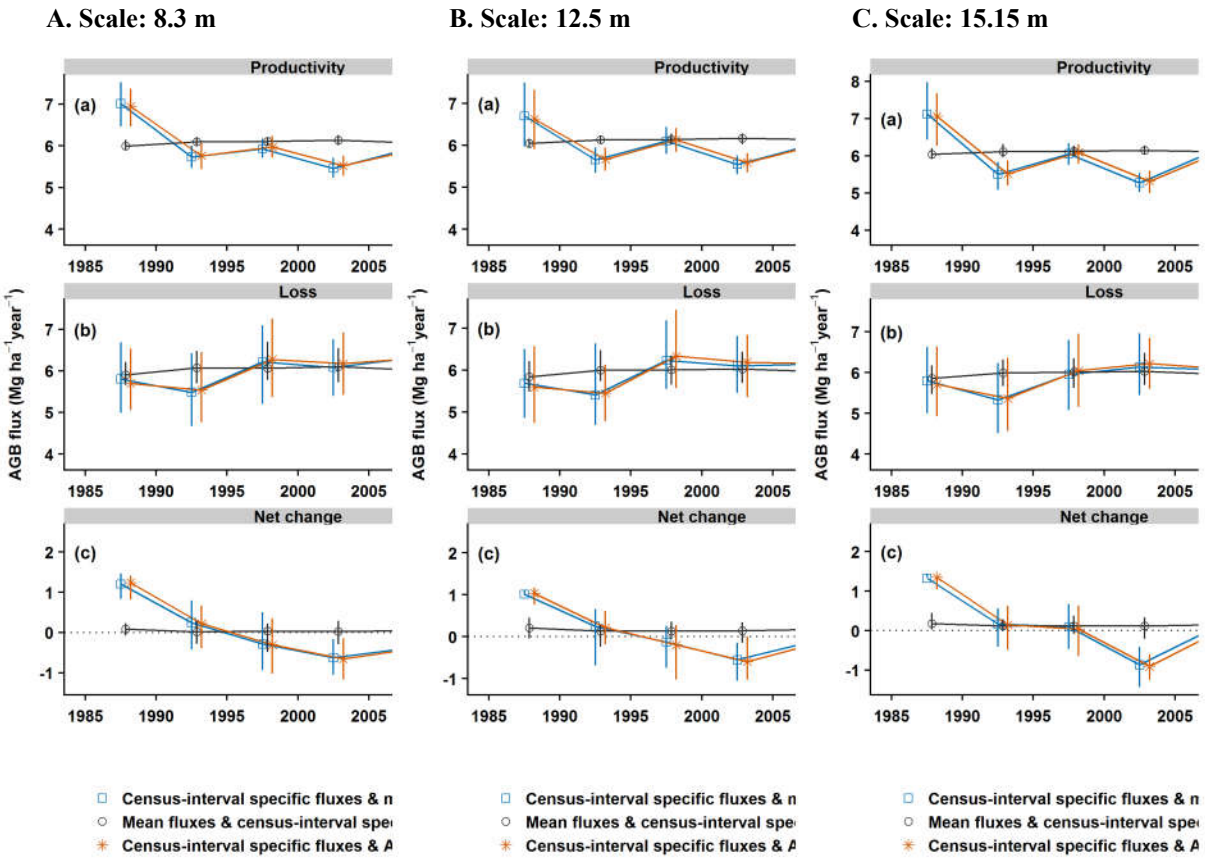

Figure S10 Comparison of qualitative patterns of hypothetical quadrat biomass fluxes across different quadrat sizes, for 8.93, 12.5 and 15.15-m square quadrats (A, B and C, respectively). Hypothetical fluxes were computed under three scenarios: census-interval fluxes and mean (i.e. across all census intervals) initial biomass (EAGBi) probability density functions (PDFs) (blue squares), mean fluxes and census-interval initial biomass PDFs (grey circles), and census-interval specific fluxes and initial biomass PDFs (red stars). Vertical lines show the 95% confidence intervals from bootstrapping over quadrats. The points are placed at the mid-points of the census intervals, and jiggered horizontally to increase readability. In all cases, missing diameter values (0.04%) were linearly interpolated, and EAGB calculations were based on equivalent diameters at 1.3 m estimated using a taper equation (see methods). In all cases, quadrats where a large strangler fig (DBH>50cm) occurred were excluded; these constituted less than 2.7% of quadrats. Note that difference in patterns are due to the substitution of extreme values (below 5th and above 95th percentiles of the overall EAGB distribution) in the hypothetical fluxes.

C1. Testing for the inclusion of 1.8 hectares of young forest at BCI

We tested for the robustness of our method and results in accounting for 1.8 hectare of 'young forest' regrowing from clear cutting about 120 years ago (Condit et al. 1996). We ran the same analysis and produce the same figures as presented in the manuscript and found no noticeable difference.

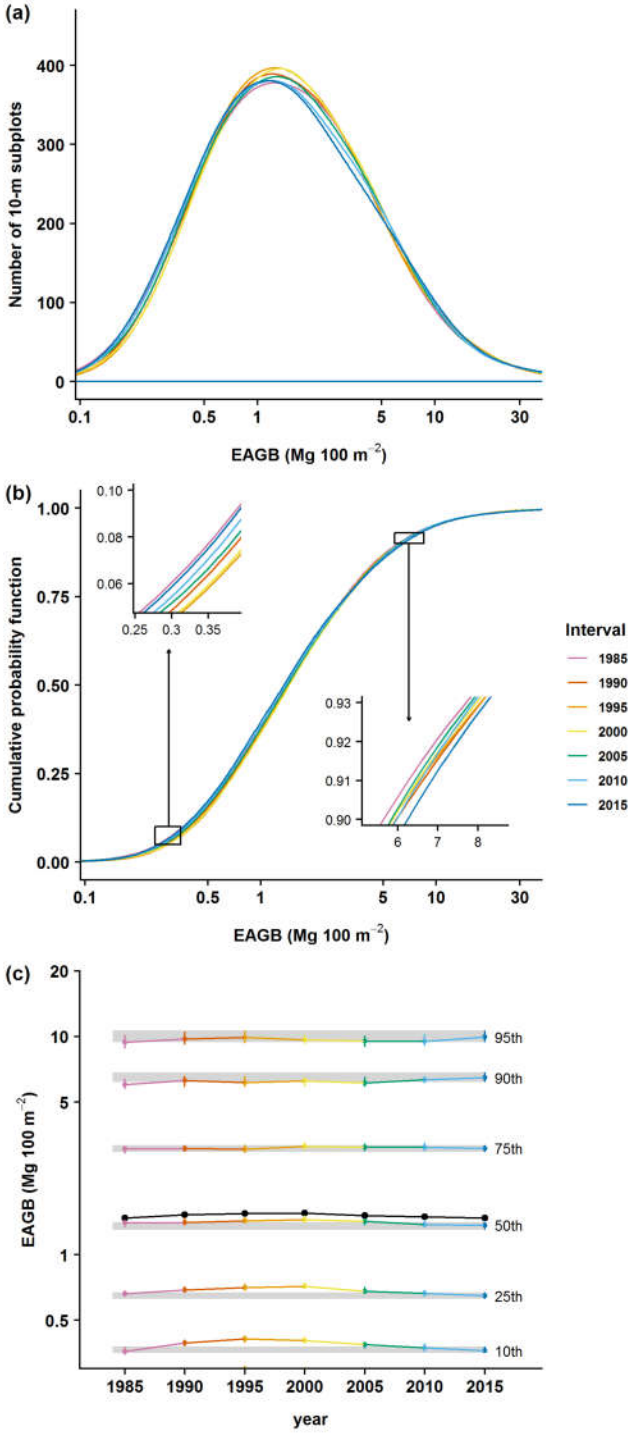

Figure S 11: Parallel figure to main text figure 6, except with secondary forest (1.8 ha) included. Probability density distribution (a) and cumulative probability distribution (b) of EAGB density across all 10 x 10 m quadrats, with insets in (b) magnified to show inter-census variation for cumulative probabilities of 0.05 to 0.1 and 0.9 to 0.95. (c) Variation over time in seven specific percentiles of the

EAGB distribution over quadrats (colored points and lines) and in the overall mean EAGB density at the 50-ha scale (black solid points and lines). In panel c, vertical lines show the 95% confidence intervals from bootstrapping over quadrats, and horizontal grey shading shows the confidence intervals for values in 2015 to enable easy visual assessment of how other years compare. The illustrated curves in panels a) and b) are truncated at the 0.2th and 99.8th percentiles of the distribution, but all values were included in analyses. Note that the EAGB densities can be converted to units of Mg ha-1 by multiplying by 100.

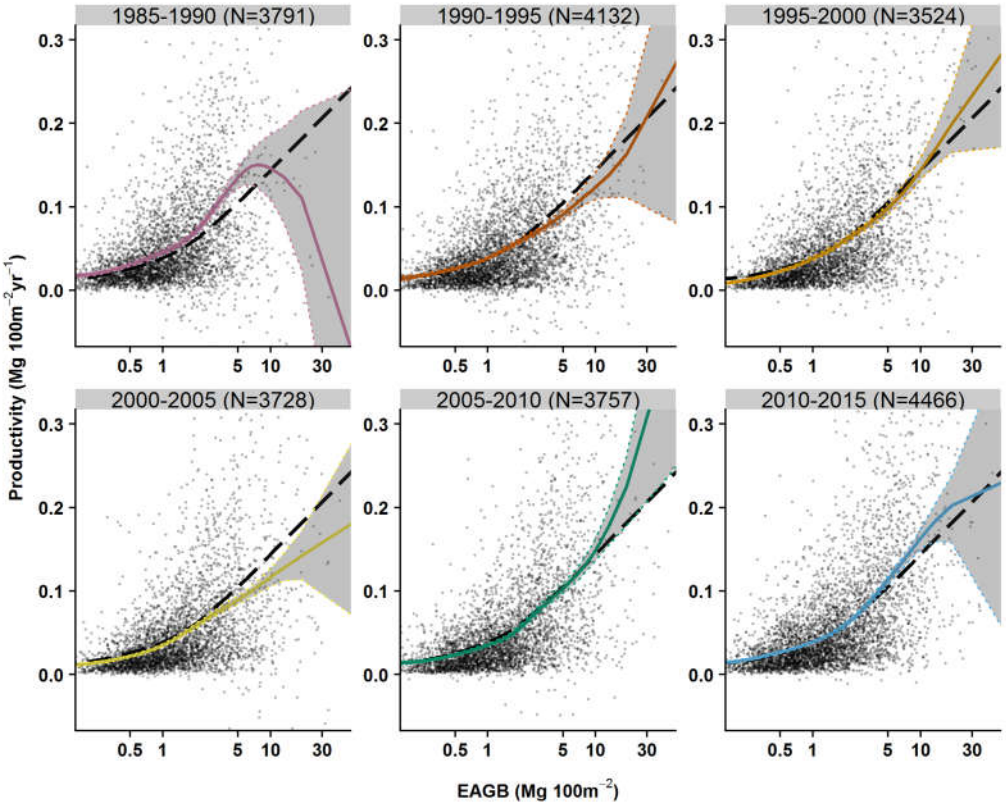

Figure S 12: Parallel figure to main text figure 3, except with secondary forest (1.8 ha) included. Quadrat-level mean annual EAGB productivity (Mg 100 m^{-2} yr^{-1}) as a function of initial quadrat biomass (EAGB in Mg 100 m^{-2}) for each 5-year census interval, for individual 10x10 m quadrats (points), together with local polynomial regression lines for individual census intervals (colored solid lines) and for all census intervals combined (black dashed lines). Confidence envelopes were computed from bootstrapping over quadrats. For each census interval, analyses excluded quadrats with problematic EAGB change measurements (see methods for details); N is the number of quadrats included for each census interval. The range of data shown here is truncated, but all points were included in the analyses. Note that EAGB stocks and fluxes can be converted to units of Mg ha^{-1} by multiplying by 100.

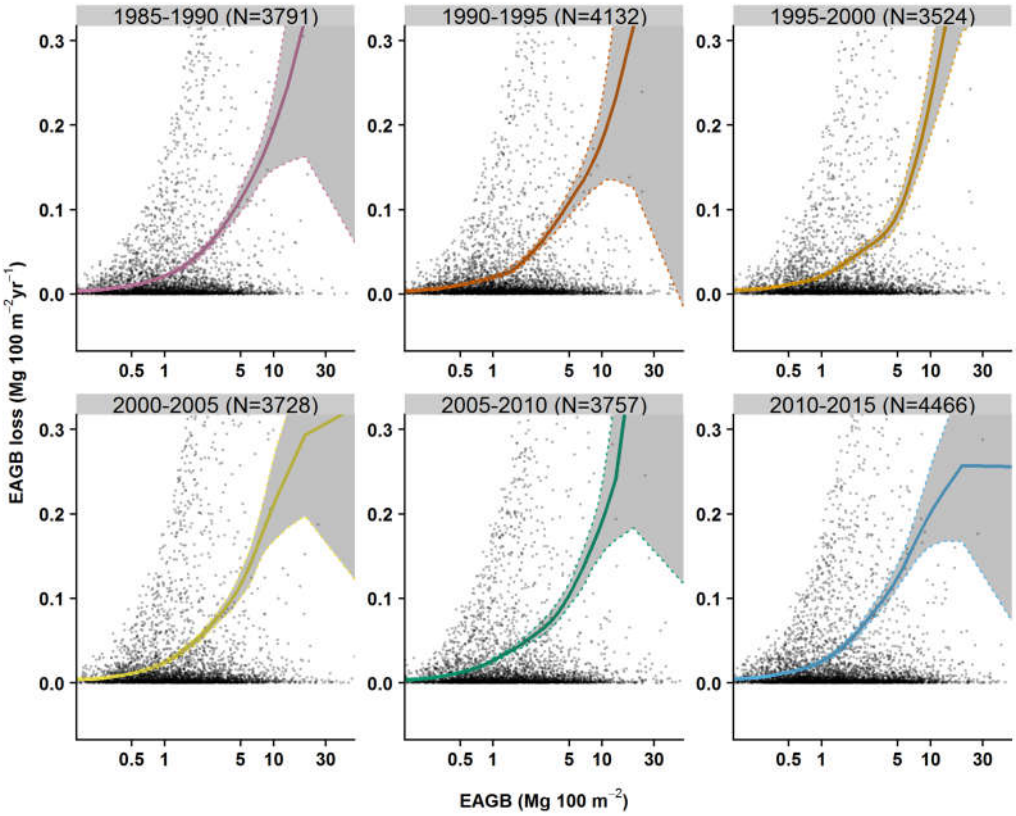

Figure S 13: Parallel figure to figure S3, except with secondary forest (1.8 ha) included. Quadrat-level annual EAGB mortality ($Mg.100m^{-2}.yr^{-1}$) as a function of initial quadrat biomass for each 5-year census interval, for 10x10 m quadrats (points) with local polynomial regression lines for individual census intervals (colored solid lines) and for all census intervals combined (black dashed lines). For each census interval, analyses excluded quadrats containing one or more trees that (a) are large strangler figs, (b) have a change in POM, or (c) have an obvious major measurement error during the census interval (see methods for details; N is the number of quadrats included for each census interval). Regression lines are shown only for the ranges of the 2nd to 98th percentile values of the respective datasets (avoiding the distribution extremes where uncertainty increases). The range of data shown here is truncated for illustration purposes, but all points (including those outside the graphed range) were included in analyses.

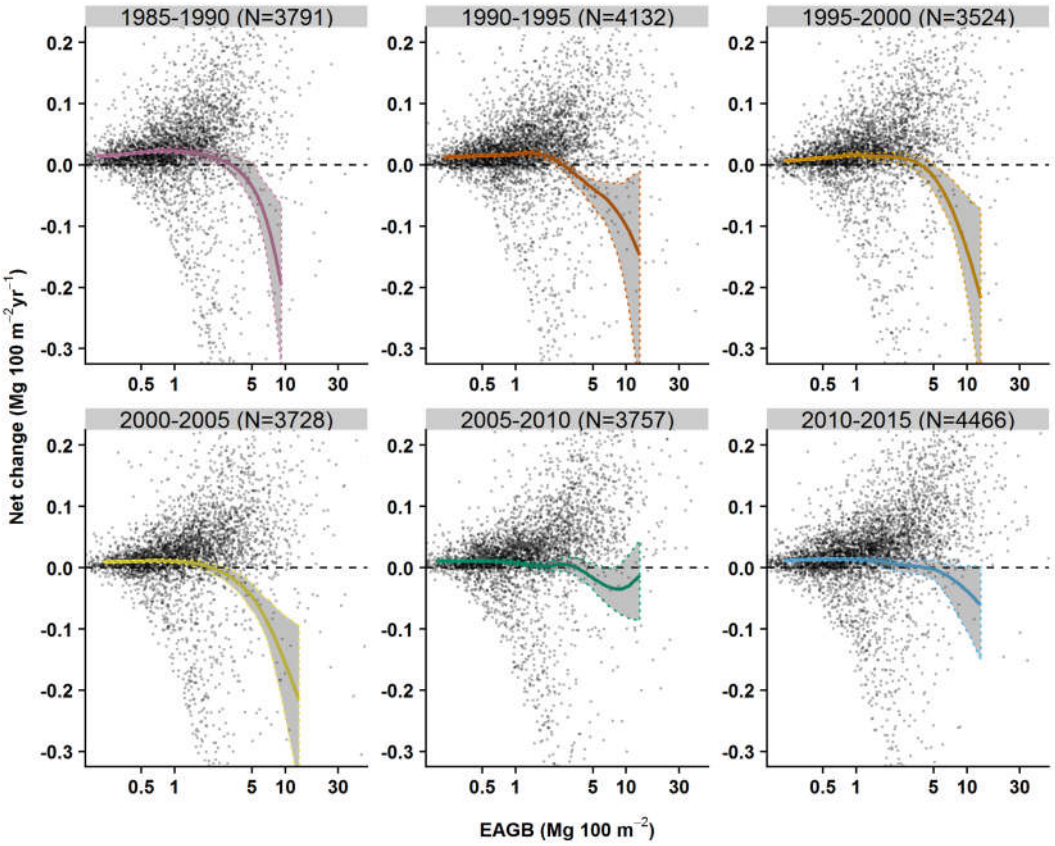

Figure S 14: Parallel figure to figure S4, except with secondary forest (1.8 ha) included. Quadrat-level annual EAGB net change ($Mg.100m^{-2}.yr^{-1}$) as a function of initial quadrat biomass for each 5-year census interval, for 10x10 m quadrats (points) with local polynomial regression lines for individual census intervals (colored solid lines) and for all census intervals combined (black dashed lines). For each census interval, analyses excluded quadrats containing one or more trees that (a) are large strangler figs, (b) have a change in POM, or (c) have an obvious major measurement error during the census interval (see methods for details; N is the number of quadrats included for each census interval). Regression lines are shown only for the ranges of the 2nd to 98th percentile values of the respective datasets (avoiding the distribution extremes where uncertainty increases). The range of data shown here is truncated for illustration purposes.

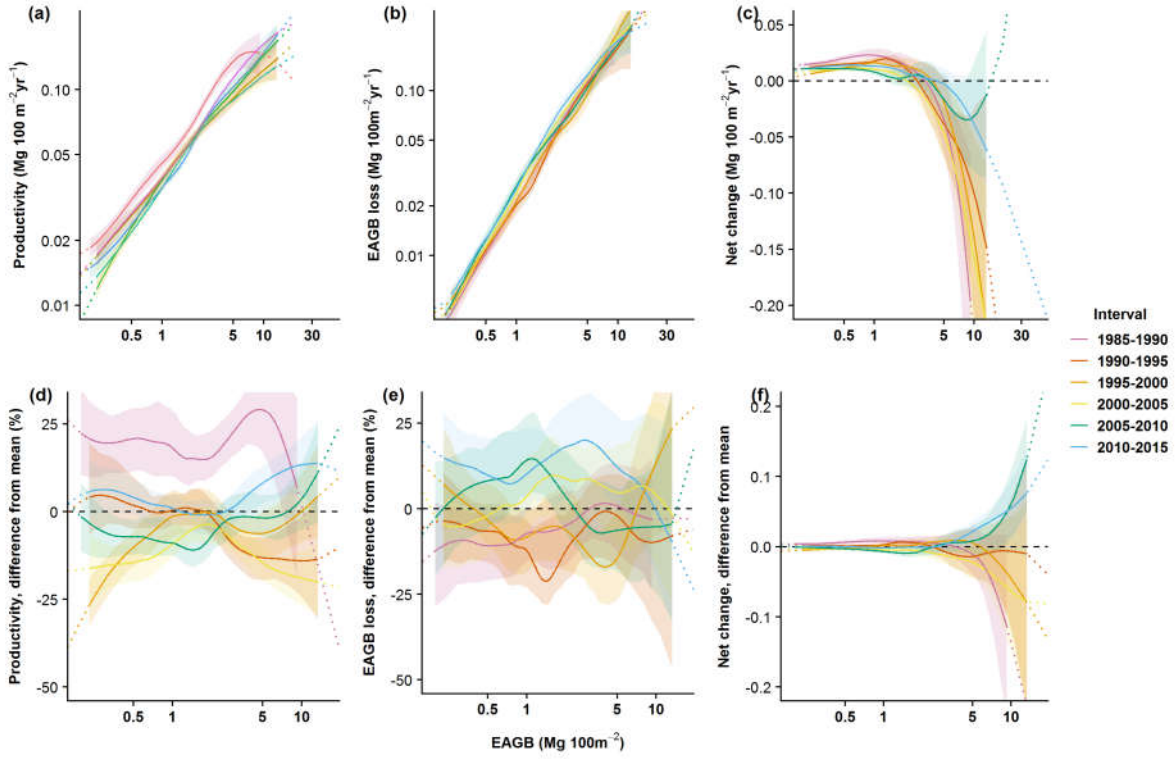

Figure S 15: Parallel figure to main text figure 4, except with secondary forest (1.8 ha) included. Variation among census intervals in quadrat EAGB productivity (a), loss (b) and net change (c) as a function of aboveground biomass (EAGB) at the initial census for 10x10 m quadrats, together with the corresponding differences from the mean (per initial EAGB) across all census intervals (d,e,f). Patterns were quantified using local polynomial regression; regression lines are displayed as solid lines for initial EAGB values spanning the 2nd to 98th percentiles of the respective census interval, and as dotted lines outside this range. Confidence envelopes were computed by bootstrapping over quadrats, and are shown for the 2nd to 98th percentiles of initial EAGB using shading. Analyses excluded quadrats with problematic EAGB change measurements (see methods for details). Note that productivity (a) and loss (b) are shown on log scales, and their differences from the mean are expressed in percentages (d,e) whereas the net change (c) and its difference from the mean (f) are shown on linear scales. Note that EAGB stocks and fluxes can be converted to units of Mg ha^{-1} by multiplying by 100.

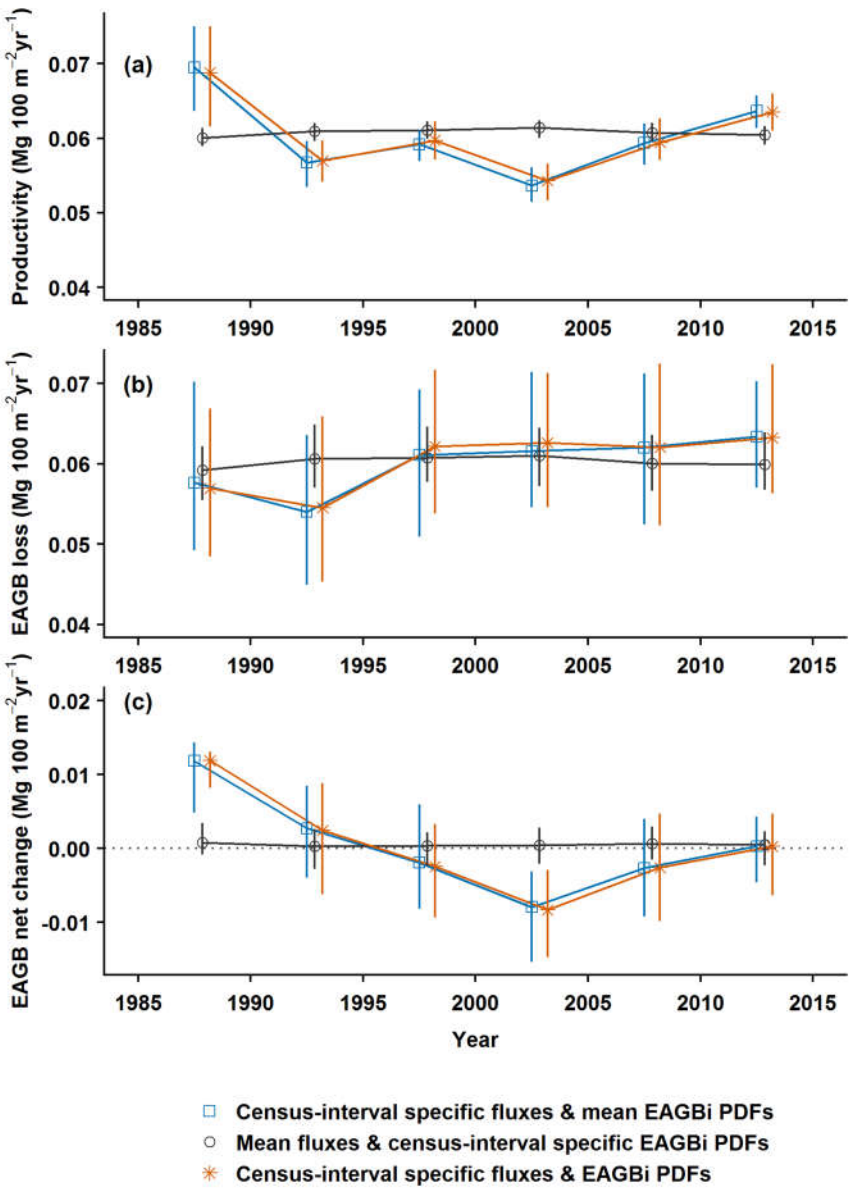

Figure S 16: Parallel figure to main text figure 7, except with secondary forest (1.8 ha) included. Time series of hypothetical whole-plot productivity (a), loss (b), and net change (c) expected with and without variation among census intervals in functions specifying how estimated above-ground biomass (EAGB) fluxes vary with initial biomass, and with and without variation among census intervals in initial EAGB distributions (EAGBi). See methods for details. Vertical lines show 95% confidence intervals obtained by bootstrapping over quadrats. The points are placed at the mid-points of the census intervals, and jiggered horizontally to increase readability. Values are given in Table S3. Note that EAGB stocks and fluxes can be converted to units of Mg ha^{-1} by multiplying by 100.

D. Empirical fluxes under different correction methods

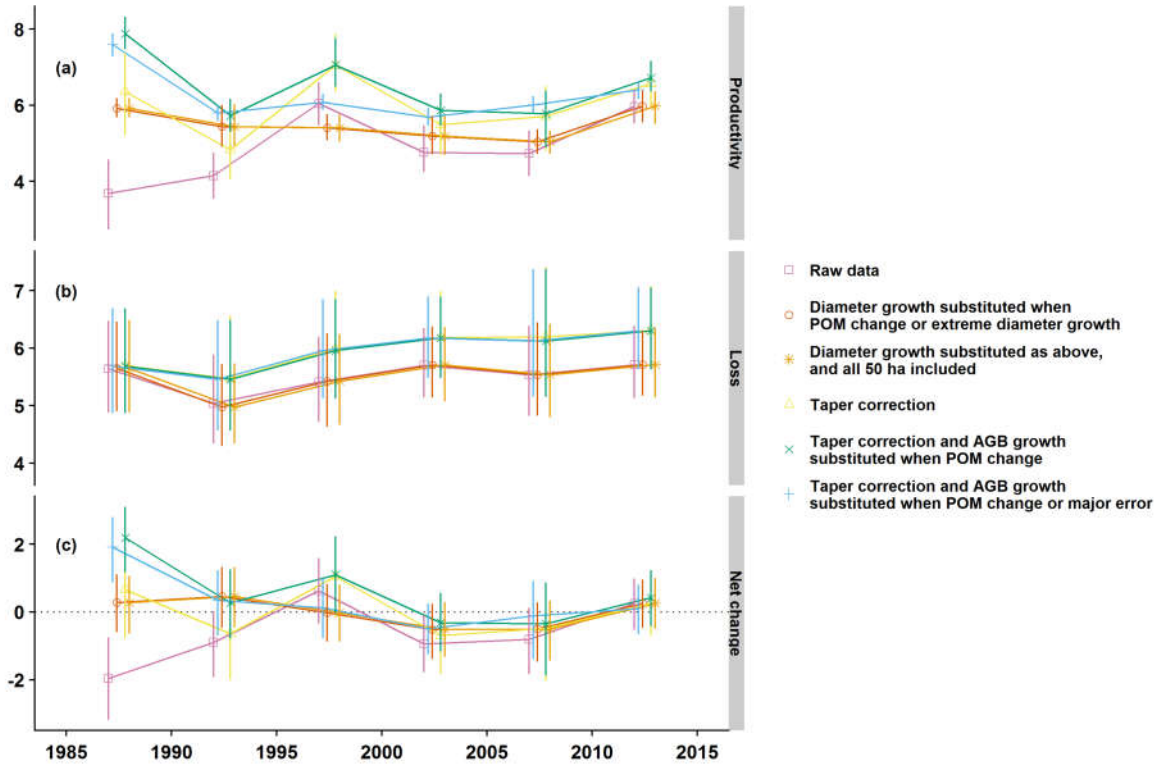

Figure S17 Estimated plot-level EAGB fluxes in woody productivity (a), loss (mortality) (b), and net change (c) for each census interval, calculated under alternative data correction procedures. (i) Original DBH data without any corrections (yellow squares). (ii) All trees that ever reached DBH ≥ 70 cm and ever exhibited extreme diameter growth (increase > 45 mm/yr or decrease of more than 5 mm/yr) without a change in the point of measurement (N=80) were checked individually and corrected by linear interpolation/extrapolation between censuses, and all other individual census interval DBH records showing extreme diameter growth or with POM change were substituted with mean diameter growth for the same size classes following the methods of Chave et al. 2008 (diameter class limits were 10, 15, 20, 25, 30, 40, 50, 100, 200, 300, 400, 500, 600, 700, and 10,000 mm) (purple circles). (iii) As under the previous scenario, except all 50 ha were included for comparison with other studies, whereas all other scenarios shown here include data only for the 48.8 ha excluding the swamp (blue stars). (iv) DBHs were taper corrected and no other corrections were done (red stars). (v) DBHs were taper corrected and DBH records involving a POM change were substituted based on mean EAGB growth in the same diameter class (taper-corrected diameter class limits were 10, 50, 100, 200, 400, and 600 mm) (green triangles). (vi) DBHs were taper corrected and DBH records involving a POM change or highly suspicious and highly influential measurement error (i.e. productivity > 20% of mean productivity for 1 ha) were substituted based on mean EAGB growth in the same EAGB class, as in the previous scenario (black crosses). Vertical lines show the 95% confidence intervals from bootstrapping over quadrats. The points are placed at the mid-points of the census intervals, and jiggered horizontally to increase readability. In all cases, missing diameter values (0.04%) were linearly interpolated. In all cases except (iii), quadrats where a large strangler fig (DBH ≥ 50cm) occurred were excluded; these constituted less than 2.7% of quadrats. Except in the case of the diameter series of large trees under (ii) and (iii), substitutions were done independently for each census interval, always affected the final diameter of the census interval, and did not carry over to the following census interval (e.g., a tree that had a change in point of measurement between 1990 and 1995 would have its 1995 diameter substituted for the 1990-1995 calculations, and its measured 1995

diameter used for 1995-2000 calculations). Size classes always included the upper bound (and for the smallest size class, also the lower bound). For cases (v) and (vi), we substituted size-class-specific mean EAGB growth rates for stems flagged for substitution. Mean EAGB growth rates were calculated for each census interval and diameter size class after excluding records with a change in measurement height or unrealistic diameter growth (Table S3), where unrealistic growth was defined as dbh growth > 75 mm/yr or second dbh measure more than 4 standard deviations in measurement error below the first (Rüger et al., 2011).

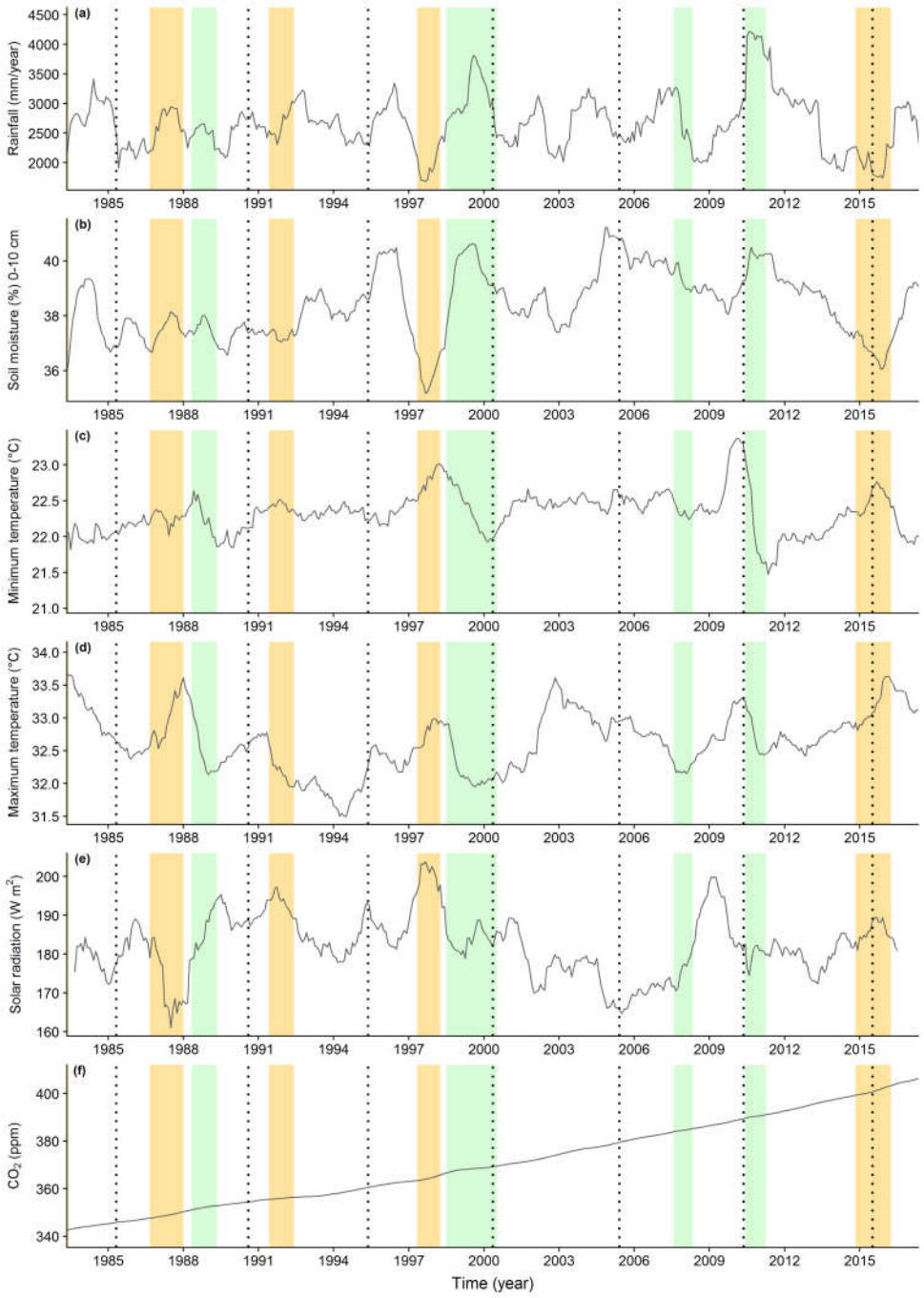

Figure S18 Temporal variation of potential drivers of biomass dynamics on BCI over the study period, including local climate drivers (a-e) and global atmospheric/climate drivers (f-g), as reflected in 12-month running sum (for a) and running means (for b to g) (grey lines). Vertical grey dashed lines indicate the mean date of each census of the 50 ha forest dynamics plot (the mean over trees of the measurement date for that census). Strong El Niño (orange) and La Niña (green) events are identified based on Oceanic Niño Index values >0.5 °C and less than −0.5 °C, respectively, for at least nine consecutive months. Local climate data were collected on Barro Colorado Island (see https://biogeodb.stri.si.edu/physical_monitoring/research/barrocolorado); Matteo Detto performed QAQC to identify errors and gap-fill missing and erroneous values of solar radiation using data from other nearby stations (Detto et al., 2018). Global mean annual atmospheric carbon dioxide (CO2)

concentrations (ppm) were obtained from the NOAA ESRL (Earth Systems Research Laboratory) website https://www.esrl.noaa.gov/gmd/ccgg/trends/full.html.

Literature cited

Condit, R. (1998). Tropical forest census plots: methods and results from Barro Colorado Island, Panama and a comparison with other plots. *Springer Science & Business Media*, 1998.

Detto, M., Wright, S. J., Calderón, O., & Muller-Landau, H. C. (2018). Resource acquisition and reproductive strategies of tropical forest in response to the El Niño–Southern Oscillation. *Nature Communications*, *9*(1), 913.

Kohyama, T. S., Kohyama, T. I., & Sheil, D. (2019). Estimating net biomass production and loss from repeated measurements of trees in forests and woodlands: Formulae, biases and recommendations. *Forest Ecology and Management*, 433, 729–740. https://doi.org/10.1016/j.foreco.2018.11.010

Rüger, N., Berger, U., Hubbell, S. P., Vieilledent, G., & Condit, R. (2011). Growth Strategies of Tropical Tree Species: Disentangling Light and Size Effects. *PLOS ONE*, *6*(9), e25330.

Wood densities arise from a local data base (Wright et al. 2010 and unpublished) and a global data base (Zanne et al. 2009). Level of assignment (level) was done first at species level using the local data base, or the global database if not present in the local data base. If the species was not present, wood density was averaged at genus level (merging both bases) or across all assigned species (stand-level) instead.

genus	species	family	WD (g/cm3)	level	source
Abarema	barbouriana	Fabaceae	**0.512**	genus	genus average
Abarema	macradenia	Fabaceae	**0.438**	species	local data base
Abarema	idiopoda	Fabaceae	**0.512**	genus	genus average
Acacia	mangium	Fabaceae	**0.507**	species	global data base
Acalypha	diversifolia	Euphorbiaceae	**0.300**	genus	genus average
Acalypha	macrostachya	Euphorbiaceae	**0.300**	genus	genus average
Acanthocereus	tetragonus	Cactaceae	**0.592**	stand-level average	
Acidoton	nicaraguensis	Euphorbiaceae	**0.592**	stand-level average	
Acrocomia	aculeata	Arecaceae	**0.592**	stand-level average	
Adelia	triloba	Euphorbiaceae	**0.574**	species	local data base
Adenaria	floribunda	Lythraceae	**0.592**	stand-level average	
Aegiphila	anomala	Lamiaceae	**0.657**	genus	genus average
Aegiphila	panamensis	Lamiaceae	**0.657**	genus	genus average
Agonandra	brasiliensis	Opiliaceae	**0.818**	species	global data base
Agouticarpa	curviflora	Rubiaceae	**0.592**	stand-level average	
Agouticarpa	williamsii	Rubiaceae	**0.592**	stand-level average	
Aiouea	vexatrix	Lauraceae	**0.370**	genus	genus average
Aiphanes	hirsuta	Arecaceae	**0.592**	stand-level average	
Albizia	adinocephala	Fabaceae	**0.556**	genus	genus average
Albizia	niopoides	Fabaceae	**0.555**	species	global data base
Albizia	procera	Fabaceae	**0.573**	species	local data base
Alchornea	costaricensis	Euphorbiaceae	**0.301**	species	local data base
Alchornea	grandis	Euphorbiaceae	**0.340**	species	global data base
Alchornea	latifolia	Euphorbiaceae	**0.425**	species	local data base
Alibertia	edulis	Rubiaceae	**0.760**	species	local data base
Alibertia	dwyeri	Rubiaceae	**0.733**	genus	genus average
Allenanthus	erythrocarpus	Rubiaceae	**0.592**	stand-level average	
Allophylus	gentryi	Sapindaceae	**0.518**	genus	genus average
Allophylus	psilospermus	Sapindaceae	**0.518**	genus	genus average
Allophylus	racemosus	Sapindaceae	**0.518**	genus	genus average
Alseis	blackiana	Rubiaceae	**0.536**	species	local data base
Amaioua	corymbosa	Rubiaceae	**0.625**	genus	genus average
Amaioua	magnicarpa	Rubiaceae	**0.625**	genus	genus average
Amaioua	pedicellata	Rubiaceae	**0.625**	genus	genus average
Amanoa	guianensis	Phyllanthaceae	**0.843**	species	global data base
Ampelocera	edentula	Ulmaceae	**0.700**	species	local data base
Ampelocera	macphersonii	Ulmaceae	**0.726**	genus	genus average
Amphitecna	latifolia	Bignoniaceae	**0.460**	genus	genus average

genus	species	family	WD (g/cm3)	level	source
Amphitecna	spathicalyx	Bignoniaceae	**0.460**	genus	genus average
Amphitecna	isthmica	Bignoniaceae	**0.460**	genus	genus average
Anacardium	excelsum	Anacardiaceae	**0.391**	species	local data base
Anacardium	occidentale	Anacardiaceae	**0.447**	species	global data base
Anaxagorea	allenii	Annonaceae	**0.530**	genus	genus average
Anaxagorea	panamensis	Annonaceae	**0.530**	genus	genus average
Anaxagorea	crassipetala	Annonaceae	**0.480**	species	global data base
Andira	inermis	Fabaceae	**0.643**	species	local data base
Aniba	hostmanniana	Lauraceae	**0.619**	species	local data base
Annona	acuminata	Annonaceae	**0.524**	genus	genus average
Annona	cherimola	Annonaceae	**0.524**	genus	genus average
Annona	glabra	Annonaceae	**0.500**	species	global data base
Annona	hayesii	Annonaceae	**0.524**	genus	genus average
Annona	montana	Annonaceae	**0.524**	genus	genus average
Annona	muricata	Annonaceae	**0.360**	species	global data base
Annona	pittieri	Annonaceae	**0.524**	genus	genus average
Annona	purpurea	Annonaceae	**0.570**	species	local data base
Annona	reticulata	Annonaceae	**0.550**	species	global data base
Annona	spraguei	Annonaceae	**0.559**	species	local data base
Annona	mucosa	Annonaceae	**0.524**	genus	genus average
Annona	papilionella	Annonaceae	**0.524**	genus	genus average
Apeiba	hybrid	Malvaceae	**0.255**	genus	genus average
Apeiba	tibourbou	Malvaceae	**0.200**	species	local data base
Apeiba	membranacea	Malvaceae	**0.255**	genus	genus average
Aphelandra	campanensis	Acanthaceae	**0.592**	stand-level average	
Aphelandra	gracilis	Acanthaceae	**0.592**	stand-level average	
Aphelandra	scabra	Acanthaceae	**0.592**	stand-level average	
Aphelandra	sinclairiana	Acanthaceae	**0.592**	stand-level average	
Appunia	seibertii	Rubiaceae	**0.592**	stand-level average	
Arachnothryx	buddleioides	Rubiaceae	**0.560**	species	global data base
Ardisia	bartlettii	Primulaceae	**0.591**	genus	genus average
Ardisia	dukei	Primulaceae	**0.591**	genus	genus average
Ardisia	glomerata	Primulaceae	**0.591**	genus	genus average
Ardisia	guianensis	Primulaceae	**0.620**	species	local data base
Ardisia	opegrapha	Primulaceae	**0.591**	genus	genus average
Ardisia	revoluta	Primulaceae	**0.591**	genus	genus average
Ardisia	solanacea	Primulaceae	**0.620**	species	global data base
Ardisia	standleyana	Primulaceae	**0.591**	genus	genus average
Ardisia	compressa	Primulaceae	**0.591**	genus	genus average
Artocarpus	altilis	Moraceae	**0.431**	species	local data base
Aspidosperma	desmanthum	Apocynaceae	**0.610**	species	global data base
Aspidosperma	excelsum	Apocynaceae	**0.792**	species	global data base
Astrocaryum	alatum	Arecaceae	**0.508**	genus	genus average
Astrocaryum	standleyanum	Arecaceae	**0.508**	genus	genus average

genus	species	family	WD (g/cm3)	level	source
Astronium	graveolens	Anacardiaceae	**0.868**	species	local data base
Attalea	rostrata	Arecaceae	**0.326**	genus	genus average
Avicennia	bicolor	Acanthaceae	**0.685**	genus	genus average
Avicennia	germinans	Acanthaceae	**0.776**	species	global data base
Bactris	barronis	Arecaceae	**0.592**	stand-level average	
Bactris	coloniata	Arecaceae	**0.592**	stand-level average	
Bactris	coloradonis	Arecaceae	**0.592**	stand-level average	
Bactris	gasipaes	Arecaceae	**0.592**	stand-level average	
Bactris	major	Arecaceae	**0.592**	stand-level average	
Bactris	maraja	Arecaceae	**0.592**	stand-level average	
Bactris	panamensis	Arecaceae	**0.592**	stand-level average	
Banara	guianensis	Salicaceae	**0.610**	species	local data base
Bauhinia	ungulata	Fabaceae	**0.755**	genus	genus average
Beilschmiedia	sulcata	Lauraceae	**0.563**	genus	genus average
Beilschmiedia	aff.tilaranensis	Lauraceae	**0.563**	genus	genus average
Beilschmiedia	tovarensis	Lauraceae	**0.563**	genus	genus average
Bellucia	pentamera	Melastomataceae	**0.485**	species	local data base
Bertiera	guianensis	Rubiaceae	**0.592**	stand-level average	
Besleria	formicaria	Gesneriaceae	**0.592**	stand-level average	
Besleria	robusta	Gesneriaceae	**0.592**	stand-level average	
Billia	rosea	Sapindaceae	**0.690**	genus	genus average
Bixa	orellana	Bixaceae	**0.360**	species	global data base
Blighia	sapida	Sapindaceae	**0.762**	species	global data base
Bocconia	frutescens	Papaveraceae	**0.592**	stand-level average	
Bonellia	macrocarpa	Primulaceae	**0.592**	stand-level average	
Bourreria	costaricensis	Boraginaceae	**0.730**	genus	genus average
Brosimum	alicastrum	Moraceae	**0.600**	species	local data base
Brosimum	costaricanum	Moraceae	**0.665**	species	local data base
Brosimum	guianense	Moraceae	**0.844**	species	local data base
Brosimum	lactescens	Moraceae	**0.656**	species	local data base
Brosimum	rubescens	Moraceae	**0.825**	species	global data base
Brosimum	utile	Moraceae	**0.506**	species	local data base
Brownea	macrophylla	Fabaceae	**1.210**	genus	genus average
Buchenavia	tetraphylla	Combretaceae	**0.617**	species	global data base
Bunchosia	dwyeri	Malpighiaceae	**0.695**	genus	genus average
Bunchosia	macrophylla	Malpighiaceae	**0.695**	genus	genus average
Bunchosia	nitida	Malpighiaceae	**0.695**	genus	genus average
Bunchosia	odorata	Malpighiaceae	**0.695**	genus	genus average
Bursera	simaruba	Burseraceae	**0.305**	species	local data base
Bursera	tomentosa	Burseraceae	**0.311**	genus	genus average
Byrsonima	crassifolia	Malpighiaceae	**0.586**	species	local data base
Byrsonima	crispa	Malpighiaceae	**0.580**	species	local data base
Byrsonima	dressleri	Malpighiaceae	**0.649**	genus	genus average
Byrsonima	spicata	Malpighiaceae	**0.614**	species	local data base

genus	species	family	WD (g/cm3)	level	source
Calatola	costaricensis	Icacinaceae	**0.566**	species	local data base
Calliandra	laxa	Fabaceae	**0.816**	genus	genus average
Calliandra	aff.grandifolia	Fabaceae	**0.816**	genus	genus average
Callicarpa	acuminata	Lamiaceae	**0.350**	genus	genus average
Calophyllum	brasiliense	Calophyllaceae	**0.589**	species	local data base
Calophyllum	inophyllum	Calophyllaceae	**0.585**	species	global data base
Calophyllum	longifolium	Calophyllaceae	**0.542**	species	local data base
Calycolpus	warszewiczianus	Myrtaceae	**0.800**	genus	genus average
Calycophyllum	candidissimum	Rubiaceae	**0.702**	species	local data base
Calyptranthes	chytraculia	Myrtaceae	**0.783**	genus	genus average
Calyptranthes	pulchella	Myrtaceae	**0.783**	genus	genus average
Calyptranthes	tumidonodia	Myrtaceae	**0.783**	genus	genus average
Calyptrogyne	costatifrons	Arecaceae	**0.592**	stand-level average	
Campnosperma	panamense	Anacardiaceae	**0.376**	genus	genus average
Capparidastrum	frondosum	Capparaceae	**0.592**	stand-level average	
Capparidastrum	discolor	Capparaceae	**0.592**	stand-level average	
Capparidastrum	aff.osmanthum	Capparaceae	**0.592**	stand-level average	
Carapa	guianensis	Meliaceae	**0.530**	species	local data base
Carica	papaya	Caricaceae	**0.188**	genus	genus average
Caryodaphnopsis	burgeri	Lauraceae	**0.592**	stand-level average	
Caryodaphnopsis	tomentosa	Lauraceae	**0.592**	stand-level average	
Casearia	aculeata	Salicaceae	**0.660**	species	local data base
Casearia	arguta	Salicaceae	**0.517**	species	local data base
Casearia	commersoniana	Salicaceae	**0.621**	genus	genus average
Casearia	coronata	Salicaceae	**0.621**	genus	genus average
Casearia	corymbosa	Salicaceae	**0.621**	genus	genus average
Casearia	guianensis	Salicaceae	**0.742**	species	local data base
Casearia	nigricans	Salicaceae	**0.621**	genus	genus average
Casearia	sylvestris	Salicaceae	**0.705**	species	local data base
Casearia	arborea	Salicaceae	**0.574**	species	local data base
Cassia	grandis	Fabaceae	**0.736**	genus	genus average
Cassia	moschata	Fabaceae	**0.805**	species	local data base
Cassipourea	enana	Rhizophoraceae	**0.650**	genus	genus average
Cassipourea	hoja_grande	Rhizophoraceae	**0.650**	genus	genus average
Cassipourea	elliptica	Rhizophoraceae	**0.650**	genus	genus average
Castilla	elastica	Moraceae	**0.524**	species	local data base
Cavanillesia	platanifolia	Malvaceae	**0.360**	species	local data base
Cecropia	garciae	Urticaceae	**0.340**	genus	genus average
Cecropia	heterochroma	Urticaceae	**0.340**	genus	genus average
Cecropia	insignis	Urticaceae	**0.318**	species	local data base
Cecropia	longipes	Urticaceae	**0.340**	genus	genus average
Cecropia	obtusifolia	Urticaceae	**0.307**	species	local data base
Cecropia	peltata	Urticaceae	**0.300**	species	local data base
Cecropia	hispidissima	Urticaceae	**0.340**	genus	genus average

genus	species	family	WD (g/cm3)	level	source
Cedrela	fissilis	Meliaceae	**0.467**	species	global data base
Cedrela	odorata	Meliaceae	**0.447**	species	local data base
Ceiba	pentandra	Malvaceae	**0.305**	species	local data base
Celtis	schippii	Cannabaceae	**0.616**	species	local data base
Centropogon	tortilis	Campanulaceae	**0.592**	stand-level average	
Cespedesia	spathulata	Ochnaceae	**0.613**	species	local data base
Cestrum	latifolium	Solanaceae	**0.592**	stand-level average	
Cestrum	racemosum	Solanaceae	**0.592**	stand-level average	
Cestrum	schlechtendahlii	Solanaceae	**0.592**	stand-level average	
Chamaedorea	pinnatifrons	Arecaceae	**0.592**	stand-level average	
Chamaedorea	tepejilote	Arecaceae	**0.592**	stand-level average	
Chamguava	schippii	Myrtaceae	**0.592**	stand-level average	
Cheiloclinium	cognatum	Celastraceae	**0.592**	stand-level average	
Chimarrhis	parviflora	Rubiaceae	**0.707**	genus	genus average
Chimarrhis	latifolia	Rubiaceae	**0.707**	genus	genus average
Chionanthus	panamensis	Oleaceae	**0.680**	genus	genus average
Chloroleucon	mangense	Fabaceae	**0.990**	species	global data base
Chomelia	spinosa	Rubiaceae	**0.530**	species	local data base
Chromolucuma	aff.rubriflora	Sapotaceae	**0.730**	genus	genus average
Chrysobalanus	icaco	Chrysobalanaceae	**0.753**	species	global data base
Chrysochlamys	eclipes	Clusiaceae	**0.430**	genus	genus average
Chrysochlamys	glauca	Clusiaceae	**0.430**	genus	genus average
Chrysochlamys	grandifolia	Clusiaceae	**0.430**	genus	genus average
Chrysophyllum	brenesii	Sapotaceae	**0.665**	genus	genus average
Chrysophyllum	cainito	Sapotaceae	**0.655**	species	local data base
Chrysophyllum	colombianum	Sapotaceae	**0.665**	genus	genus average
Chrysophyllum	hirsutum	Sapotaceae	**0.665**	genus	genus average
Chrysophyllum	venezuelanense	Sapotaceae	**0.665**	genus	genus average
Chrysophyllum	argenteum	Sapotaceae	**0.777**	species	local data base
Cinnamomum	triplinerve	Lauraceae	**0.467**	genus	genus average
Cinnamomum	tonduzii	Lauraceae	**0.467**	genus	genus average
Citharexylum	caudatum	Verbenaceae	**0.667**	genus	genus average
Citrus	sinensis	Rutaceae	**0.780**	species	local data base
Clarisia	biflora	Moraceae	**0.498**	species	local data base
Clarisia	racemosa	Moraceae	**0.585**	species	local data base
Clavija	biborrana	Primulaceae	**0.592**	stand-level average	
Clavija	costaricana	Primulaceae	**0.592**	stand-level average	
Clavija	mezii	Primulaceae	**0.592**	stand-level average	
Clethra	mexicana	Clethraceae	**0.550**	species	global data base
Clidemia	crenulata	Melastomataceae	**0.592**	stand-level average	
Clidemia	densiflora	Melastomataceae	**0.592**	stand-level average	
Clidemia	dentata	Melastomataceae	**0.592**	stand-level average	
Clidemia	hammelii	Melastomataceae	**0.592**	stand-level average	
Clidemia	octona	Melastomataceae	**0.592**	stand-level average	

genus	species	family	WD (g/cm3)	level	source
Clidemia	septuplinervia	Melastomataceae	**0.592**	stand-level average	
Clidemia	discolor	Melastomataceae	**0.592**	stand-level average	
Clitoria	glaberrima	Fabaceae	**0.592**	stand-level average	
Clusia	cretosa	Clusiaceae	**0.676**	genus	genus average
Clusia	divaricata	Clusiaceae	**0.676**	genus	genus average
Clusia	pratensis	Clusiaceae	**0.676**	genus	genus average
Clusia	rosea	Clusiaceae	**0.605**	species	global data base
Clusia	stenophylla	Clusiaceae	**0.676**	genus	genus average
Cnidoscolus	urens	Euphorbiaceae	**0.427**	genus	genus average
Coccoloba	acuminata	Polygonaceae	**0.580**	species	global data base
Coccoloba	ascendens	Polygonaceae	**0.687**	genus	genus average
Coccoloba	caracasana	Polygonaceae	**0.430**	species	global data base
Coccoloba	coronata	Polygonaceae	**0.687**	genus	genus average
Coccoloba	johnstonii	Polygonaceae	**0.687**	genus	genus average
Coccoloba	lasseri	Polygonaceae	**0.687**	genus	genus average
Coccoloba	manzinellensis	Polygonaceae	**0.687**	genus	genus average
Coccoloba	mollis	Polygonaceae	**0.675**	species	local data base
Coccoloba	padiformis	Polygonaceae	**0.800**	species	local data base
Coccoloba	tuerckheimii	Polygonaceae	**0.687**	genus	genus average
Coccoloba	uvifera	Polygonaceae	**0.700**	species	global data base
Coccoloba	obovata	Polygonaceae	**0.687**	genus	genus average
Cochlospermum	vitifolium	Bixaceae	**0.218**	species	global data base
Cocos	nucifera	Arecaceae	**0.592**	stand-level average	
Coffea	arabica	Rubiaceae	**0.620**	species	global data base
Cojoba	hoja_grande	Fabaceae	**0.592**	stand-level average	
Cojoba	rufescens	Fabaceae	**0.592**	stand-level average	
Colpothrinax	aphanopetala	Arecaceae	**0.592**	stand-level average	
Colubrina	glandulosa	Rhamnaceae	**0.739**	species	local data base
Colubrina	heteroneura	Rhamnaceae	**0.970**	species	local data base
Colubrina	spinosa	Rhamnaceae	**0.495**	species	global data base
Compsoneura	rigidifolia	Myristicaceae	**0.592**	stand-level average	
Compsoneura	mexicana	Myristicaceae	**0.592**	stand-level average	
Conceveiba	pleiostemona	Euphorbiaceae	**0.266**	species	local data base
Conchocarpus	nicaraguensis	Rutaceae	**0.592**	stand-level average	
Condaminea	corymbosa	Rubiaceae	**0.592**	stand-level average	
Conocarpus	erectus	Combretaceae	**0.845**	species	global data base
Conostegia	bracteata	Melastomataceae	**0.592**	stand-level average	
Conostegia	cinnamomea	Melastomataceae	**0.592**	stand-level average	
Conostegia	cuatrecasii	Melastomataceae	**0.592**	stand-level average	
Conostegia	rufescens	Melastomataceae	**0.592**	stand-level average	
Conostegia	speciosa	Melastomataceae	**0.592**	stand-level average	
Conostegia	xalapensis	Melastomataceae	**0.592**	stand-level average	
Conostegia	montana	Melastomataceae	**0.592**	stand-level average	
Copaifera	aromatica	Fabaceae	**0.620**	species	local data base

genus	species	family	WD (g/cm3)	level	source
Cordia	alliodora	Boraginaceae	**0.520**	species	local data base
Cordia	bicolor	Boraginaceae	**0.475**	species	local data base
Cordia	collococca	Boraginaceae	**0.420**	species	global data base
Cordia	cymosa	Boraginaceae	**0.538**	genus	genus average
Cordia	dentata	Boraginaceae	**0.500**	species	global data base
Cordia	eriostigma	Boraginaceae	**0.538**	genus	genus average
Cordia	lasiocalyx	Boraginaceae	**0.397**	species	local data base
Cordia	lucidula	Boraginaceae	**0.538**	genus	genus average
Cordia	megalantha	Boraginaceae	**0.390**	species	global data base
Cordia	panamensis	Boraginaceae	**0.330**	species	local data base
Cordia	porcata	Boraginaceae	**0.538**	genus	genus average
Cordia	dwyeri	Boraginaceae	**0.538**	genus	genus average
Cordia	correae	Boraginaceae	**0.538**	genus	genus average
Cordiera	garapatica	Rubiaceae	**0.592**	stand-level average	
Cornutia	pyramidata	Lamiaceae	**0.600**	genus	genus average
Cosmibuena	macrocarpa	Rubiaceae	**0.592**	stand-level average	
Couepia	chocolate	Chrysobalanaceae	**0.798**	genus	genus average
Couratari	guianensis	Lecythidaceae	**0.507**	species	local data base
Coussarea	cerroazulensis	Rubiaceae	**0.618**	genus	genus average
Coussarea	curvigemmia	Rubiaceae	**0.618**	genus	genus average
Coussarea	latifolia	Rubiaceae	**0.618**	genus	genus average
Coussarea	loftonii	Rubiaceae	**0.618**	genus	genus average
Coutarea	hexandra	Rubiaceae	**0.600**	species	local data base
Crateva	tapia	Capparaceae	**0.519**	species	local data base
Cremastosperma	panamense	Annonaceae	**0.592**	stand-level average	
Crescentia	cujete	Bignoniaceae	**0.634**	species	global data base
Crossopetalum	parviflorum	Celastraceae	**0.592**	stand-level average	
Croton	billbergianus	Euphorbiaceae	**0.510**	genus	genus average
Croton	draco	Euphorbiaceae	**0.510**	genus	genus average
Croton	pachypodus	Euphorbiaceae	**0.510**	genus	genus average
Croton	schiedeanus	Euphorbiaceae	**0.510**	genus	genus average
Croton	smithianus	Euphorbiaceae	**0.510**	genus	genus average
Croton	matourensis	Euphorbiaceae	**0.388**	species	global data base
Crudia	acuminata	Fabaceae	**0.777**	genus	genus average
Cryosophila	warscewiczii	Arecaceae	**0.400**	species	local data base
Cryptocarya	panamensis	Lauraceae	**0.561**	genus	genus average
Cupania	cinerea	Sapindaceae	**0.500**	species	local data base
Cupania	guatemalensis	Sapindaceae	**0.688**	species	local data base
Cupania	latifolia	Sapindaceae	**0.618**	genus	genus average
Cupania	rufescens	Sapindaceae	**0.618**	genus	genus average
Cupania	scrobiculata	Sapindaceae	**0.628**	species	local data base
Cupania	seemannii	Sapindaceae	**0.618**	genus	genus average
Curatella	americana	Dilleniaceae	**0.650**	species	global data base
Cyathea	multiflora	Cyatheaceae	**0.592**	stand-level average	

genus	species	family	WD (g/cm3)	level	source
Cyathea	petiolata	Cyatheaceae	**0.592**	stand-level average	
Cybianthus	schlimii	Primulaceae	**0.593**	genus	genus average
Cymbopetalum	lanugipetalum	Annonaceae	**0.552**	genus	genus average
Cymbopetalum	costaricense	Annonaceae	**0.552**	genus	genus average
Cynometra	bauhiniifolia	Fabaceae	**0.812**	genus	genus average
Cynophalla	flexuosa	Capparaceae	**0.592**	stand-level average	
Cynophalla	verrucosa	Capparaceae	**0.592**	stand-level average	
Cyrilla	racemiflora	Cyrillaceae	**0.590**	species	global data base
Dalbergia	retusa	Fabaceae	**0.863**	species	local data base
Damburneya	umbrosa	Lauraceae	**0.592**	stand-level average	
Damburneya	martinicensis	Lauraceae	**0.592**	stand-level average	
Daphnopsis	americana	Thymelaeaceae	**0.520**	genus	genus average
Daphnopsis	correae	Thymelaeaceae	**0.520**	genus	genus average
Delonix	regia	Fabaceae	**0.579**	species	global data base
Dendropanax	sessiliflorus	Araliaceae	**0.420**	genus	genus average
Dendropanax	arboreus	Araliaceae	**0.420**	species	local data base
Dendropanax	punctatus	Araliaceae	**0.420**	genus	genus average
Dendropanax	globosus	Araliaceae	**0.420**	genus	genus average
Desmopsis	maxonii	Annonaceae	**0.764**	genus	genus average
Desmopsis	panamensis	Annonaceae	**0.764**	species	local data base
Dialium	guianense	Fabaceae	**0.896**	species	local data base
Dichapetalum	axillare	Dichapetalaceae	**0.761**	genus	genus average
Dilodendron	costaricense	Sapindaceae	**0.592**	stand-level average	
Diospyros	artanthifolia	Ebenaceae	**0.683**	genus	genus average
Diphysa	americana	Fabaceae	**1.080**	genus	genus average
Diplotropis	purpurea	Fabaceae	**0.762**	species	global data base
Dipteryx	oleifera	Fabaceae	**0.848**	species	local data base
Discophora	guianensis	Stemonuraceae	**0.560**	species	local data base
Drypetes	standleyi	Putranjivaceae	**0.675**	species	local data base
Drypetes	coba	Putranjivaceae	**0.695**	genus	genus average
Drypetes	aff.amazonica	Putranjivaceae	**0.695**	genus	genus average
Duguetia	confusa	Annonaceae	**0.729**	genus	genus average
Duguetia	panamensis	Annonaceae	**0.729**	genus	genus average
Dussia	atropurpurea	Fabaceae	**0.553**	genus	genus average
Dussia	macroprophyllata	Fabaceae	**0.563**	species	local data base
Dussia	tessmannii	Fabaceae	**0.553**	genus	genus average
Dystovomita	paniculata	Clusiaceae	**0.592**	stand-level average	
Ecclinusa	lanceolata	Sapotaceae	**0.580**	species	local data base
Elaeagia	auriculata	Rubiaceae	**0.592**	stand-level average	
Elaeagia	nitidifolia	Rubiaceae	**0.592**	stand-level average	
Elaeis	oleifera	Arecaceae	**0.592**	stand-level average	
Endlicheria	browniana	Lauraceae	**0.495**	genus	genus average
Enterolobium	cyclocarpum	Fabaceae	**0.391**	species	local data base
Enterolobium	schomburgkii	Fabaceae	**0.699**	species	local data base

genus	species	family	WD (g/cm3)	level	source
Erblichia	odorata	Passifloraceae	**0.592**	stand-level average	
Erisma	blancoa	Vochysiaceae	**0.571**	genus	genus average
Erythrina	costaricensis	Fabaceae	**0.289**	genus	genus average
Erythrina	fusca	Fabaceae	**0.299**	species	global data base
Erythrina	poeppigiana	Fabaceae	**0.305**	species	global data base
Erythrina	rubrinervia	Fabaceae	**0.289**	genus	genus average
Erythroxylum	citrifolium	Erythroxylaceae	**0.710**	species	local data base
Erythroxylum	panamense	Erythroxylaceae	**0.790**	genus	genus average
Erythroxylum	macrophyllum	Erythroxylaceae	**0.710**	species	local data base
Eschweilera	amplexifolia	Lecythidaceae	**0.825**	genus	genus average
Eschweilera	calyculata	Lecythidaceae	**0.825**	genus	genus average
Eschweilera	jacquelyniae	Lecythidaceae	**0.825**	genus	genus average
Eschweilera	pittieri	Lecythidaceae	**0.860**	species	local data base
Eschweilera	sessilis	Lecythidaceae	**0.825**	genus	genus average
Eschweilera	panamensis	Lecythidaceae	**0.825**	genus	genus average
Eschweilera	aff.compressa	Lecythidaceae	**0.825**	genus	genus average
Esenbeckia	panamensis	Rutaceae	**1.077**	genus	genus average
Eugenia	coloradoensis	Myrtaceae	**0.721**	genus	genus average
Eugenia	cricamolensis	Myrtaceae	**0.721**	genus	genus average
Eugenia	galalonensis	Myrtaceae	**0.721**	genus	genus average
Eugenia	nesiotica	Myrtaceae	**0.721**	genus	genus average
Eugenia	oerstediana	Myrtaceae	**0.721**	genus	genus average
Eugenia	venezuelensis	Myrtaceae	**0.820**	species	local data base
Eugenia	principium	Myrtaceae	**0.721**	genus	genus average
Eugenia	austin-smithii	Myrtaceae	**0.721**	genus	genus average
Eugenia	octopleura	Myrtaceae	**0.721**	genus	genus average
Eugenia	hiraeifolia	Myrtaceae	**0.721**	genus	genus average
Euphorbia	sinclairiana	Euphorbiaceae	**0.457**	genus	genus average
Euterpe	precatoria	Arecaceae	**0.388**	species	local data base
Exostema	mexicanum	Rubiaceae	**0.995**	genus	genus average
Fairchildia	panamensis	Fabaceae	**0.592**	stand-level average	
Faramea	eurycarpa	Rubiaceae	**0.585**	genus	genus average
Faramea	luteovirens	Rubiaceae	**0.585**	genus	genus average
Faramea	multiflora	Rubiaceae	**0.585**	genus	genus average
Faramea	occidentalis	Rubiaceae	**0.585**	species	local data base
Faramea	papillata	Rubiaceae	**0.585**	genus	genus average
Faramea	papirifolia	Rubiaceae	**0.585**	genus	genus average
Faramea	suerrensis	Rubiaceae	**0.585**	genus	genus average
Faramea	coba	Rubiaceae	**0.585**	genus	genus average
Faramea	parvibractea	Rubiaceae	**0.585**	genus	genus average
Faramea	calophylla	Rubiaceae	**0.585**	genus	genus average
Ferdinandusa	panamensis	Rubiaceae	**0.725**	genus	genus average
Ficus	citrifolia	Moraceae	**0.400**	species	local data base
Ficus	colubrinae	Moraceae	**0.406**	genus	genus average

genus	species	family	WD (g/cm3)	level	source
Ficus	costaricana	Moraceae	**0.406**	genus	genus average
Ficus	insipida	Moraceae	**0.377**	species	local data base
Ficus	maxima	Moraceae	**0.361**	species	local data base
Ficus	nymphaeifolia	Moraceae	**0.415**	species	local data base
Ficus	obtusifolia	Moraceae	**0.406**	genus	genus average
Ficus	pertusa	Moraceae	**0.420**	species	local data base
Ficus	popenoei	Moraceae	**0.406**	genus	genus average
Ficus	tonduzii	Moraceae	**0.406**	genus	genus average
Ficus	yoponensis	Moraceae	**0.406**	genus	genus average
Ficus	apollinaris	Moraceae	**0.406**	genus	genus average
Ficus	brevibracteata	Moraceae	**0.406**	genus	genus average
Ficus	benjamina	Moraceae	**0.459**	species	global data base
Ficus	unidentified	Moraceae	**0.406**	genus	genus average
Ficus	trigonata	Moraceae	**0.430**	species	global data base
Ficus	matiziana	Moraceae	**0.406**	genus	genus average
Fissicalyx	fendleri	Fabaceae	**0.592**	stand-level average	
Flacourtia	jangomas	Salicaceae	**0.923**	species	global data base
Flemingia	strobilifera	Fabaceae	**0.592**	stand-level average	
Freziera	calophylla	Pentaphylacaceae	**0.580**	genus	genus average
Galipea	panamensis	Rutaceae	**0.997**	genus	genus average
Garcinia	madruno	Clusiaceae	**0.727**	species	local data base
Garcinia	magnifolia	Clusiaceae	**0.742**	genus	genus average
Garcinia	recondita	Clusiaceae	**0.742**	genus	genus average
Genipa	americana	Rubiaceae	**0.634**	species	local data base
Geonoma	congesta	Arecaceae	**0.592**	stand-level average	
Geonoma	cuneata	Arecaceae	**0.592**	stand-level average	
Geonoma	deversa	Arecaceae	**0.592**	stand-level average	
Geonoma	interrupta	Arecaceae	**0.592**	stand-level average	
Gliricidia	sepium	Fabaceae	**0.618**	species	global data base
Gloeospermum	blakeanum	Violaceae	**0.592**	stand-level average	
Gloeospermum	sphaerocarpum	Violaceae	**0.592**	stand-level average	
Gloeospermum	eneidense	Violaceae	**0.592**	stand-level average	
Gmelina	arborea	Lamiaceae	**0.430**	species	local data base
Godmania	aesculifolia	Bignoniaceae	**0.520**	species	global data base
Gonzalagunia	panamensis	Rubiaceae	**0.592**	stand-level average	
Gonzalagunia	rudis	Rubiaceae	**0.592**	stand-level average	
Gordonia	fruticosa	Theaceae	**0.519**	species	local data base
Gordonia	brenesii	Theaceae	**0.589**	genus	genus average
Gossypium	barbadense	Malvaceae	**0.680**	genus	genus average
Graffenrieda	galeottii	Melastomataceae	**0.592**	stand-level average	
Grias	cauliflora	Lecythidaceae	**0.620**	genus	genus average
Guapira	campochagres	Nyctaginaceae	**0.671**	genus	genus average
Guapira	standleyana	Nyctaginaceae	**0.671**	genus	genus average
Guapira	costaricana	Nyctaginaceae	**0.671**	genus	genus average

genus	species	family	WD (g/cm3)	level	source
Guarea	glabra	Meliaceae	**0.478**	species	local data base
Guarea	arbusto	Meliaceae	**0.607**	genus	genus average
Guarea	sherman	Meliaceae	**0.607**	genus	genus average
Guarea	grandifolia	Meliaceae	**0.545**	species	local data base
Guarea	guidonia	Meliaceae	**0.565**	species	local data base
Guarea	pterorhachis	Meliaceae	**0.770**	species	local data base
Guarea	bullata	Meliaceae	**0.607**	genus	genus average
Guarea	kunthiana	Meliaceae	**0.616**	species	local data base
Guarea	rhopalocarpa	Meliaceae	**0.607**	genus	genus average
Guarea	cf.macrophylla	Meliaceae	**0.607**	genus	genus average
Guarea	hoffmanniana	Meliaceae	**0.607**	genus	genus average
Guatteria	amplifolia	Annonaceae	**0.511**	species	local data base
Guatteria	aberrans	Annonaceae	**0.577**	genus	genus average
Guatteria	alata	Annonaceae	**0.577**	genus	genus average
Guatteria	allenii	Annonaceae	**0.577**	genus	genus average
Guatteria	dolichopoda	Annonaceae	**0.577**	genus	genus average
Guatteria	jefensis	Annonaceae	**0.577**	genus	genus average
Guatteria	sessilicarpa	Annonaceae	**0.577**	genus	genus average
Guatteria	lucens	Annonaceae	**0.577**	genus	genus average
Guatteria	ucayalina	Annonaceae	**0.577**	genus	genus average
Guazuma	ulmifolia	Malvaceae	**0.519**	species	local data base
Guettarda	crispiflora	Rubiaceae	**0.728**	genus	genus average
Guettarda	foliacea	Rubiaceae	**0.728**	genus	genus average
Guettarda	odorata	Rubiaceae	**0.728**	genus	genus average
Guettarda	ramuliflora	Rubiaceae	**0.728**	genus	genus average
Gustavia	dubia	Lecythidaceae	**0.638**	genus	genus average
Gustavia	fosteri	Lecythidaceae	**0.638**	genus	genus average
Gustavia	hexapetala	Lecythidaceae	**0.716**	species	global data base
Gustavia	nana	Lecythidaceae	**0.638**	genus	genus average
Gustavia	superba	Lecythidaceae	**0.580**	species	local data base
Gyranthera	darienensis	Malvaceae	**0.370**	genus	genus average
Hamelia	axillaris	Rubiaceae	**0.618**	species	local data base
Hamelia	patens	Rubiaceae	**0.763**	species	local data base
Hampea	appendiculata	Malvaceae	**0.245**	species	local data base
Hampea	micrantha	Malvaceae	**0.318**	genus	genus average
Handroanthus	guayacan	Bignoniaceae	**0.592**	stand-level average	
Handroanthus	impetiginosus	Bignoniaceae	**0.592**	stand-level average	
Handroanthus	ochraceus	Bignoniaceae	**0.592**	stand-level average	
Hasseltia	floribunda	Salicaceae	**0.530**	species	local data base
Hedyosmum	bonplandianum	Chloranthaceae	**0.450**	genus	genus average
Hedyosmum	scaberrimum	Chloranthaceae	**0.450**	genus	genus average
Heisteria	acuminata	Olacaceae	**0.696**	genus	genus average
Heisteria	concinna	Olacaceae	**0.640**	species	local data base
Heisteria	costaricensis	Olacaceae	**0.696**	genus	genus average

genus	species	family	WD (g/cm3)	level	source
Helicostylis	tovarensis	Moraceae	**0.669**	genus	genus average
Helicteres	guazumifolia	Malvaceae	**0.592**	stand-level average	
Heliocarpus	americanus	Malvaceae	**0.221**	species	global data base
Henriettea	succosa	Melastomataceae	**0.690**	genus	genus average
Henriettea	fascicularis	Melastomataceae	**0.690**	genus	genus average
Henriettea	tuberculosa	Melastomataceae	**0.690**	genus	genus average
Henriettea	trachyphylla	Melastomataceae	**0.690**	genus	genus average
Hernandia	didymantha	Hernandiaceae	**0.280**	species	local data base
Hernandia	stenura	Hernandiaceae	**0.292**	genus	genus average
Herrania	nycterodendron	Malvaceae	**0.592**	stand-level average	
Herrania	purpurea	Malvaceae	**0.592**	stand-level average	
Hevea	brasiliensis	Euphorbiaceae	**0.467**	species	local data base
Hieronyma	oblonga	Phyllanthaceae	**0.592**	stand-level average	
Hieronyma	alchorneoides	Phyllanthaceae	**0.592**	stand-level average	
Hippomane	mancinella	Euphorbiaceae	**0.500**	species	global data base
Hippotis	panamensis	Rubiaceae	**0.592**	stand-level average	
Hirtella	americana	Chrysobalanaceae	**0.793**	genus	genus average
Hirtella	guatemalensis	Chrysobalanaceae	**0.793**	genus	genus average
Hirtella	latifolia	Chrysobalanaceae	**0.793**	genus	genus average
Hirtella	racemosa	Chrysobalanaceae	**0.775**	species	local data base
Hirtella	triandra	Chrysobalanaceae	**0.683**	species	local data base
Hirtella	tubiflora	Chrysobalanaceae	**0.793**	genus	genus average
Homalium	racemosum	Salicaceae	**0.795**	species	global data base
Hortia	brasiliana	Rutaceae	**0.901**	genus	genus average
Humiriastrum	diguense	Humiriaceae	**0.690**	genus	genus average
Hura	crepitans	Euphorbiaceae	**0.367**	species	local data base
Hybanthus	denticulatus	Violaceae	**0.670**	genus	genus average
Hymenaea	courbaril	Fabaceae	**0.792**	species	local data base
Hymenandra	pittieri	Primulaceae	**0.592**	stand-level average	
Hymenolobium	mesoamericanum	Fabaceae	**0.642**	genus	genus average
Hyperbaena	tonduzii	Menispermaceae	**0.592**	stand-level average	
Ilex	guianensis	Aquifoliaceae	**0.563**	genus	genus average
Inga	ciliata	Fabaceae	**0.578**	genus	genus average
Inga	alba	Fabaceae	**0.586**	species	local data base
Inga	bella	Fabaceae	**0.578**	genus	genus average
Inga	capitata	Fabaceae	**0.592**	species	local data base
Inga	chocoensis	Fabaceae	**0.578**	genus	genus average
Inga	multijuga	Fabaceae	**0.578**	genus	genus average
Inga	dwyeri	Fabaceae	**0.578**	genus	genus average
Inga	edulis	Fabaceae	**0.587**	species	global data base
Inga	filiformis	Fabaceae	**0.578**	genus	genus average
Inga	goldmanii	Fabaceae	**0.578**	genus	genus average
Inga	jefensis	Fabaceae	**0.578**	genus	genus average
Inga	marginata	Fabaceae	**0.552**	species	local data base

genus	species	family	WD (g/cm3)	level	source
Inga	mucuna	Fabaceae	**0.578**	genus	genus average
Inga	pauciflora	Fabaceae	**0.578**	genus	genus average
Inga	pezizifera	Fabaceae	**0.607**	species	local data base
Inga	polita	Fabaceae	**0.578**	genus	genus average
Inga	portobellensis	Fabaceae	**0.578**	genus	genus average
Inga	punctata	Fabaceae	**0.560**	species	local data base
Inga	ruiziana	Fabaceae	**0.578**	genus	genus average
Inga	sapindoides	Fabaceae	**0.578**	genus	genus average
Inga	sertulifera	Fabaceae	**0.650**	species	local data base
Inga	spectabilis	Fabaceae	**0.578**	genus	genus average
Inga	cocleensis	Fabaceae	**0.578**	genus	genus average
Inga	umbellifera	Fabaceae	**0.724**	species	local data base
Inga	urceolata	Fabaceae	**0.578**	genus	genus average
Inga	venusta	Fabaceae	**0.578**	genus	genus average
Inga	vera	Fabaceae	**0.577**	species	local data base
Inga	acuminata	Fabaceae	**0.578**	genus	genus average
Inga	laurina	Fabaceae	**0.661**	species	local data base
Inga	nobilis	Fabaceae	**0.560**	species	local data base
Inga	oerstediana	Fabaceae	**0.425**	species	local data base
Inga	thibaudiana	Fabaceae	**0.578**	genus	genus average
Inga	acrocephala	Fabaceae	**0.513**	species	local data base
Inga	leiocalycina	Fabaceae	**0.560**	species	local data base
Inga	sierrae	Fabaceae	**0.578**	genus	genus average
Inga	aff.stenophylla	Fabaceae	**0.578**	genus	genus average
Inga	mortoniana	Fabaceae	**0.578**	genus	genus average
Inga	unidentified	Fabaceae	**0.578**	genus	genus average
Iriartea	deltoidea	Arecaceae	**0.267**	species	local data base
Iryanthera	juruensis	Myristicaceae	**0.633**	species	global data base
Isertia	haenkeana	Rubiaceae	**0.548**	genus	genus average
Isertia	laevis	Rubiaceae	**0.520**	species	global data base
Ixora	floribunda	Rubiaceae	**0.793**	genus	genus average
Jacaranda	caucana	Bignoniaceae	**0.473**	genus	genus average
Jacaranda	copaia	Bignoniaceae	**0.351**	species	local data base
Jacaratia	spinosa	Caricaceae	**0.265**	genus	genus average
Jatropha	curcas	Euphorbiaceae	**0.170**	species	global data base
Jatropha	gossypiifolia	Euphorbiaceae	**0.325**	genus	genus average
Jatropha	integerrima	Euphorbiaceae	**0.325**	genus	genus average
Khaya	senegalensis	Meliaceae	**0.626**	species	global data base
Klarobelia	anomala	Annonaceae	**0.592**	stand-level average	
Koanophyllon	wetmorei	Compositae	**0.592**	stand-level average	
Lacistema	aggregatum	Lacistemataceae	**0.506**	species	local data base
Lacmellea	panamensis	Apocynaceae	**0.472**	species	local data base
Lacmellea	speciosa	Apocynaceae	**0.513**	genus	genus average
Ladenbergia	brenesii	Rubiaceae	**0.490**	genus	genus average

genus	species	family	WD (g/cm3)	level	source
Ladenbergia	macrocarpa	Rubiaceae	**0.490**	genus	genus average
Laetia	procera	Salicaceae	**0.648**	species	local data base
Laetia	thamnia	Salicaceae	**0.660**	species	local data base
Lafoensia	punicifolia	Lythraceae	**0.705**	species	local data base
Lagerstroemia	speciosa	Lythraceae	**0.595**	species	global data base
Laguncularia	racemosa	Combretaceae	**0.610**	species	global data base
Lantana	camara	Verbenaceae	**0.592**	stand-level average	
Laxoplumeria	tessmannii	Apocynaceae	**0.592**	stand-level average	
Leandra	roja	Melastomataceae	**0.592**	stand-level average	
Leandra	dichotoma	Melastomataceae	**0.592**	stand-level average	
Leandra	granatensis	Melastomataceae	**0.592**	stand-level average	
Lecointea	amazonica	Fabaceae	**0.893**	species	local data base
Lecythis	ampla	Lecythidaceae	**0.750**	species	local data base
Lennea	viridiflora	Fabaceae	**0.592**	stand-level average	
Leonia	glycycarpa	Violaceae	**0.600**	species	local data base
Leptolobium	panamense	Fabaceae	**0.592**	stand-level average	
Libidibia	coriaria	Fabaceae	**0.592**	stand-level average	
Licania	affinis	Chrysobalanaceae	**0.820**	genus	genus average
Licania	arborea	Chrysobalanaceae	**0.622**	species	local data base
Licania	cruegeriana	Chrysobalanaceae	**0.820**	genus	genus average
Licania	fasciculata	Chrysobalanaceae	**0.820**	genus	genus average
Licania	hypoleuca	Chrysobalanaceae	**0.909**	species	local data base
Licania	morii	Chrysobalanaceae	**0.820**	genus	genus average
Licania	platypus	Chrysobalanaceae	**0.620**	species	local data base
Licania	coba	Chrysobalanaceae	**0.820**	genus	genus average
Licania	macrocarpa	Chrysobalanaceae	**0.820**	genus	genus average
Licania	kallunkiae	Chrysobalanaceae	**0.820**	genus	genus average
Licaria	guianensis	Lauraceae	**0.748**	species	global data base
Licaria	excelsa	Lauraceae	**0.787**	genus	genus average
Licaria	misantlae	Lauraceae	**0.787**	genus	genus average
Licaria	cannella	Lauraceae	**0.939**	species	global data base
Lindackeria	laurina	Achariaceae	**0.560**	genus	genus average
Lisianthius	jefensis	Gentianaceae	**0.592**	stand-level average	
Lonchocarpus	atropurpureus	Fabaceae	**0.758**	genus	genus average
Lonchocarpus	sericeus	Fabaceae	**0.705**	species	global data base
Lonchocarpus	velutinus	Fabaceae	**0.750**	species	global data base
Lonchocarpus	heptaphyllus	Fabaceae	**0.687**	species	local data base
Lonchocarpus	oliganthus	Fabaceae	**0.758**	genus	genus average
Lonchocarpus	ferrugineus	Fabaceae	**0.758**	genus	genus average
Lozania	pittieri	Lacistemataceae	**0.592**	stand-level average	
Luehea	seemannii	Malvaceae	**0.417**	species	local data base
Luehea	speciosa	Malvaceae	**0.440**	species	local data base
Lunania	mexicana	Salicaceae	**0.580**	species	global data base
Lunania	parviflora	Salicaceae	**0.635**	species	local data base

genus	species	family	WD (g/cm3)	level	source
Lycianthes	maxonii	Solanaceae	**0.440**	genus	genus average
Mabea	occidentalis	Euphorbiaceae	**0.608**	genus	genus average
Machaerium	biovulatum	Fabaceae	**0.732**	genus	genus average
Maclura	tinctoria	Moraceae	**0.794**	species	local data base
Macoubea	mesoamericana	Apocynaceae	**0.414**	genus	genus average
Macrocnemum	roseum	Rubiaceae	**0.450**	species	local data base
Macrolobium	pittieri	Fabaceae	**0.619**	genus	genus average
Macrolobium	costaricense	Fabaceae	**0.619**	genus	genus average
Malmea	dimera	Annonaceae	**0.390**	genus	genus average
Malouetia	quadricasarum	Apocynaceae	**0.527**	genus	genus average
Malpighia	albiflora	Malpighiaceae	**0.592**	stand-level average	
Malpighia	romeroana	Malpighiaceae	**0.592**	stand-level average	
Mammea	immansueta	Calophyllaceae	**0.779**	genus	genus average
Mangifera	indica	Anacardiaceae	**0.553**	species	local data base
Manihot	esculenta	Euphorbiaceae	**0.592**	stand-level average	
Manilkara	bidentata	Sapotaceae	**0.873**	species	local data base
Manilkara	zapota	Sapotaceae	**0.810**	species	local data base
Manilkara	chicle	Sapotaceae	**1.040**	species	global data base
Maprounea	guianensis	Euphorbiaceae	**0.588**	species	local data base
Maquira	guianensis	Moraceae	**0.766**	species	local data base
Maranthes	panamensis	Chrysobalanaceae	**0.830**	genus	genus average
Margaritaria	nobilis	Phyllanthaceae	**0.616**	species	local data base
Marila	lactogena	Calophyllaceae	**0.592**	stand-level average	
Marila	laxiflora	Calophyllaceae	**0.592**	stand-level average	
Marila	pluricostata	Calophyllaceae	**0.592**	stand-level average	
Marila	domingensis	Calophyllaceae	**0.592**	stand-level average	
Matayba	apetala	Sapindaceae	**0.771**	genus	genus average
Matayba	glaberrima	Sapindaceae	**0.771**	genus	genus average
Matayba	scrobiculata	Sapindaceae	**0.771**	genus	genus average
Matisia	aff.idroboi	Malvaceae	**0.535**	genus	genus average
Matisia	bracteolosa	Malvaceae	**0.535**	genus	genus average
Matisia	jefensis	Malvaceae	**0.535**	genus	genus average
Matisia	obliquifolia	Malvaceae	**0.535**	genus	genus average
Matisia	sanblasensis	Malvaceae	**0.535**	genus	genus average
Matisia	exalata	Malvaceae	**0.535**	genus	genus average
Mayna	grandifolia	Achariaceae	**0.592**	stand-level average	
Mayna	odorata	Achariaceae	**0.592**	stand-level average	
Maytenus	schippii	Celastraceae	**0.713**	genus	genus average
Melicoccus	bijugatus	Sapindaceae	**0.980**	genus	genus average
Meliosma	glabrata	Sabiaceae	**0.479**	genus	genus average
Meliosma	grandiflora	Sabiaceae	**0.479**	genus	genus average
Meliosma	idiopoda	Sabiaceae	**0.479**	genus	genus average
Meliosma	occidentalis	Sabiaceae	**0.479**	genus	genus average
Meliosma	hoja_grande	Sabiaceae	**0.479**	genus	genus average

genus	species	family	WD (g/cm3)	level	source
Meliosma	frondosa	Sabiaceae	**0.479**	genus	genus average
Miconia	affinis	Melastomataceae	**0.634**	genus	genus average
Miconia	argentea	Melastomataceae	**0.589**	species	local data base
Miconia	centronioides	Melastomataceae	**0.634**	genus	genus average
Miconia	centrosperma	Melastomataceae	**0.634**	genus	genus average
Miconia	chrysophylla	Melastomataceae	**0.620**	species	global data base
Miconia	dodecandra	Melastomataceae	**0.634**	genus	genus average
Miconia	elata	Melastomataceae	**0.470**	species	local data base
Miconia	hondurensis	Melastomataceae	**0.634**	genus	genus average
Miconia	impetiolaris	Melastomataceae	**0.747**	species	local data base
Miconia	lacera	Melastomataceae	**0.634**	genus	genus average
Miconia	ligulata	Melastomataceae	**0.634**	genus	genus average
Miconia	minutiflora	Melastomataceae	**0.634**	genus	genus average
Miconia	multispicata	Melastomataceae	**0.634**	genus	genus average
Miconia	nervosa	Melastomataceae	**0.634**	genus	genus average
Miconia	oinochrophylla	Melastomataceae	**0.634**	genus	genus average
Miconia	pileata	Melastomataceae	**0.634**	genus	genus average
Miconia	poeppigii	Melastomataceae	**0.597**	species	local data base
Miconia	prasina	Melastomataceae	**0.699**	species	local data base
Miconia	punctata	Melastomataceae	**0.634**	genus	genus average
Miconia	reducens	Melastomataceae	**0.620**	species	local data base
Miconia	rubiginosa	Melastomataceae	**0.634**	genus	genus average
Miconia	serrulata	Melastomataceae	**0.634**	genus	genus average
Miconia	simplex	Melastomataceae	**0.634**	genus	genus average
Miconia	stenostachya	Melastomataceae	**0.634**	genus	genus average
Miconia	trinervia	Melastomataceae	**0.620**	species	local data base
Miconia	dorsiloba	Melastomataceae	**0.634**	genus	genus average
Miconia	umbriensis	Melastomataceae	**0.634**	genus	genus average
Miconia	doniana	Melastomataceae	**0.634**	genus	genus average
Micropholis	guyanensis	Sapotaceae	**0.657**	species	global data base
Micropholis	melinoniana	Sapotaceae	**0.530**	species	local data base
Micropholis	venulosa	Sapotaceae	**0.670**	species	local data base
Mimosa	tenuiflora	Fabaceae	**1.120**	species	global data base
Mimusops	elengi	Sapotaceae	**0.849**	species	global data base
Minquartia	guianensis	Olacaceae	**0.787**	species	local data base
Mollinedia	viridiflora	Monimiaceae	**0.592**	stand-level average	
Morella	cerifera	Myricaceae	**0.592**	stand-level average	
Morinda	panamensis	Rubiaceae	**0.490**	species	global data base
Morinda	citrifolia	Rubiaceae	**0.630**	species	global data base
Mortoniodendron	anisophyllum	Malvaceae	**0.510**	genus	genus average
Mosannona	garwoodii	Annonaceae	**0.592**	stand-level average	
Mosquitoxylum	jamaicense	Anacardiaceae	**0.592**	stand-level average	
Mouriri	gleasoniana	Melastomataceae	**0.840**	genus	genus average
Mouriri	myrtilloides	Melastomataceae	**0.840**	genus	genus average

genus	species	family	WD (g/cm3)	level	source
Mouriri	panamensis	Melastomataceae	**0.840**	genus	genus average
Mouriri	coba	Melastomataceae	**0.840**	genus	genus average
Mouriri	aff.exilis	Melastomataceae	**0.840**	genus	genus average
Mouriri	cf.completens	Melastomataceae	**0.840**	genus	genus average
Muntingia	calabura	Muntingiaceae	**0.300**	species	global data base
Myrcia	splendens	Myrtaceae	**0.800**	species	global data base
Myrcia	panamensis	Myrtaceae	**0.816**	genus	genus average
Myrcia	fosteri	Myrtaceae	**0.816**	genus	genus average
Myrcia	zetekiana	Myrtaceae	**0.816**	genus	genus average
Myrciaria	floribunda	Myrtaceae	**0.785**	species	global data base
Myriocarpa	longipes	Urticaceae	**0.592**	stand-level average	
Myrospermum	frutescens	Fabaceae	**0.830**	species	local data base
Myrsine	coriacea	Primulaceae	**0.647**	species	global data base
Naucleopsis	naga	Moraceae	**0.651**	genus	genus average
Naucleopsis	ulei	Moraceae	**0.670**	species	local data base
Naucleopsis	straminea	Moraceae	**0.651**	genus	genus average
Naucleopsis	capirensis	Moraceae	**0.651**	genus	genus average
Nectandra	bicolor	Lauraceae	**0.562**	genus	genus average
Nectandra	cissiflora	Lauraceae	**0.590**	species	local data base
Nectandra	cuspidata	Lauraceae	**0.518**	species	local data base
Nectandra	fuzzy	Lauraceae	**0.562**	genus	genus average
Nectandra	lineata	Lauraceae	**0.562**	genus	genus average
Neea	roja	Nyctaginaceae	**0.640**	genus	genus average
Neea	amplifolia	Nyctaginaceae	**0.640**	genus	genus average
Neea	delicatula	Nyctaginaceae	**0.640**	genus	genus average
Neea	laetevirens	Nyctaginaceae	**0.640**	genus	genus average
Ochoterenaea	colombiana	Anacardiaceae	**0.592**	stand-level average	
Ochroma	pyramidale	Malvaceae	**0.158**	species	local data base
Ocotea	arcuata	Lauraceae	**0.542**	genus	genus average
Ocotea	atirrensis	Lauraceae	**0.480**	species	local data base
Ocotea	cernua	Lauraceae	**0.454**	species	local data base
Ocotea	dendrodaphne	Lauraceae	**0.530**	species	local data base
Ocotea	endresiana	Lauraceae	**0.542**	genus	genus average
Ocotea	insularis	Lauraceae	**0.542**	genus	genus average
Ocotea	leucoxylon	Lauraceae	**0.462**	species	local data base
Ocotea	meziana	Lauraceae	**0.390**	species	global data base
Ocotea	oblonga	Lauraceae	**0.386**	species	local data base
Ocotea	rubrinervis	Lauraceae	**0.542**	genus	genus average
Ocotea	tonduzii	Lauraceae	**0.542**	genus	genus average
Ocotea	veraguensis	Lauraceae	**0.735**	species	local data base
Ocotea	puberula	Lauraceae	**0.433**	species	local data base
Ocotea	whitei	Lauraceae	**0.542**	genus	genus average
Ocotea	hartshorniana	Lauraceae	**0.380**	species	global data base
Ocotea	jorge-escobarii	Lauraceae	**0.542**	genus	genus average

genus	species	family	WD (g/cm3)	level	source
Ocotea	helicterifolia	Lauraceae	**0.542**	genus	genus average
Oenocarpus	mapora	Arecaceae	**0.713**	species	local data base
Opuntia	elatior	Cactaceae	**0.592**	stand-level average	
Oreopanax	capitatus	Araliaceae	**0.520**	genus	genus average
Ormosia	amazonica	Fabaceae	**0.579**	genus	genus average
Ormosia	macrocalyx	Fabaceae	**0.579**	genus	genus average
Ormosia	coccinea	Fabaceae	**0.625**	species	local data base
Ormosia	velutina	Fabaceae	**0.579**	genus	genus average
Ossaea	spicata	Melastomataceae	**0.592**	stand-level average	
Osteophloeum	platyspermum	Myristicaceae	**0.466**	species	local data base
Otoba	acuminata	Myristicaceae	**0.389**	genus	genus average
Otoba	latialata	Myristicaceae	**0.389**	genus	genus average
Otoba	novogranatensis	Myristicaceae	**0.350**	species	local data base
Otoba	parvifolia	Myristicaceae	**0.426**	species	local data base
Ouratea	knappiae	Ochnaceae	**0.743**	genus	genus average
Ouratea	lucens	Ochnaceae	**0.743**	genus	genus average
Ouratea	prominens	Ochnaceae	**0.743**	genus	genus average
Ouratea	sulcatinervia	Ochnaceae	**0.743**	genus	genus average
Oxandra	longipetala	Annonaceae	**0.737**	genus	genus average
Oxandra	panamensis	Annonaceae	**0.737**	genus	genus average
Oxandra	venezuelana	Annonaceae	**0.737**	genus	genus average
Pachira	aquatica	Malvaceae	**0.377**	species	local data base
Pachira	sessilis	Malvaceae	**0.420**	species	local data base
Palicourea	allenii	Rubiaceae	**0.550**	genus	genus average
Palicourea	guianensis	Rubiaceae	**0.540**	species	local data base
Palicourea	triphylla	Rubiaceae	**0.550**	genus	genus average
Palicourea	crocea	Rubiaceae	**0.560**	species	global data base
Palicourea	umbelliformis	Rubiaceae	**0.550**	genus	genus average
Palicourea	hondensis	Rubiaceae	**0.550**	genus	genus average
Palicourea	acuminata	Rubiaceae	**0.550**	genus	genus average
Palicourea	brachiata	Rubiaceae	**0.550**	genus	genus average
Palicourea	capitata	Rubiaceae	**0.550**	genus	genus average
Palicourea	cyanococca	Rubiaceae	**0.550**	genus	genus average
Palicourea	deflexa	Rubiaceae	**0.550**	genus	genus average
Palicourea	elata	Rubiaceae	**0.550**	genus	genus average
Palicourea	glomerulata	Rubiaceae	**0.550**	genus	genus average
Palicourea	gracilenta	Rubiaceae	**0.550**	genus	genus average
Palicourea	hoffmannseggiana	Rubiaceae	**0.550**	genus	genus average
Palicourea	longicuspis	Rubiaceae	**0.550**	genus	genus average
Palicourea	luxurians	Rubiaceae	**0.550**	genus	genus average
Palicourea	tomentosa	Rubiaceae	**0.550**	genus	genus average
Palicourea	pubescens	Rubiaceae	**0.550**	genus	genus average
Palicourea	racemosa	Rubiaceae	**0.550**	genus	genus average
Palicourea	suerrensis	Rubiaceae	**0.550**	genus	genus average

genus	species	family	WD (g/cm3)	level	source
Panopsis	suaveolens	Proteaceae	**0.512**	genus	genus average
Parathesis	amplifolia	Primulaceae	**0.620**	genus	genus average
Parinari	chocoensis	Chrysobalanaceae	**0.713**	genus	genus average
Parkia	nitida	Fabaceae	**0.383**	species	local data base
Parkinsonia	aculeata	Fabaceae	**0.622**	species	global data base
Parmentiera	cereifera	Bignoniaceae	**0.592**	stand-level average	
Parmentiera	macrophylla	Bignoniaceae	**0.592**	stand-level average	
Pavonia	dasypetala	Malvaceae	**0.592**	stand-level average	
Pelliciera	rhizophorae	Tetrameristaceae	**0.592**	stand-level average	
Pentagonia	gymnopoda	Rubiaceae	**0.592**	stand-level average	
Pentagonia	macrophylla	Rubiaceae	**0.592**	stand-level average	
Pentagonia	parvifolia	Rubiaceae	**0.592**	stand-level average	
Pentagonia	wendlandii	Rubiaceae	**0.592**	stand-level average	
Pentagonia	costaricensis	Rubiaceae	**0.592**	stand-level average	
Pera	arborea	Peraceae	**0.730**	species	local data base
Pera	oppositifolia	Peraceae	**0.666**	genus	genus average
Perebea	angustifolia	Moraceae	**0.517**	species	local data base
Perebea	guianensis	Moraceae	**0.560**	species	local data base
Perebea	xanthochyma	Moraceae	**0.560**	species	local data base
Pereskia	bleo	Cactaceae	**0.592**	stand-level average	
Persea	americana	Lauraceae	**0.549**	species	global data base
Photinia	microcarpa	Rosaceae	**0.724**	genus	genus average
Phyllanthus	acuminatus	Phyllanthaceae	**0.613**	genus	genus average
Phytelephas	seemannii	Arecaceae	**0.592**	stand-level average	
Picramnia	latifolia	Picramniaceae	**0.592**	stand-level average	
Pinus	caribaea	Pinaceae	**0.571**	species	global data base
Piper	hispidum	Piperaceae	**0.393**	species	local data base
Piper	aduncum	Piperaceae	**0.393**	genus	genus average
Piper	aequale	Piperaceae	**0.393**	genus	genus average
Piper	amalago	Piperaceae	**0.393**	genus	genus average
Piper	arboreum	Piperaceae	**0.393**	genus	genus average
Piper	augustum	Piperaceae	**0.393**	genus	genus average
Piper	auritum	Piperaceae	**0.393**	genus	genus average
Piper	cordulatum	Piperaceae	**0.393**	genus	genus average
Piper	fimbriulatum	Piperaceae	**0.393**	genus	genus average
Piper	grande	Piperaceae	**0.393**	genus	genus average
Piper	hirtellipetiolum	Piperaceae	**0.393**	genus	genus average
Piper	longispicum	Piperaceae	**0.393**	genus	genus average
Piper	marginatum	Piperaceae	**0.393**	genus	genus average
Piper	perlasense	Piperaceae	**0.393**	genus	genus average
Piper	phytolaccifolium	Piperaceae	**0.393**	genus	genus average
Piper	reticulatum	Piperaceae	**0.330**	species	local data base
Piper	colonense	Piperaceae	**0.393**	genus	genus average
Piper	schiedeanum	Piperaceae	**0.393**	genus	genus average

genus	species	family	WD (g/cm3)	level	source
Piper	imperiale	Piperaceae	**0.393**	genus	genus average
Piptocoma	discolor	Compositae	**0.470**	species	global data base
Pithecellobium	hymenaeifolium	Fabaceae	**0.502**	genus	genus average
Pithecellobium	lanceolatum	Fabaceae	**0.502**	genus	genus average
Pithecellobium	unguis-cati	Fabaceae	**0.502**	genus	genus average
Pittoniotis	trichantha	Rubiaceae	**0.592**	stand-level average	
Platymiscium	pinnatum	Fabaceae	**0.721**	species	local data base
Platypodium	elegans	Fabaceae	**0.806**	species	local data base
Pleuranthodendron	lindenii	Salicaceae	**0.680**	species	local data base
Pleurothyrium	aff.hexaglandulosum	Lauraceae	**0.470**	genus	genus average
Pleurothyrium	racemosum	Lauraceae	**0.470**	genus	genus average
Plinia	povedae	Myrtaceae	**0.950**	genus	genus average
Plumeria	rubra	Apocynaceae	**0.500**	species	global data base
Pochota	quinata	Malvaceae	**0.592**	stand-level average	
Podocarpus	guatemalensis	Podocarpaceae	**0.400**	species	global data base
Podocarpus	oleifolius	Podocarpaceae	**0.453**	species	local data base
Pogonopus	exsertus	Rubiaceae	**0.592**	stand-level average	
Pombalia	prunifolia	NA	**0.592**	stand-level average	
Posoqueria	latifolia	Rubiaceae	**0.570**	species	local data base
Posoqueria	coriacea	Rubiaceae	**0.575**	genus	genus average
Potalia	turbinata	Gentianaceae	**0.592**	stand-level average	
Poulsenia	armata	Moraceae	**0.350**	species	local data base
Pourouma	bicolor	Urticaceae	**0.353**	species	local data base
Pourouma	minor	Urticaceae	**0.436**	species	local data base
Pouteria	glomerata	Sapotaceae	**0.679**	species	local data base
Pouteria	buenaventurensis	Sapotaceae	**0.560**	species	local data base
Pouteria	bulliformis	Sapotaceae	**0.688**	genus	genus average
Pouteria	calistophylla	Sapotaceae	**0.688**	genus	genus average
Pouteria	campechiana	Sapotaceae	**0.790**	species	local data base
Pouteria	cuspidata	Sapotaceae	**0.900**	species	local data base
Pouteria	fossicola	Sapotaceae	**0.688**	genus	genus average
Pouteria	foveolata	Sapotaceae	**0.688**	genus	genus average
Pouteria	leptopedicellata	Sapotaceae	**0.688**	genus	genus average
Pouteria	aff.sclerocarpa	Sapotaceae	**0.688**	genus	genus average
Pouteria	stipitata	Sapotaceae	**0.688**	genus	genus average
Pouteria	torta	Sapotaceae	**0.769**	species	local data base
Pouteria	reticulata	Sapotaceae	**0.794**	species	local data base
Pouteria	congestifolia	Sapotaceae	**0.688**	genus	genus average
Pouteria	durlandii	Sapotaceae	**0.690**	species	local data base
Pouteria	silvestris	Sapotaceae	**0.688**	genus	genus average
Pouteria	sapota	Sapotaceae	**0.855**	species	global data base
Preslianthus	panamensis	NA	**0.592**	stand-level average	
Preslianthus	pittieri	NA	**0.592**	stand-level average	
Prestoea	decurrens	Arecaceae	**0.250**	species	local data base

genus	species	family	WD (g/cm3)	level	source
Prioria	copaifera	Fabaceae	**0.414**	species	local data base
Prockia	crucis	Salicaceae	**0.580**	species	local data base
Prosopis	juliflora	Fabaceae	**0.794**	species	global data base
Protium	tenuifolium	Burseraceae	**0.570**	species	local data base
Protium	aff.guianense	Burseraceae	**0.568**	genus	genus average
Protium	costaricense	Burseraceae	**0.568**	genus	genus average
Protium	glabrum	Burseraceae	**0.568**	genus	genus average
Protium	panamense	Burseraceae	**0.452**	species	local data base
Protium	trifoliolatum	Burseraceae	**0.685**	species	local data base
Protium	confusum	Burseraceae	**0.568**	genus	genus average
Pseudima	frutescens	Sapindaceae	**0.800**	species	global data base
Pseudobombax	septenatum	Malvaceae	**0.212**	species	local data base
Pseudolmedia	spuria	Moraceae	**0.713**	species	local data base
Pseudolmedia	laevigata	Moraceae	**0.629**	species	local data base
Pseudosamanea	guachapele	Fabaceae	**0.592**	stand-level average	
Psidium	friedrichsthalianum	Myrtaceae	**0.855**	genus	genus average
Psidium	guajava	Myrtaceae	**0.652**	species	global data base
Psychotria	calophylla	Rubiaceae	**0.496**	genus	genus average
Psychotria	chagrensis	Rubiaceae	**0.496**	genus	genus average
Psychotria	graciliflora	Rubiaceae	**0.496**	genus	genus average
Psychotria	grandis	Rubiaceae	**0.295**	species	local data base
Psychotria	horizontalis	Rubiaceae	**0.496**	genus	genus average
Psychotria	limonensis	Rubiaceae	**0.496**	genus	genus average
Psychotria	marginata	Rubiaceae	**0.496**	genus	genus average
Psychotria	micrantha	Rubiaceae	**0.496**	genus	genus average
Psychotria	nervosa	Rubiaceae	**0.496**	genus	genus average
Psychotria	panamensis	Rubiaceae	**0.496**	genus	genus average
Psychotria	psychotriifolia	Rubiaceae	**0.496**	genus	genus average
Psychotria	remota	Rubiaceae	**0.496**	genus	genus average
Psychotria	tenuifolia	Rubiaceae	**0.496**	genus	genus average
Pterocarpus	acapulcensis	Fabaceae	**0.627**	genus	genus average
Pterocarpus	officinalis	Fabaceae	**0.383**	species	local data base
Pterocarpus	hayesii	Fabaceae	**0.627**	genus	genus average
Quadrella	cynophallophora	Capparaceae	**0.592**	stand-level average	
Quadrella	antonensis	Capparaceae	**0.592**	stand-level average	
Quadrella	indica	Capparaceae	**0.592**	stand-level average	
Qualea	polychroma	Vochysiaceae	**0.647**	genus	genus average
Quararibea	asterolepis	Malvaceae	**0.454**	species	local data base
Quararibea	platyphylla	Malvaceae	**0.488**	genus	genus average
Quararibea	pumila	Malvaceae	**0.488**	genus	genus average
Quararibea	pterocalyx	Malvaceae	**0.488**	genus	genus average
Quassia	amara	Simaroubaceae	**0.470**	species	local data base
Quetzalia	occidentalis	Celastraceae	**0.592**	stand-level average	
Quiina	schippii	Ochnaceae	**0.862**	genus	genus average

genus	species	family	WD (g/cm3)	level	source
Randia	campo_chagres	Rubiaceae	**0.671**	genus	genus average
Randia	aculeata	Rubiaceae	**0.671**	genus	genus average
Randia	armata	Rubiaceae	**0.668**	species	local data base
Randia	grandifolia	Rubiaceae	**0.671**	genus	genus average
Randia	lasiantha	Rubiaceae	**0.671**	genus	genus average
Randia	hondensis	Rubiaceae	**0.671**	genus	genus average
Raphia	taedigera	Arecaceae	**0.592**	stand-level average	
Raritebe	palicoureoides	Rubiaceae	**0.592**	stand-level average	
Rauvolfia	littoralis	Apocynaceae	**0.486**	genus	genus average
Rauvolfia	purpurascens	Apocynaceae	**0.476**	species	global data base
Rhizophora	mangle	Rhizophoraceae	**0.898**	species	global data base
Richeria	grandis	Phyllanthaceae	**0.577**	species	global data base
Ricinus	communis	Euphorbiaceae	**0.592**	stand-level average	
Rinorea	apiculata	Violaceae	**0.681**	genus	genus average
Rinorea	crenata	Violaceae	**0.681**	genus	genus average
Rinorea	dasyadena	Violaceae	**0.681**	genus	genus average
Rinorea	lindeniana	Violaceae	**0.681**	genus	genus average
Rinorea	squamata	Violaceae	**0.681**	genus	genus average
Rinorea	sylvatica	Violaceae	**0.681**	genus	genus average
Rinorea	hummelii	Violaceae	**0.681**	genus	genus average
Rogiera	amoena	Rubiaceae	**0.592**	stand-level average	
Ronabea	latifolia	Rubiaceae	**0.592**	stand-level average	
Rondeletia	hameliifolia	Rubiaceae	**0.500**	genus	genus average
Rondeletia	panamensis	Rubiaceae	**0.500**	genus	genus average
Rosenbergiodendron	formosum	Rubiaceae	**0.592**	stand-level average	
Roupala	montana	Proteaceae	**0.783**	species	local data base
Roupala	percoriacea	Proteaceae	**0.837**	genus	genus average
Roystonea	regia	Arecaceae	**0.592**	stand-level average	
Rudgea	cornifolia	Rubiaceae	**0.570**	genus	genus average
Rudgea	isthmensis	Rubiaceae	**0.570**	genus	genus average
Rudgea	pittieri	Rubiaceae	**0.570**	genus	genus average
Rudgea	skutchii	Rubiaceae	**0.570**	genus	genus average
Ruprechtia	costata	Polygonaceae	**0.653**	genus	genus average
Ruptiliocarpon	caracolito	Lepidobotryaceae	**0.592**	stand-level average	
Ryania	speciosa	Salicaceae	**0.592**	stand-level average	
Sacoglottis	ovicarpa	Humiriaceae	**0.775**	genus	genus average
Sacoglottis	trichogyna	Humiriaceae	**0.775**	genus	genus average
Salacia	juruana	Celastraceae	**0.760**	genus	genus average
Salacia	petenensis	Celastraceae	**0.760**	genus	genus average
Samanea	saman	Fabaceae	**0.592**	stand-level average	
Sapindus	saponaria	Sapindaceae	**0.712**	species	local data base
Sapium	broadleaf	Euphorbiaceae	**0.419**	genus	genus average
Sapium	glandulosum	Euphorbiaceae	**0.415**	species	local data base
Sapium	laurifolium	Euphorbiaceae	**0.419**	genus	genus average

genus	species	family	WD (g/cm3)	level	source
Sarcaulus	brasiliensis	Sapotaceae	**0.615**	species	local data base
Saurauia	yasicae	Actinidiaceae	**0.411**	genus	genus average
Schefflera	morototoni	Araliaceae	**0.456**	species	local data base
Schizolobium	parahyba	Fabaceae	**0.347**	species	local data base
Schoenobiblus	panamensis	Thymelaeaceae	**0.592**	stand-level average	
Sciadodendron	excelsum	Araliaceae	**0.530**	species	local data base
Senegalia	riparia	Fabaceae	**0.592**	stand-level average	
Senna	bicapsularis	Fabaceae	**0.603**	genus	genus average
Senna	reticulata	Fabaceae	**0.450**	species	global data base
Senna	dariensis	Fabaceae	**0.603**	genus	genus average
Sideroxylon	capiri	Sapotaceae	**0.760**	species	global data base
Sideroxylon	celastrinum	Sapotaceae	**0.849**	genus	genus average
Sideroxylon	persimile	Sapotaceae	**0.849**	genus	genus average
Sideroxylon	cf.contrerasii	Sapotaceae	**0.849**	genus	genus average
Simaba	cedron	Simaroubaceae	**0.474**	species	global data base
Simaba	polyphylla	Simaroubaceae	**0.410**	genus	genus average
Simarouba	amara	Simaroubaceae	**0.383**	species	local data base
Simira	maxonii	Rubiaceae	**0.615**	species	global data base
Siparuna	conica	Siparunaceae	**0.662**	genus	genus average
Siparuna	cuspidata	Siparunaceae	**0.655**	species	local data base
Siparuna	grandiflora	Siparunaceae	**0.662**	genus	genus average
Siparuna	guianensis	Siparunaceae	**0.662**	genus	genus average
Siparuna	pauciflora	Siparunaceae	**0.662**	genus	genus average
Siparuna	thecaphora	Siparunaceae	**0.662**	genus	genus average
Siparuna	cristata	Siparunaceae	**0.662**	genus	genus average
Sloanea	laurifolia	Elaeocarpaceae	**0.816**	species	local data base
Sloanea	megaphylla	Elaeocarpaceae	**0.609**	genus	genus average
Sloanea	meianthera	Elaeocarpaceae	**0.609**	genus	genus average
Sloanea	zuliaensis	Elaeocarpaceae	**0.609**	genus	genus average
Sloanea	terniflora	Elaeocarpaceae	**0.609**	genus	genus average
Sloanea	medusula	Elaeocarpaceae	**0.609**	genus	genus average
Sloanea	obtusifolia	Elaeocarpaceae	**0.609**	genus	genus average
Socratea	exorrhiza	Arecaceae	**0.230**	species	local data base
Solanum	enves_purpura	Solanaceae	**0.412**	genus	genus average
Solanum	arboreum	Solanaceae	**0.412**	genus	genus average
Solanum	asperum	Solanaceae	**0.412**	genus	genus average
Solanum	hayesii	Solanaceae	**0.412**	genus	genus average
Solanum	jamaicense	Solanaceae	**0.412**	genus	genus average
Solanum	circinatum	Solanaceae	**0.412**	genus	genus average
Solanum	cordovense	Solanaceae	**0.412**	genus	genus average
Solanum	lepidotum	Solanaceae	**0.412**	genus	genus average
Sorocea	pubivena	Moraceae	**0.605**	genus	genus average
Sorocea	affinis	Moraceae	**0.605**	genus	genus average
Spachea	correae	Malpighiaceae	**0.595**	genus	genus average

genus	species	family	WD (g/cm3)	level	source
Spachea	membranacea	Malpighiaceae	**0.595**	genus	genus average
Spathodea	campanulata	Bignoniaceae	**0.351**	species	global data base
Spondias	dulcis	Anacardiaceae	**0.370**	species	local data base
Spondias	mombin	Anacardiaceae	**0.391**	species	local data base
Spondias	purpurea	Anacardiaceae	**0.330**	species	global data base
Spondias	radlkoferi	Anacardiaceae	**0.434**	species	local data base
Stachyarrhena	heterochroa	Rubiaceae	**0.820**	genus	genus average
Stauranthus	perforatus	Rutaceae	**0.592**	stand-level average	
Stemmadenia	alfaroi	Apocynaceae	**0.500**	genus	genus average
Sterculia	costaricana	Malvaceae	**0.405**	genus	genus average
Sterculia	apetala	Malvaceae	**0.392**	species	local data base
Sterculia	recordiana	Malvaceae	**0.490**	species	local data base
Stylogyne	turbacensis	Primulaceae	**0.483**	genus	genus average
Swartzia	simplex	Fabaceae	**0.849**	genus	genus average
Swartzia	aff.sumorum	Fabaceae	**0.849**	genus	genus average
Swietenia	macrophylla	Meliaceae	**0.520**	species	local data base
Symphonia	globulifera	Clusiaceae	**0.600**	species	local data base
Symplocos	panamensis	Symplocaceae	**0.534**	genus	genus average
Synechanthus	warscewiczianus	Arecaceae	**0.592**	stand-level average	
Syzygium	jambos	Myrtaceae	**0.700**	species	global data base
Syzygium	malaccense	Myrtaceae	**0.562**	species	global data base
Tabebuia	rosea	Bignoniaceae	**0.531**	species	local data base
Tabebuia	striata	Bignoniaceae	**0.762**	genus	genus average
Tabernaemontana	arborea	Apocynaceae	**0.526**	genus	genus average
Tabernaemontana	longipes	Apocynaceae	**0.526**	genus	genus average
Tabernaemontana	panamensis	Apocynaceae	**0.526**	genus	genus average
Tabernaemontana	undulata	Apocynaceae	**0.585**	species	local data base
Tabernaemontana	grandiflora	Apocynaceae	**0.526**	genus	genus average
Tachigali	panamensis	Fabaceae	**0.577**	genus	genus average
Tachigali	costaricensis	Fabaceae	**0.577**	genus	genus average
Talauma	gloriensis	Magnoliaceae	**0.592**	stand-level average	
Talauma	sambuensis	Magnoliaceae	**0.592**	stand-level average	
Taliparitи	tiliaceum	Malvaceae	**0.543**	species	global data base
Talisia	nervosa	Sapindaceae	**0.833**	genus	genus average
Talisia	croatii	Sapindaceae	**0.833**	genus	genus average
Tamarindus	indica	Fabaceae	**0.978**	species	global data base
Tapirira	guianensis	Anacardiaceae	**0.457**	species	local data base
Tapura	cubensis	Dichapetalaceae	**0.640**	genus	genus average
Tecoma	stans	Bignoniaceae	**0.466**	species	global data base
Tectona	grandis	Lamiaceae	**0.601**	species	global data base
Terminalia	amazonia	Combretaceae	**0.674**	species	local data base
Terminalia	catappa	Combretaceae	**0.478**	species	global data base
Terminalia	oblonga	Combretaceae	**0.694**	species	local data base
Terminalia	bucidoides	Combretaceae	**0.630**	genus	genus average

genus	species	family	WD (g/cm3)	level	source
Terminalia	buceras	Combretaceae	**0.630**	genus	genus average
Ternstroemia	tepezapote	Pentaphylacaceae	**0.616**	genus	genus average
Tetragastris	panamensis	Burseraceae	**0.717**	species	local data base
Tetrathylacium	johansenii	Salicaceae	**0.620**	genus	genus average
Tetrathylacium	macrophyllum	Salicaceae	**0.620**	species	local data base
Tetrorchidium	euryphyllum	Euphorbiaceae	**0.455**	genus	genus average
Tetrorchidium	robledoanum	Euphorbiaceae	**0.455**	genus	genus average
Theobroma	bernoullii	Malvaceae	**0.532**	genus	genus average
Theobroma	cacao	Malvaceae	**0.420**	species	local data base
Theobroma	simiarum	Malvaceae	**0.532**	genus	genus average
Theobroma	speciosum	Malvaceae	**0.630**	species	local data base
Theobroma	bicolor	Malvaceae	**0.532**	genus	genus average
Thevetia	ahouai	Apocynaceae	**0.720**	genus	genus average
Tococa	guianensis	Melastomataceae	**0.592**	stand-level average	
Tocoyena	pittieri	Rubiaceae	**0.620**	genus	genus average
Tovomita	longifolia	Clusiaceae	**0.695**	genus	genus average
Tovomita	stylosa	Clusiaceae	**0.695**	genus	genus average
Tovomita	weddelliana	Clusiaceae	**0.695**	genus	genus average
Trattinnickia	aspera	Burseraceae	**0.424**	species	local data base
Trattinnickia	burserifolia	Burseraceae	**0.460**	species	local data base
Trema	micrantha	Cannabaceae	**0.319**	species	local data base
Trema	integerrima	Cannabaceae	**0.300**	species	global data base
Trema	unidentified	Cannabaceae	**0.342**	genus	genus average
Trichanthera	gigantea	Acanthaceae	**0.450**	species	local data base
Trichilia	hirta	Meliaceae	**0.569**	species	local data base
Trichilia	martiana	Meliaceae	**0.470**	species	local data base
Trichilia	pleeana	Meliaceae	**0.675**	species	local data base
Trichilia	poeppigii	Meliaceae	**0.645**	genus	genus average
Trichilia	quadrijuga	Meliaceae	**0.548**	species	local data base
Trichilia	septentrionalis	Meliaceae	**0.645**	genus	genus average
Trichilia	trifolia	Meliaceae	**0.800**	species	global data base
Trichilia	pallida	Meliaceae	**0.700**	species	local data base
Trichilia	tuberculata	Meliaceae	**0.628**	species	local data base
Trichospermum	galeottii	Malvaceae	**0.270**	species	local data base
Triplaris	cumingiana	Polygonaceae	**0.520**	species	local data base
Triumfetta	bogotensis	Malvaceae	**0.592**	stand-level average	
Trophis	racemosa	Moraceae	**0.659**	species	local data base
Trophis	caucana	Moraceae	**0.470**	species	local data base
Turnera	panamensis	Passifloraceae	**0.592**	stand-level average	
Turpinia	occidentalis	Staphyleaceae	**0.342**	species	local data base
Unidentified	pubescente	NA	**0.592**	stand-level average	
Unidentified	species	NA	**0.592**	stand-level average	
Unonopsis	panamensis	Annonaceae	**0.534**	genus	genus average
Unonopsis	pittieri	Annonaceae	**0.368**	species	local data base

genus	species	family	WD (g/cm3)	level	source
Unonopsis	theobromifolia	Annonaceae	**0.534**	genus	genus average
Unonopsis	aff.veneficiorum	Annonaceae	**0.534**	genus	genus average
Unonopsis	peludo	Annonaceae	**0.534**	genus	genus average
Unonopsis	bullata	Annonaceae	**0.534**	genus	genus average
Unonopsis	storkii	Annonaceae	**0.534**	genus	genus average
Urera	baccifera	Urticaceae	**0.220**	species	local data base
Urera	caracasana	Urticaceae	**0.316**	species	global data base
Urera	laciniata	Urticaceae	**0.342**	genus	genus average
Vachellia	melanoceras	Fabaceae	**0.592**	stand-level average	
Vachellia	collinsii	Fabaceae	**0.592**	stand-level average	
Vantanea	depleta	Humiriaceae	**0.837**	genus	genus average
Varronia	curassavica	Boraginaceae	**0.592**	stand-level average	
Vasconcellea	cauliflora	Caricaceae	**0.592**	stand-level average	
Vatairea	erythrocarpa	Fabaceae	**0.673**	genus	genus average
Verbesina	gigantea	Compositae	**0.592**	stand-level average	
Verbesina	lanata	Compositae	**0.592**	stand-level average	
Vernonia	patens	Compositae	**0.330**	genus	genus average
Virola	elongata	Myristicaceae	**0.523**	species	local data base
Virola	koschnyi	Myristicaceae	**0.408**	species	local data base
Virola	macrocarpa	Myristicaceae	**0.484**	genus	genus average
Virola	megacarpa	Myristicaceae	**0.484**	genus	genus average
Virola	sebifera	Myristicaceae	**0.445**	species	local data base
Virola	multiflora	Myristicaceae	**0.458**	species	local data base
Virola	guatemalensis	Myristicaceae	**0.520**	species	global data base
Virola	nobilis	Myristicaceae	**0.484**	genus	genus average
Vismia	baccifera	Hypericaceae	**0.430**	species	local data base
Vismia	billbergiana	Hypericaceae	**0.493**	genus	genus average
Vismia	jefensis	Hypericaceae	**0.493**	genus	genus average
Vismia	macrophylla	Hypericaceae	**0.494**	species	local data base
Vitex	cooperi	Lamiaceae	**0.565**	genus	genus average
Vitex	cymosa	Lamiaceae	**0.563**	species	local data base
Vochysia	ferruginea	Vochysiaceae	**0.410**	species	local data base
Vochysia	jefensis	Vochysiaceae	**0.486**	genus	genus average
Vochysia	guatemalensis	Vochysiaceae	**0.353**	species	local data base
Waltheria	glomerata	Malvaceae	**0.592**	stand-level average	
Warszewiczia	coccinea	Rubiaceae	**0.557**	species	local data base
Welfia	regia	Arecaceae	**0.400**	species	local data base
Wettinia	quinaria	Arecaceae	**0.592**	stand-level average	
Witheringia	solanacea	Solanaceae	**0.592**	stand-level average	
Ximenia	americana	Olacaceae	**0.856**	species	local data base
Xylopia	aromatica	Annonaceae	**0.561**	species	local data base
Xylopia	bocatorena	Annonaceae	**0.591**	genus	genus average
Xylopia	frutescens	Annonaceae	**0.593**	species	local data base
Xylopia	macrantha	Annonaceae	**0.874**	species	local data base

genus	species	family	WD (g/cm3)	level	source
Xylopia	sericea	Annonaceae	**0.591**	genus	genus average
Xylopia	roubik	Annonaceae	**0.591**	genus	genus average
Xylosma	chlorantha	Salicaceae	**0.661**	genus	genus average
Xylosma	oligandra	Salicaceae	**0.661**	genus	genus average
Xylosma	panamensis	Salicaceae	**0.661**	genus	genus average
Zamia	fairchildiana	Zamiaceae	**0.592**	stand-level average	
Zanthoxylum	acuminatum	Rutaceae	**0.618**	genus	genus average
Zanthoxylum	panamense	Rutaceae	**0.490**	species	local data base
Zanthoxylum	setulosum	Rutaceae	**0.469**	species	local data base
Zanthoxylum	ekmanii	Rutaceae	**0.618**	genus	genus average
Ziziphus	chloroxylon	Rhamnaceae	**0.778**	genus	genus average
Ziziphus	mauritiana	Rhamnaceae	**0.618**	species	global data base
Zuelania	guidonia	Salicaceae	**0.583**	species	local data base
Zygia	dinizii	Fabaceae	**0.820**	genus	genus average
Zygia	englesingii	Fabaceae	**0.820**	genus	genus average
Zygia	latifolia	Fabaceae	**0.750**	species	global data base
Zygia	longifolia	Fabaceae	**0.710**	species	global data base